Tiago Alexandre Ramos Teixeira de Sousa Santos

THERAPEUTIC POTENTIAL OF RETINOIC ACID-LOADED NANOPARTICLES FOR BRAIN REPAIR

Doctoral Thesis in Biosciences (Specialization in Neuroscience), Supervised by Doctor Liliana Inácio Bernardino and Doctor Emília da Conceição Pedrosa Duarte, and presented to the Faculty of Sciences and Technology of the University of Coimbra

September 2015

· U C ·

UNIVERSIDADE DE COIMBRA

Therapeutic potential of retinoic acid-loaded nanoparticles for brain repair

---

Potencial terapêutico de nanopartículas com ácido retinóico encapsulado para reparação cerebral

UNIVERSIDADE DE COIMBRA

Tiago Alexandre Ramos Teixeira de Sousa Santos, MSc

Faculdade de Ciências e Tecnologia

Departamento de Ciências da Vida

Universidade de Coimbra

Coimbra, Setembro de 2015

Cover: Subventricular zone cells labeled for beta-III tubulin (neuronal marker, red) and glial fibrillary acidic protein (astrocytic marker, green). Cell nuclei are stained with Hoechst 33342 (blue).

PUBLICATIONS

The results presented in this Doctoral Thesis resulted in several publications, namely one research article concerning Chapter 3, and another research article currently being prepared for submission concerning the results described in Chapter 4:

Santos, T., Ferreira, R., Maia, J., Agasse, F., Xapelli, S., Cortes, L., Bragança, J., Malva, J. O., Ferreira, L. and Bernardino, L. (2012). "Polymeric Nanoparticles to Control the Differentiation of Neural Stem Cells in the Subventricular Zone of the Brain." *ACS Nano* 6(12): 10463-10474. (Chapter 3)

Santos, T., Ferreira, R., Quartin, E., Boto, C., Saraiva, C. M., Cristóvão A.C., Bragança, J., Ferreira, L., Bernardino, L. " Enhanced Neuronal Differentiation of Neural Stem Cells by Blue Light-Responsive Retinoic Acid-Loaded Polymeric Nanoparticles" (Chapter 4)

In addition, two review articles in international peer-reviewed journals were published or submitted:

Santos, T., Maia, J., Agasse, F., Xapelli, S., Ferreira, L. and Bernardino, L. (2012). "Nanomedicine Boosts Neurogenesis: New Strategies for Brain Repair." *Integr Biol* 4(9): 973-981.

Santos, T., Boto, C., Saraiva, C. M., Bernardino, L. and Ferreira, L. (2015). "Nanomedicine approaches to modulate stem cells in brain repair" *Trends Biotechnol.* (Submitted)

ACKNOWLEDGEMENTS

I would like to express my acknowledgements in my native language

O meu agradecimento sentido e profundo a todos que me ajudaram a tornar não só um melhor investigador mas também uma melhor pessoa. A todos os mentores, colaboradores, colegas, amigos e familiares que fizeram parte deste meu percurso e que espero que continuem a fazê-lo no futuro!!!

Quero ainda assim destacar especialmente o meu agradecimento à Doutora Liliana Bernardino, minha orientadora científica e já amiga de longa data, por me ter recebido como o seu aluno de Doutoramento *impecável*!!! Agradeço também à minha co-orientadora Doutora Emília Duarte e ao colaborador Doutor Lino Ferreira que possibilitou o desenvolvimento deste trabalho.

Destaco ainda os meus pais, por serem o meu exemplo de vida e pelo vosso amor incondicional. Faço o meu melhor não só por mim, mas também para deixar-vos orgulhosos! Agradeço também aos meus irmãos, meus grandes *sócios* na vida.

Por fim, quero agradecer à Raquel, minha namorada e companheira que sempre me apoiou activa e incansavelmente. Obrigado por estares sempre *à minha beira*!

O meu sincero obrigado!!!

Tiago

iv

INDEX

ABBREVIATIONS AND ACRONYMS

8-oxo-dG	8-oxo-7,8-dihydro-2-deoxyguanosine
AD	Alzheimer's disease
BBB	Blood-brain barrier
BDNF	Brain-derived neurotrophic factor
bHLH	Basic helix-loop-helix
BMP-4	Bone morphogenetic protein 4
CSF	Cerebrospinal fluid
DA	Dopamine
DCFDA	2',7'-dichlorodihydrofluorescein diacetate
DCX	Doublecortin
DG	Dentate gyrus
Dlx2	Distal-less homeobox 2
DMNC	4,5-dimethoxy-2-nitrobenzyl chloroformate
DMSO	Dimethyl sulfoxide
DS	Dextran sulphate
Dvl2	Dishevelled 2
ECM	Extracellular matrix
EGF	Endothelial growth factor
EPO	Erythropoietin
Erk	Extracellular signal-regulated kinase
ESC	Embryonic stem cells
FGF-2	Fibroblast growth factor-2
FITC	Fluorescein isothiocyanate
GAPDH	Glyceraldehyde 3-phosphate dehydrogenase
GCL	Granule cell layer
GFAP	Glial fibrillary acidic protein

GTF	General transcription factors
HAT	Histone acetyl transferase
HD	Huntington's disease
HDAC	Histone deacetylase
Hes	Hairy and enhancer of split
HGF	Hepatocyte growth factor
i.c.v.	Intracerebroventricular
i.v.	Intravenous
JNK	c-Jun N-terminal
LIF	Leukemia inhibitory factor
LTD	Long-term depression
LR-NP	Retinoic acid-loaded light-responsive nanoparticles
LTP	Long-term potentiation
LV	Lateral ventricle
MAPK	Mitogen-activated protein kinases
Mash1	Achaete-scute complex homolog-like 1, Ascl1
MCAO	Middle cerebral artery occlusion
mDNA	Mitochondrial deoxyribonucleic acid
miRNA	Micro ribonucleic acid
mRNA	Messenger ribonucleic acid
mROS	Mitochondrial reactive oxygen species
Ngn	Neurogenin
NIR	Near-infrared
NO	Nitric oxide
Nox	Nicotinamide adenine dinucleotide phosphate oxidase
NP	Nanoparticles
NRX	Nucleoredoxin
NSC	Neural stem cells
OB	Olfactory bulb

Oct-4	Octamer-binding transcription factor 4
Olig2	Oligodendrocyte transcription factor 2
PBS	Phosphate-buffered saline
PD	Parkinson's disease
PEG	Polyethylene glycol
PEI	Polyethyleneimine
P-JNK	Phospho-c-Jun N-terminal
PSA-NCAM	Polysialylated neural cell adhesion molecule
qChIP	Quantitative chromatin immunoprecipitation
qRT-PCR	Quantitative real-time polymerase chain reaction
RA	Retinoic acid
Rac1	Rho family, small GTP binding protein Rac1
RA-NP	Retinoic acid-loaded nanoparticles
RAR	Retinoic acid receptor
RARE	Retinoic acid-response element
RMS	Rostral migratory stream
ROS	Reactive oxygen species
RT	Room temperature
RXR	Retinoid X receptor
SCCI	Single cell calcium imaging
SDF-1α	Stromal cell-derived factor-1 alpha
SFM	Serum-free media
SGZ	Subgranular zone
siRNA	small interfering ribonucleic acid
Sox2	Sex determining region Y-box 2
STAT3	Signal transducer and activator of transcription 3
SVZ	Subventricular zone
TNF-α	Tumour necrosis factor alpha
UV	Ultraviolet

VEGF	Vascular endothelial growth factor
VPA	Valproic acid
βIII-tubulin	Neuron-specific class III beta-tubulin

ABSTRACT

The subventricular zone (SVZ) and the hippocampal subgranular zone (SGZ) comprise two main germinal niches in the adult mammalian brain. Within these regions there are self-renewing and multipotent neural stem cells (NSC) which can ultimately give rise to new neurons, astrocytes and oligodendrocytes. Understanding how to efficiently trigger NSC differentiation is crucial to devise new cellular therapies aimed at repairing the damaged brain. A vast array of proteins and molecules have been described to modulate NSC fate and tested in innovative therapeutic applications, however with little success so far. Of note, retinoic acid (RA) is a potent differentiating factor critical for both developing and adult neurogenesis. Unfortunately, concerns related to solubility, stability, concentration or spatial and temporal positioning can hinder its desirable effects. The use of biomaterials emerges as the ideal support to overcome these limitations and consequently boost NSC differentiation. Therefore, the aim of this thesis was to develop a safer and more efficient therapeutic platform based on RA-loaded nanoparticles to induce neurogenesis from the resident NSC present in the adult brain.

In Chapter 3 we reported the use of RA-loaded polymeric nanoparticles as a potent tool to induce the neuronal differentiation of SVZ cells. Intracellular delivery of RA by nanoparticles activated RA receptors, decreased stemness and increased proneurogenic gene expression. Importantly, this work reported for the first time a nanoparticle formulation able to modulate the SVZ neurogenic niche *in vivo*. We further compared the dynamics of the initial stages of differentiation between SVZ cells treated with RA-loaded polymeric nanoparticles and solubilized RA. However, the balance between biomaterials and differentiating factors must be well established, since bioaccumulation in off-target areas and the uncontrolled release can generate undesired side-effects. For that reason, we further optimized our formulation to be remotely controllable. Accordingly, in Chapter 4 we developed a light-responsive nanoparticle formulation to control the release of RA while delivering it intracellularly with spatial and temporal precision. The stimulus used to trigger RA release from nanoparticles was light (405

nm laser), which demonstrated neurogenic capabilities by itself by activating β-catenin through the transient induction of mitochondrial- and NADPH oxidase-mediated reactive oxygen species (ROS). This cellular response to light culminated in the upregulation of RA receptor alpha (RARα), resulting in enhanced RA-induced neurogenesis. In conclusion, this combinatory therapy induces an amplified neurogenic effect, offering great advantages to potentiate neuronal differentiation of NSC while allowing a temporal and spatial remote control of RA release.

The nanoparticle formulations herein developed may ultimately offer new perspectives for brain regenerative strategies, focused in the modulation of endogenous NSC found in the adult brain. The protection of RA from degradation, intracellular delivery and spatial and temporal precision gathered by RA-loaded nanoparticles may be the grounds for the development of an innovative therapy for brain regeneration against injury and degeneration.

Resumo

As zonas subventricular (SVZ) e subgranular do hipocampo (SGZ) constituem os dois principais nichos neurogénicos no cérebro do mamífero adulto. Nestas regiões, existem células estaminais dotadas de multipotência e auto-renovação, e que podem originar novos neurónios, astrócitos e oligodendrócitos. A compreensão dos mecanismos de diferenciação neuronal é crucial para o desenvolvimento de novas terapias celulares dirigidas à reparação do cérebro lesionado. Para este propósito, têm sido descritas e testadas várias proteínas e moléculas promissoras, embora com pouco sucesso. O ácido retinóico (RA) é um destes agentes pro-neurogénicos que se tem destacado por potenciar a neurogénese durante o desenvolvimento e na idade adulta. Infelizmente, parâmetros tais como a solubilidade, estabilidade e concentração ou posicionamento espácio-temporal comprometem o seu potencial terapêutico. A utilização de biomateriais surge assim como o suporte ideal para contornar estas limitações e consequentemente potenciar a diferenciação neuronal. Assim, o objectivo principal desta tese foi desenvolver uma plataforma mais segura e eficaz baseada na aplicação de nanopartículas com RA encapsulado para impulsionar o processo neurogénico em células estaminais neurais no cérebro adulto.

No Capítulo 3, reportamos a utilização de nanopartículas com RA encapsulado como uma ferramenta com potencial de induzir diferenciação neuronal de células da SVZ. A entrega intracelular de RA através de nanopartículas levou à ativação de recetores de RA, diminuiu a capacidade estaminal e aumentou a expressão de genes pró-neurogénicos. É de salientar que este trabalho demonstrou a capacidade destas mesmas nanopartículas modularem o nicho neurogénico da SVZ *in vivo*. Adicionalmente, comparamos a dinâmica da expressão genética das fases iniciais de diferenciação induzida pelas nanopartículas com RA encapsulado ou por RA solubilizado. No entanto, a bioacumulação em áreas do organismo que não as pretendidas e a libertação contínua destes agentes podem induzir efeitos secundários indesejados. Neste sentido, otimizamos a formulação previamente descrita no Capítulo 3 de forma a ser controlada remotamente. Assim, no Capítulo 4 desenvolvemos uma formulação que é sensível à luz

permitindo a libertação intracelular de RA com precisão espácio-temporal. O estímulo utilizado para desencadear a libertação de RA foi luz com comprimento de onda de 405 nm. O estímulo com luz promoveu o aumento transiente de espécies reativas de oxigénio (ROS) mediadas pela NADPH oxidase e presentes na mitocôndria culminando com a ativação da β-catenina e aumento de diferenciação neuronal. Esta resposta celular à luz aumentou ainda os níveis de expressão do receptor RA-alfa (RARα), resultando num aumento de neurogénese induzida por RA.

Em suma, as formulações de nanopartículas desenvolvidas no curso deste trabalho oferecem novas perspetivas para o desenvolvimento de estratégias de regeneração cerebral, com o enfoque na modulação das fontes endógenas de NSC no cérebro adulto. A proteção do RA contra a degradação, a entrega intracelular e precisão espácio-temporais mediados por nanopartículas com RA encapsulado podem ser os fundamentos para o desenvolvimento de uma terapia inovadora para a regeneração do cérebro contra lesões e degeneração.

PALAVRAS-CHAVE: Ácido retinoico, células estaminais, diferenciação celular, nanopartículas, reparação cerebral

CHAPTER 1

Introduction

1.1 - NEURAL STEM CELL NICHES

The classical view of adult mammalian brain presented it as an immutable organ, incapable of generating new neurons. However, in the past decades, exciting data revealed that multipotent and self-renewing neural stem cells (NSC) with the ability to differentiate into neurons, astrocytes, and oligodendrocytes existed in defined neurogenic niches (Reznikov 1991; Luskin 1993; Alvarez-Buylla *et al.* 1998; Sanai *et al.* 2004). Thus, the persistence of these germinal regions through life further reinforces the idea that new neurons may be used to restore dysfunctional circuitries. Therefore, the modulation of endogenous neurogenesis raises many expectations for the treatment of several brain disorders such as neurodegenerative diseases, stroke, head trauma, among others.

In rodents, neurogenesis is primarily confined to two germinal niches, the subventricular zone (SVZ) located between the lateral ventricles and the parenchyma of the striatum and the subgranular zone (SGZ) of the hippocampus and (Lim *et al.* 2014). Outside these two regions, neurogenesis is limited, being the SVZ the largest germinal center in the adult brain. This region contains slowly dividing radial astrocyte-like NSC that express phenotypic markers of immaturity such as nestin and sex determining region Y-box 2 (Sox2). These cells are known as type B cells and represent a small subset of the total astrocytic population in the SVZ. Type B cells hold stem cell properties, a feature that discriminates this astrocytic subtype from mature, differentiated astrocytes (Doetsch *et al.* 1999a). In fact, in opposition to multiciliated ependymal cells (E cells) that line the lateral walls of the ventricle, B cells possess a single short cilium that is in direct contact with the cerebrospinal fluid (CSF). Hence, these cells are responsive to external cues from both ventricle lumen (*via* CSF) and blood vessels. Neural stem cells (type B) give rise to actively proliferating type C cells, which in turn generate immature neuroblasts (type A cells) (Morshead *et al.* 1994). Neuroblasts, as well as clusters of rapidly dividing type C cells, are surrounded by processes of type B cells (Doetsch *et al.* 1997). In the anterior and dorsal SVZ, chains of neuroblasts condense to form the rostral migratory stream (RMS) (Lois *et al.* 1996; Lledo *et al.* 2006). Therefore, neuroblasts migrate through the RMS towards the olfactory bulb along tubular structures formed by specialized astrocytes. After

reaching the olfactory bulb, neuroblasts integrate the cortical layers, mainly as new GABAergic granule- and GABAergic or dopaminergic periglomerular-interneurons (Lledo *et al.* 2006; Ming *et al.* 2011a). These SVZ-derived newly-born neurons contribute to olfactory discrimination and memory (Chambers *et al.* 2004). Figure 1.1a represents the SVZ cytoarchitecture as well as a representative digital image of neuroblasts (doublecortin-positive) present in both the dorsal SVZ and RMS (Figure 1.1b).

The SGZ is located in the dentate gyrus, between the hippocampal molecular layer and the hilus, and contains radial (known as type I or B cells) and nonradial glia-like (type II or D) cells that are tightly associated with blood vessels to form *foci* of proliferating cells (Palmer *et al.* 2000). Similarly to their subventricular counterparts (type B), SGZ astrocytes seem to operate as NSC and give rise to transiently amplifying progenitors that, in turn, generate neuroblasts (type III or G cells).
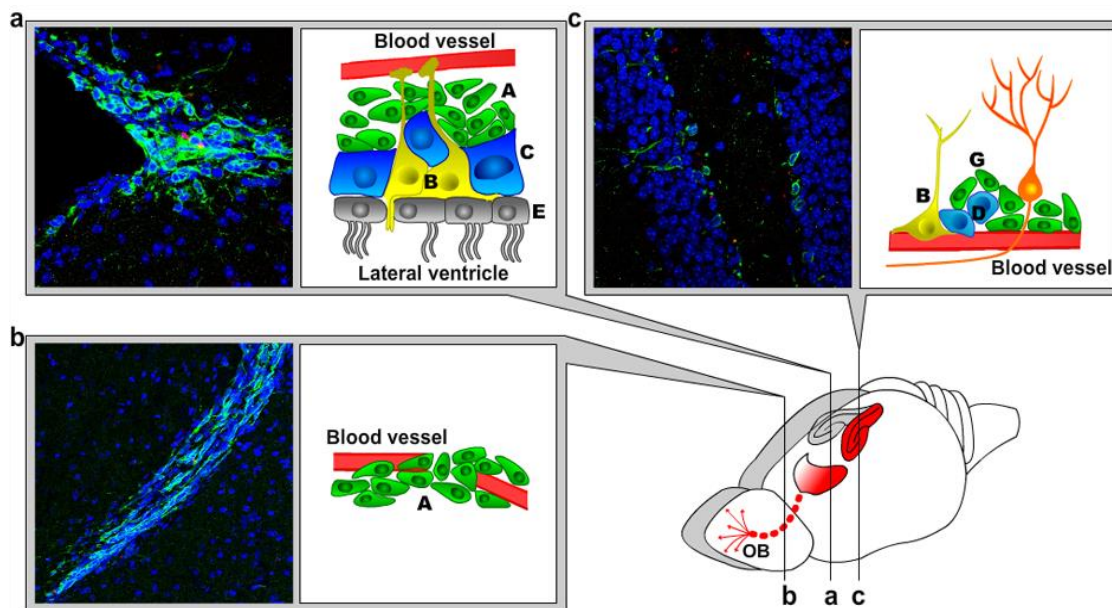
Figure 1.1 - Neurogenesis in the adult rodent brain. (a) Schematic representation of the cytoarchitecture of the subventricular zone (SVZ) stem cell niche. Neural stem cells (type B cells) proliferate and give rise to transit amplifying progenitors (type C cells) that differentiate into neuroblasts (type A cells). Neuroblasts then migrate long distances through the rostral migratory stream (RMS; b) towards the olfactory bulb (OB), where they fully differentiate into GABAergic or dopaminergic interneurons. (c) In parallel, neural stem cells (type B or type I cells) present in the subgranular layer of the hippocampus, give rise to type D (or type II) progenitors that initially differentiate into new neurons (type G or type III cells) that migrate short distances into the granular cell layer, where they ultimately differentiate into mature granular neurons. Newly born neurons present in both the SVZ (a), RMS (b) and SGZ (c) were labeled with doublecortin (green). Hoechst staining (blue) labels cell nuclei. From Santos *et al.* 2012b.

Unlike SVZ, the progeny of SGZ astrocytes does not migrate a long distance before maturation. Instead, differentiating SGZ neuroblasts migrate locally to the granule cell layer (GCL) where they spread dendrites and project axons towards CA3 to form new granule neurons (Seri *et al.* 2004). These new neurons extend their dendrites deeper into the molecular layers as they differentiate and become involved in processes of learning and memory (Shors *et al.* 2001; Schmidt-Hieber *et al.* 2004; Tashiro *et al.* 2006). Figure 1.1c illustrates the SGZ structure and includes a representative digital image of newborn neurons (stained with doublecortin; green) present in the dentate gyrus (DG) of the adult rodent brain hippocampus.

SVZ and SGZ type B cells share multiple characteristics with astrocytes. These cells express the intermediate filament component glial fibrillary acidic protein (GFAP), a typical marker of mature astrocytes and, structurally, they display bundles of intermediate filaments and gap junction complexes (Doetsch *et al.* 1999a; Seri *et al.* 2001). The physical and chemical contact with blood vessels allows the maintenance of an undifferentiated stem cell state (Shen *et al.* 2004; Shen *et al.* 2008; Tavazoie *et al.* 2008). Additionally, in response to injury, NSC proliferate, migrate towards the injured site and differentiate into new neurons. Due to these unique characteristics, NSC were considered to be an inexhaustible source of new neurons that can be recruited to promote brain repair in a context of neurodegeneration. Nevertheless, this endogenous regenerative program is inefficient and only a few NSC-derived newly born neurons are able to survive under the injured environment (Santos *et al.* 2012a). For that reason, the study of molecular cues able to promote survival, proliferation, differentiation, or migration is crucial. The *in vitro* study of NSC is possible through the neurosphere assay (Figure 1.2). This assay consists of growing isolated NSC in serum-free medium (SFM) containing mitogenic growth factors in a nonadhesive substrate. However, *in vitro* expansion of NSC artificially selects clones with proliferative and self-renewal properties. This is caused by the presence of growth factors namely endothelial growth factor (EGF) and fibroblast growth factor-2 (FGF-2). EGF-responsive cells include type C cells and a small subset of activated type B cells. Type C cells represent about 70% of neurosphere-forming cells isolated from SVZ (Doetsch *et al.* 2002). Thus, neurospheres do not fully represent the stem cell population present *in vivo*. Moreover, the higher number of passages neurospheres are subjected to, the

more biological properties are changed. In fact, it was reported that 67% of adult NSC genes are lost in C17.2 NSC cell line-derived neurospheres and 29% of C17.2-derived neurosphere genes are not present in adult NSC (Parker *et al.* 2005). Although its limitations, the neurosphere assay is still considered a reliable tool to expand stem/progenitor cells for use in basic research or replacement therapies (Gil-Perotín *et al.* 2013) (Figure 1.2).
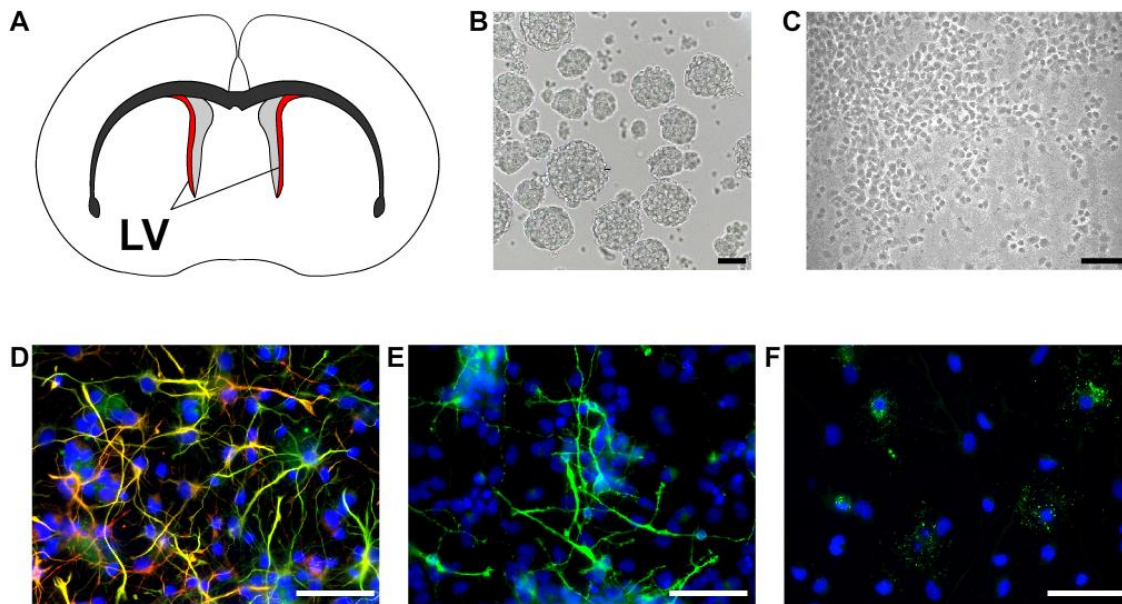
Figure 1.2 - Neural stem cells present in the subventricular zone can give rise to neurons, astrocytes and oligodendrocytes. *In vitro*, the stem/progenitor cells dissected from the subventricular region (SVZ- in red; A), constantly proliferate in serum-free medium under the continuous presence of growth factors, originating free floating spherical neurospheres (B). (C) Removal of growth factors and adherence onto a matrix such as poly-lysine induces differentiation and migration at the border of neurospheres to form a pseudomonolayer of cells. Nestin (green; D) immature SVZ cells co-expressing or not GFAP (red; D) can give rise to astrocytes, neurons (immunoreactive to doublecortin - in green; E) and oligodendrocytes (immunoreactive to oligodendrocyte marker O4 - in green; F). Hoechst staining (blue) labels cell nuclei. Scale bar is 50 μm; LV, lateral ventricles. From Santos *et al.* 2012b.

In 1998 a landmark paper by Eriksson et al. unequivocally demonstrated that neurogenesis was also occurring in the adult human brain, particularly in the SGZ. In fact, the same study also reported the presence of proliferating cells with a morphology similar to rat neural progenitor cells in the SVZ (Eriksson *et al.* 1998). The human SGZ niche cytoarchitecture is similar to the rodent one. However, conservation of structure across species

does not imply identical function or proliferation ratios. In rodents, proliferation is high in both the SVZ and SGZ, while in humans proliferation is prominent in the SVZ but limited in the SGZ (Curtis *et al.* 2012). On the other hand, SVZ cytoarchitecture in the adult human brain is distinguishable from the rodent one. SVZ astrocytes (GFAP-positive) do not contact directly with ependymal cells, instead, there is a gap devoid of cells that separate these two. However, these astrocytes present NSC features *in vitro*, with some astrocytes exhibiting *in vivo* a long process that contacts the ventricular surface, a characteristic similar to rodent type B cells (Sanai *et al.* 2004; Quiñones-Hinojosa *et al.* 2006). Regarding cellular phenotypic distribution, the human SVZ exhibits less neuroblasts than the rodent brain, demonstrating a ratio of type B : C : A cells of 3 : 1 : 1 in human compared to 2 : 1 : 3 in rodent (Doetsch *et al.* 1997; Curtis *et al.* 2005). Additionally, thus far there is no consensus regarding the existence of an adult human RMS. A ventral extension of the lateral ventricle presenting DCX- and GFAP-positive cells, resembling the RMS, was described during the second trimester of gestation. However, in this period no neuroblast chain-like structures were detected in the olfactory bulb, indicating that migration might occur to other destination (Guerrero-Cazares *et al.* 2011). In fact, new neurons generated from SVZ were found to migrate not only to the olfactory bulb but also to the prefrontal cortex in children up to 18 months old (Sanai *et al.* 2011). After birth, it has been described that SVZ proliferation and migration tends to decrease, with no detectable RMS during adulthood (Quiñones-Hinojosa *et al.* 2006; Sanai *et al.* 2011). Moreover, new neurons were also described to migrate and incorporate the adjacent striatum in the adult brain (Ernst *et al.* 2014). Conversely, a migratory chain of early progenitor cells (CD133-positive), proliferating cells (PCNA-positive), astrocytes and type B cells (GFAP-positive) and migrating neuroblasts (polysialylated neural cell adhesion molecule (PSA-NCAM)-positive) was detected in a unpredictably organized fashion around a lateral ventricular extension in a path resembling rodent RMS but rotated 75 degrees (Curtis *et al.* 2007; Kam *et al.* 2009). The displacement of human RMS compared to rodent is explained by the overdeveloped human frontal lobe, pushing the olfactory tract more caudally (Kam *et al.* 2009). Nevertheless, assuming that the ventriculo-olfactory system is endowed with progenitor cells and that it covers a greater brain extention than the SGZ, the SVZ niche comprises a broader potential for brain repair therapies.

1.1.1 - CONTACT AND SOLUBLE FACTORS THAT MEDIATE NEURAL STEM CELL DIFFERENTIATION

The differentiation of NSC progeny is regulated by diffusible signals and contact with neighboring cells and extracellular matrix (ECM) components (Ming *et al.* 2011b; Watt *et al.* 2013). A profound knowledge of the cellular and molecular mechanisms driving/inhibiting differentiation in the neurogenic niches is crucial to identify molecules that can be used for brain therapy. For instance, astrocytes from the SGZ and SVZ, the so-called "niche astrocytes" secrete factors supporting the emergence of neurons from stem/progenitor cells. The astrocyte-derived Neurogenesin-1 binds to the bone morphogenetic protein 4 (BMP-4), blocking its pro-gliogenic effect on hippocampal progenitors (Ueki *et al.* 2003). Moreover, astrocytes from both the SGZ and SVZ release sonic hedgehog that, in turn, induces proliferation and instructs progenitor cells to differentiate into neurons (Jiao *et al.* 2008a). On the other hand, astrocytes from non-neurogenic areas such as the adult neocortex secrete ephrin-A2 and -A3 that bind to EphA7 receptors and limit endogenous neural progenitor cell proliferation (Jiao *et al.* 2008b) (Figure 1.3).

One of the most studied and complex family of soluble factors belong to the Wnt pathway. The Wnt family includes 19 secreted glycolipoproteins able to bind to different receptors and trigger different cellular responses. These responses are divided into canonical (β-catenin-dependent) and non-canonical (β-catenin-independent) Wnt signaling pathways. Such processes include neural induction and patterning of the developing brain, cell proliferation, fate specification, polarization and migration, axon guidance, synaptogenesis, neuronal maintenance and regeneration and most importantly adult neurogenesis (reviewed by (Niehrs 2012)). Importantly, both canonical and non-canonical pathways are required for neuronal differentiation in adult neural stem cells. Lentiviral expression of a dominant-negative form of Canonical Wnt1 in the dentate gyrus is capable of decreasing neurogenesis in an expression level-dependent way. Rats with strongly reduced levels of neurogenesis revealed impaired long-term retention of spatial and object recognition memory. On the other hand, social transmission of food preference behavior was not altered, confirming that only

neurogenesis-dependent functions of the hippocampus are affected (Jessberger *et al.* 2009). Moreover, knockout of Wnt-7a was followed by a reduction in the number of SGZ newborn neurons and impaired mouse dendritic development in a canonical fashion (Qu *et al.* 2013). Similarly, the SVZ niche is also regulated by Wnt7a. Wnt7a is secreted by niche astrocytes (but not olfactory bulb astrocytes), and it is responsible for enhancing NSC self-renewal and proliferation through a non-canonical mechanism (Moreno-Estelles *et al.* 2012). Therefore, Wnt7a displays a dual role by activating both canonical and non-canonical pathways depending on the neurogenic niches. The complexity exhibited by the Wnt pathway indicates a tight control of neurogenesis by these secreted factors.
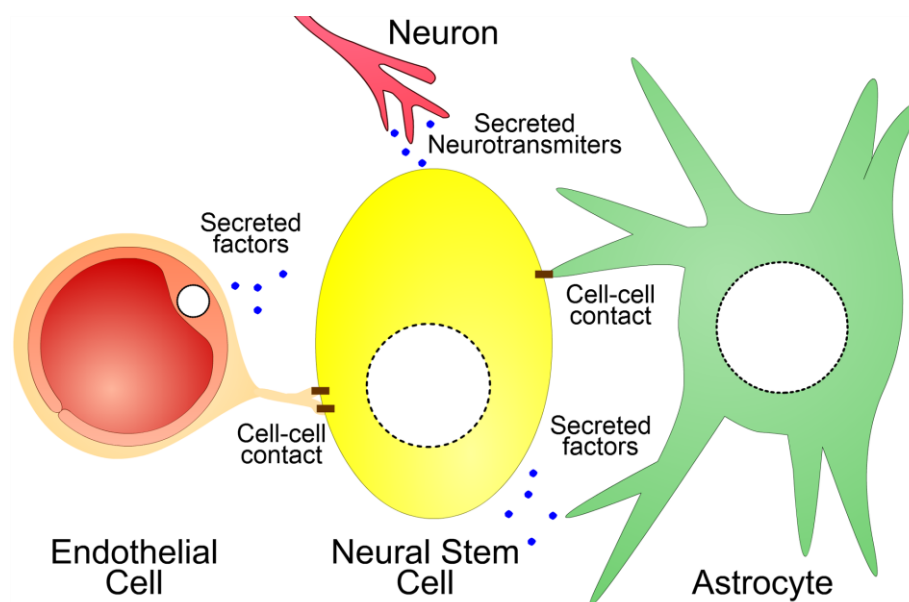
Figure 1.3 - Factors mediating neural stem cell differentiation. Astrocytes and basal lamina extensions (fractones) from endothelial cells can establish contact with neural stem cells and induce neuronal differentiation. Differentiation can also be induced by factors secreted by these cells plus neuron-derived neurotransmitters.

Similarly to astrocytes, endothelial cells of the brain vasculature are a source of factors that regulates neurogenesis (Shen *et al.* 2004). Endothelial cell-derived factors such as brain-derived neurotrophic factor (BDNF), angiopoietins and vascular endothelial growth factor (VEGF), mediate neuronal differentiation of progenitor cells in the SVZ and/or the SGZ (Jin *et al.* 2002; Lee *et al.* 2009; Liu *et al.* 2009; Rosa *et al.* 2010). Additionally, SVZ ependymal cells secrete

Noggin to antagonize BMP-4 favoring neuronal over glial fate (Lim *et al.* 2000). Finally, neurotransmitters and neuropeptides co-released from neuronal projections were shown to influence neurogenesis. Pharmacological studies and specific neuronal projection ablation point to a pro-neurogenic effect of both dopamine and serotonin in the SVZ (reviewed by (Young *et al.* 2011)) (Figure 1.3).

In addition to soluble factors, cell-to-cell contact was also shown to increase the neurogenic capacity of NSC. Contact-mediated neurogenesis in the SVZ niche was reported to involve Ephrin-B2, a membrane-bound protein found in astrocytes (Nomura *et al.* 2010). This process was later unveiled in the SGZ. Astrocytic Ephrin-B2 interacts with EphB4 receptor present in NSC and induces neurogenesis through β-catenin activation (Ashton *et al.* 2012). Astrocytes can also negatively regulate neurogenesis through the Notch pathway. Notch ligand, Jagged1, increases Notch signaling in neural stem cells, and inhibits neuronal differentiation (Wilhelmsson *et al.* 2012). Moreover, the basal lamina secreted by brain endothelial cells in the SVZ extends its projections to contact stem/progenitor cells (Mercier *et al.* 2002). These protruding structures, named fractones, are rich in laminin and N-sulfated heparan sulfates and capture FGF-2 to regulate neurogenesis in the SVZ (Kerever *et al.* 2007; Mercier *et al.* 2012) (Figure 1.3).

1.1.2 - MOLECULAR FEATURES REGULATING NEURAL STEM CELL IDENTITY

NSC differentiation and fate determination is not only established by extracellular cues (as mentioned previously), but also by intracellular events (e.g. DNA methylation, histone modifications, transcription factors, non-coding RNA) on several distinct signaling pathways (Mohamed Ariff *et al.* 2012). Different transcription factors, and their spatial and temporal action, result in different outcomes on the neurogenic process. Classic transcription factors involved in self-renewal and undifferentiated state of embryonic stem cells (ESC) are Sox2, octamer-binding transcription factor 4 (Oct-4) and Nanog (Takahashi *et al.* 2007). Noteworthy, the induced expression of these factors is capable of reversing the differentiated state of mature fibroblasts into induced pluripotent stem cells, presenting the same cardinal features as ESC (Suh *et al.* 2007). Sox2 is constitutively expressed in NSC, however, its downregulation

accompanies the process of differentiation. Thereby, Sox2 can be used as a marker for multipotent NSC able to self-renew and differentiate (Suh *et al.* 2007). In addition, Oct-4 is known to induce pluripotency not only in adult mouse cells (Kim *et al.* 2009c), but also in human NSC (Kim *et al.* 2009b). Most importantly, Oct-4 gene knockdown induces cell differentiation (Niwa *et al.* 2000; Zaehres *et al.* 2005). Accordingly, Nanog expression was shown to be required for the maintenance of NSC pluripotency (Mitsui *et al.* 2003; Kim *et al.* 2009b). These key regulators are involved in embryonic neurogenesis and maintain their functions throughout adulthood (Suh *et al.* 2009a).

Gene expression results from a tight cooperation between transcription factors and epigenetic modulators. Epigenetics refer to heritable changes in gene expression or cellular phenotype without altering the underlying DNA sequence (Ma *et al.* 2010). Epigenetic regulation may include covalent DNA methylation, non-coding RNA and histone modifications. DNA methylation strongly regulates NSC multipotency throughout development. During midgestation, NSC differentiate exclusively into neurons, even when exposed to astrocytogenic factors (e.g. ciliary neurotrophic factor) (Takizawa *et al.* 2001). This selective differentiation occurs because the astrocytic gene promoters are hypermethylated, and for that reason binding of signal transducer and activator of transcription 3 (STAT3)-complex to the glial fibrillary acidic protein (GFAP) sequence is hampered. At late gestation, astrocytic gene promoters become demethylated enabling both neuronal and glial differentiation (Qian *et al.* 2000).

Histone modifications are more complex and considered the most important epigenetic events during NSC differentiation. In order to compact the eukaryotic genome, DNA is wrapped around histones, forming the nucleosome. Condensed chromatin (heterochromatin) is associated with gene silencing whereas active loose euchromatin is required for transcriptionally active sites (Jenuwein *et al.* 2001). Two of the core histones (H3 and H4) have an N-terminal tail protruding from the nucleosome. This tail is subjected to post-translational modifications including acetylation, methylation, phosphorylation, ubiquitylation, sumoylation, glycosylation, and adenosine diphosphate ribosylation (Kouzarides 2007). Therefore, histone modifications on specific aminoacid residues play a key role in the regulation of gene transcription, by controling how genomic DNA is packaged, and therefore its access to

transcriptional machinery. Among all the histone modifications, acetylation and methylation of lysine (K) residues are the most intensely studied and decoded.

Histone acetylation is a mechanism involved in the control of adult neurogenesis especially in the differentiation of SVZ and SGZ NSC (Hsieh *et al.* 2004). Histone acetylation is mediated by two enzymes, histone acetyl transferase (HAT) and histone deacetylase (HDAC) (Hsieh *et al.* 2005). HAT catalyzes the acetylation of N-terminal lysine residues, hampering their positive charge and consequently reducing the interaction with the negatively charged DNA. This conformational change from heterochromatin to euchromatin facilitates gene expression. On the other hand, HDAC promotes the deacetylation of histones and consequently the condensation of chromatin to heterochromatin, impeding gene transcription (Hsieh *et al.* 2005). Importantly, Jawerka and colleagues have recently demonstrated that HDAC2 controls neurogenesis, possibly involving the suppression of Sox2 after NSC differentiation (Jawerka *et al.* 2010). Moreover, using a pharmacological approach with valproic acid (VPA), an inhibitor of HDAC, NSC differentiate into a neuronal phenotype. The increased neurogenesis and impaired gliogenesis is obtained due to NeuroD, a neurogenic transcription factor that becomes upregulated with the inhibition of HDAC (Hsieh *et al.* 2004). Using another HDAC inhibitor, sodium butyrate, NSC proliferation following cerebral ischemia is further increased in both SVZ and SGZ (Kim *et al.* 2009a). Noteworthy, oligodendrogenesis also relies on HDAC activity, since postnatal administration of VPA has been shown to delay the myelin-forming oligodendrogenesis (Marin-Husstege *et al.* 2002; Shen *et al.* 2005) (Figure 1.4).

Histone methylation is considered to be the most enduring histone modification. However, the recently confirmed existence of histone demethylases started questioning this idea. Histone methylation occurs when methyl groups are added to lysine (K) or arginine (R) residues of histone tails and are catalyzed by a family of conserved proteins, the histone methyltransferases (Wen *et al.* 2009). Unlike histone acetylation, histone methylation depends on the methylation site to induce or repress gene transcription. For example, histone H3 methylation at K9 and K27 along with histone H4 methylation at K59 results in gene-silent heterochromatin, whereas histone H3 methylation at K4, K36, and K79 is associated with transcription-active euchromatin (Yoo *et al.* 2006; Kouzarides 2007).

Recently, various studies focusing on lineage specification genes such as *Dlx2*, *Mash1*, *Ngn1*, *Olig2* and *Hes1*, revealed that a tight control of epigenetic activation and repression is required for cell lineage differentiation. *Dlx2* (distal-less homeobox 2) was shown to instruct neuronal differentiation and maintain proliferation of SVZ precursors (Brill *et al.* 2008; Suh *et al.* 2009b). *Mash1* (achaete-scute complex homolog-like 1, also known as *Ascl1*) is a key basic helix-loop-helix (bHLH) transcription factor essential during neurogenesis, being involved in the production and commitment of NSC while inhibiting their astrocytic potential (Ito *et al.* 2003; Kageyama *et al.* 2005). In addition to its role in neurogenesis, *Mash1* also plays a role in oligodendrocyte development (Kim *et al.* 2007; Jessberger *et al.* 2008). Accordingly, Jessberger and colleagues reported that induced over-expression of *Mash1* in hippocampal NSC, *in vivo*, redirected their fate from neurons to oligodendrocytes (Jessberger *et al.* 2008). *Ngn1* (Neurogenin1) is another bHLH transcription factor that was described to suppress astrocytic differentiation *in vitro* and *in vivo*, *via* the suppression of STAT3 target genes (Cai *et al.* 2000). *Ngn1* is expressed during the neurogenic period of neocortical development. Also, *Ngn1* is induced and essential for NSC neuronal differentiation (Sun *et al.* 2001). Moreover, Kim and collaborators have shown that *Ngn1* is able to commit pluripotent embryonal carcinoma P19 cells to adopt a neural cell phenotype. The authors have identified the epigenetic events on the *Ngn1* gene throughout the stages of differentiation. The first stage is repressive and it is characterized by the recruitment of H3K27-trimethylated(me3) on the *Ngn1* promoter region. The following stages include the association of H3K4me3 and the resultant *Ngn1* gene activation (Kim *et al.* 2004). *Olig2* (Oligodendrocyte transcription factor 2), also a bHLH transcription factor, is required for oligodendrocyte and motor neuron specification in the spinal cord (Takebayashi *et al.* 2002). However, the sustained expression of *Olig2* in motoneuron progenitors prevents their terminal differentiation by inhibiting *Ngn2* (Neurogenin2) (Lee *et al.* 2005). Moreover, constitutive overexpression of *Olig2* in human NSC promotes oligodendrocytic differentiation (Maire *et al.* 2009) (Figure 1.4). Functions of the above mentioned transcription factors are downregulated by another set of factors, *Hes1* and *Hes5* (Kageyama *et al.* 2008). Hes1 and Hes5 are bHLH transcription factors, but they have a distinct DNA-binding site resulting in transcriptional repression (Kageyama *et al.* 2015).
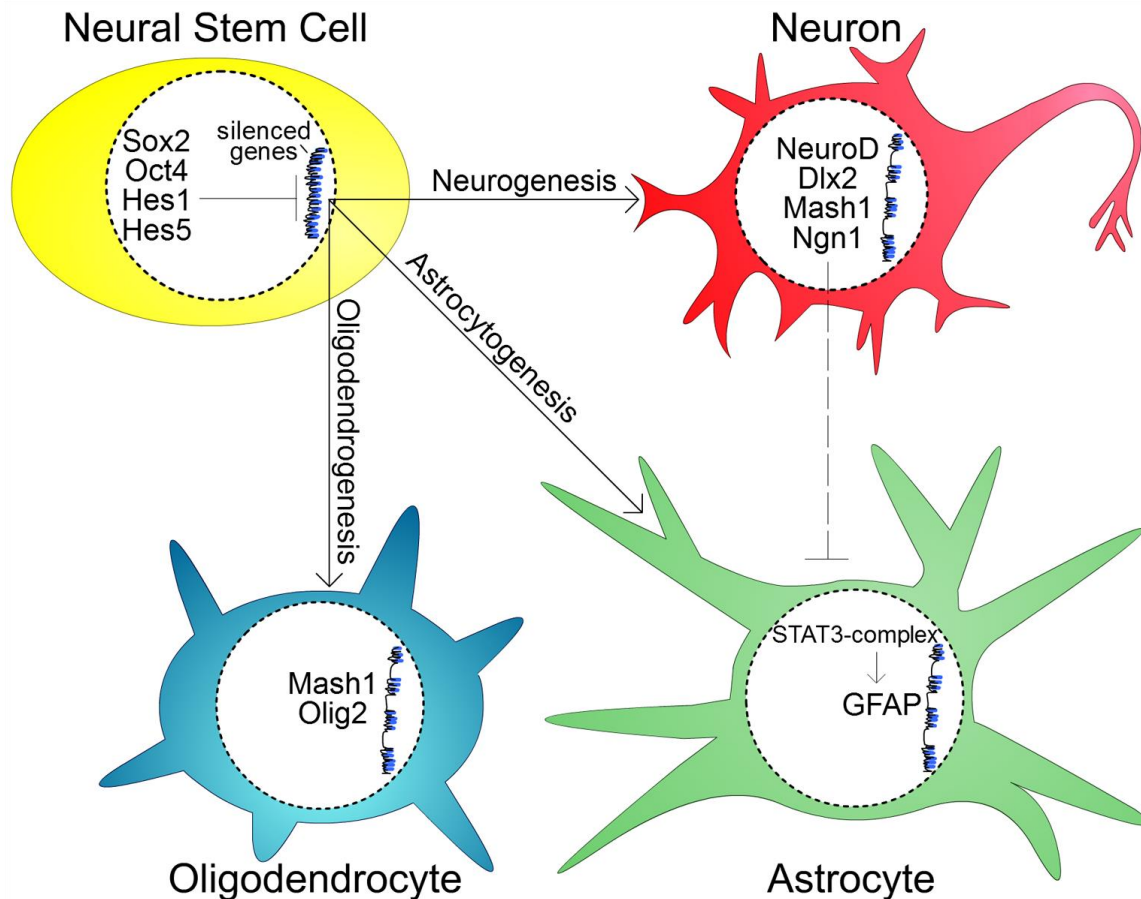
Figure 1.4 - Epigenetic alterations define neural stem-cell identity. The presence of condensed chromatin at several genes on neural stem cells impedes differentiation and favors the immature stem cell state. When stem cells are exposed to differentiating factors, histone modification and chromatin remodeling promotes gene transcription. The main genes involved in the maintenance of multipotency and in the processes of neurogenesis, astrocytogenesis and oligodendrogenesis by neural stem cells are depicted. Neurogenic genes such as Mash1 and Ngn1 are also capable of repressing astrocytogenesis.

The most recently discovered small non-coding RNA (small interfering RNA (siRNA), microRNA (miRNA) and piwi-interacting RNA (piRNA)) are known to affect gene regulation (He *et al.* 2004). The role of miRNA has been extensively studied in NSC differentiation. miRNA is generally characterized by a single strand RNA composed of 20-25 nucleotides that can bind to the 3' or 5' untranslated region of mRNA (Lytle *et al.* 2007). This binding causes the formation of a tight complex that represses translation (Rana 2007). Among other actions, the overexpression of miR-9 and miR-124, two predominantly neural miRNA expressed by SVZ cells, promotes neuronal differentiation (Akerblom *et al.* 2012). miR-124 downregulates several target genes, among them the Notch ligand Jagged1, the astrocytic transcription factor

Sox9, and the enzyme histone H3 Lys-27 histone methyltransferase, Ezh2 (Neo *et al.* 2014). miR-9 targets members of the *Hes* (hairy and enhancer of split) gene family. When expressed, this family of genes inhibit differentiation by repressing pro-neural genes (Coolen *et al.* 2013). These miRs are complex and target various transcription factors, but both result in the inhibition of STAT3-complex activation. This complex, as mentioned previously, is responsible for the expression of GFAP and astrocytogenesis. Different miRNA regulate neurogenesis in the SGZ. The most predominant are miR-184 and miR-137. The increment in their levels leads to an increase in NSC proliferation whereas lower levels results in neuronal and astrocytic differentiation (Mohamed Ariff *et al.* 2012) In this case, miR-184 binds to Mbd1, a protein that represses methylation-induced gene expression (Liu *et al.* 2010) while miR-137 reduces lysine 27 of histone H3 methylation *via* the inhibition of methyltransferases (Szulwach *et al.* 2010).

1.2 - REGULATION OF NEUROGENESIS IN BRAIN HEALTH AND DISEASE

Dementia conditions induced by AD, PD and stroke (among others), had an estimated global economic impact in 2010 of $604 billion US dollars. Additionally, the number of people with dementia is expected to double every 20 years, together with the global ageing of the population (Abbott 2011). An integrated approach to tackle such epidemia is needed, including preventive strategies to protect the evolution of dementia. Currently, there is no cure for AD or PD. But, the recovery of the injured areas by repopulation with new neurons and the stimulation of the reestablishment of neural circuitry will likely be part of the solution. Given that adult NSC have the potential to differentiate and migrate in response to brain damage, the disclosure of mechanisms and molecules involved in this process will contribute to the development of novel therapeutic strategies. SVZ is the most proliferative neurogenic niche and its neuroblasts naturally possess the ability to migrate long distances. Therefore, SVZ is the neurogenic niche of choice for the development of broad therapeutic strategies for brain repair. Though, the chemoattraction and disengagement of migration processes are yet to be fully understood. Cell replacement therapy will greatly benefit from the ability to control the mechanisms involved in

modulating the migration of neuroblasts. Changes that occur upon brain injury such as altered levels of growth factors, neurotransmitters, hormones, cytokines and chemokines, among other signaling molecules, may affect neurogenic regions. Remarkably, these alterations seem to work together with the objective of restoring brain integrity (Martino *et al.* 2011).

In the injured brain, NSC receive external cues from activated astrocytes and microglia as well as from the blood vessels surrounding their niches (Kernie *et al.* 2010). Some of these cues have already been described. For example, excitotoxicity-derived glutamate release is detrimental but, on the other hand, the same glutamate directly and indirectly (*via* production of neurotrophic factors) induces the proliferation and neuronal differentiation of NSC (Mattson 2008). In addition, inflammatory mediators released by immune cells, such as tumor necrosis factor alpha (TNF-α), nitric oxide (NO) and reactive oxygen species (ROS) also promote post-injury neurogenesis (Estrada *et al.* 2005; Bernardino *et al.* 2008; Carreira *et al.* 2010). However, a fine tuning of concentrations and temporal resolution is required, since an exacerbated or chronic inflammatory response can significantly reduce both proliferation and differentiation of NSC (Ekdahl *et al.* 2009).

Among these, ROS are particularly interesting since they are part of the normal NSC self-renewal, proliferation, differentiation and survival processes (Prozorovski *et al.* 2015). Endogenous sources of ROS are vital for the dynamic regulation of these processes. Human neurogenic niches are physiologically under a relatively hypoxic environment and this environment is responsible for supporting and maintaining NSC in their undifferentiated state (Mohyeldin *et al.* 2010). Moderate ROS levels are required for stem-cell differentiation and renewal, mainly *via* the activation of mitogen-activated protein kinases (MAPK) whereas high ROS levels lead to stem-cell exhaustion or apoptosis. On the other hand, decreased ROS levels impair stem cell function (Schieber *et al.* 2014). Increased mitochondrial ROS production is responsible for growth factor withdrawal-induced neurogenesis *in vitro* (Rharass *et al.* 2014). Hydrogen peroxide is considered the primary type of signaling ROS and acts mainly *via* the oxidation of proteins containing thiol groups (Sena *et al.* 2012). Accordingly, superoxide dismutase knockout mice, which have deficient superoxide conversion into hydrogen peroxide, present increased glial differentiation of SGZ cells (Huang *et al.* 2012a).

Stroke is the consequence of blood supply disruption to the brain, mainly caused by ischemia, hemorrhage or cardiac arrest. Importantly, cell proliferation in neurogenic niches is increased after ischemia and newly-generated neurons are found on areas external to the SVZ (Lin *et al.* 2015). In the SVZ niche, the number of type B GFAP-positive NSC that are in contact with the CSF via their apical processes were found to be increased 30 days after permanent middle cerebral artery occlusion (MCAO) in mice (Zhang *et al.* 2014a). This phenomenon further highlights the responsiveness of NSC to external cues and the potential of neurogenic regions present in the adult mammalian brain. Notably, migration towards ischemic regions continues for up to a year after stroke in rats (Thored *et al.* 2007). Neuroblasts that departed from SVZ were found differentiated into striatal neurons within the lesioned area (striatum) of rodent models of ischemia (Arvidsson *et al.* 2002). Noteworthy, this detour in migration also seems to depend on existing vasculature, just like in the RMS, indicating that post-injury angiogenesis is a critical requisite for brain repair (Thored *et al.* 2007). However, as a consequence of redirected neuroblasts, fewer cells reach the olfactory bulb (Kernie *et al.* 2010). Several factors were identified as responsible for neuroblast-detoured migration towards peri-infarct regions. In broad terms, these factors include matrix metalloproteases, chemokines and pro-angiogenic factors (Kernie *et al.* 2010). From the total number of neuroblasts that reach the lesioned region, only few of them survive, differentiate and/or integrate as new mature neurons. Though the reason for this failure is uncertain, studies point at inflammatory microenvironment as the limiting step (Arvidsson *et al.* 2002; Parent *et al.* 2002). In fact, the human SVZ of post-mortem ischemic patients has an increased overall cell proliferation that includes an increase in neuronal precursors (reactive for neuron-specific class III beta-tubulin (βIII-tubulin) and PSA-NCAM antibodies) (Marti-Fabregas *et al.* 2010). Additionally, proliferative neuroblasts (Ki67 and DCX double positive cells) are increased in the infarct core of stroke patients (Jin *et al.* 2006).

In a chronic condition such as Alzheimer's disease (AD), neurogenesis is also affected. AD is the most prevalent type of dementia characterized by synaptic and neuronal loss in areas as the entorhinal cortex, hippocampus and neocortex, which are essential areas for memory and other mental abilities. How neurogenesis is altered in AD is still a matter of debate. Jin and

colleagues reported the presence of proliferating (TUC-4-positive) neuroblasts by immunohistochemistry (DCX, PSA-NCAM, neurogenic differentiation 1 (NeuroD)) in both SGZ of dentate gyrus and in CA1 of hippocampus, the main region affected by AD pathology. Additionally, the presence of neuroblast markers was higher in AD patients *versus* control (Jin *et al.* 2004). Nevertheless, as also referred by the authors, this comparison was made by western blotting technique in separate membranes, where AD samples-loaded membrane had one single same-blot control which does not clearly demonstrate this assumption. Contrarily, neurogenesis does not seem to increase in young pre-senile AD patients. There was an increased proliferation (Ki67-positive) in AD hippocampus but it was not associated with neurogenesis (DCX-positive). It was rather reflecting a gliotic (GFAP-positive) and vascular (Von Willebrand factor (VWF)-positive) response (Boekhoorn *et al.* 2006). One possibility is that neurogenesis is only triggered after the pre-senile phase and that AD pathology initially affects both glial and vascular components. On the other hand, in Parkinson's disease (PD) neurogenesis seems to be decreased. PD is a neurodegenerative disorder characterized by the degeneration of dopamine (DA) neurons in the *substantia nigra pars compacta* (SNpc) leading to striatal DA depletion. Post-mortem brains of PD patients present reduced SVZ proliferation and decreased βIII-tubulin- and nestin-positive cells in the SGZ. Importantly, this decrease is more robust in PD patients with dementia (Hoglinger *et al.* 2004). In the same study, the authors suggest that the generation of neural precursor cells is impaired as a consequence of dopaminergic denervation, a hallmark of PD (Hoglinger *et al.* 2004). Accordingly, in non-demented patients treated with levodopa (the precursor of dopamine used to treat PD), SVZ proliferation was increased (O'Sullivan *et al.* 2011).

Overall, increased cell proliferation and neuronal differentiation following lesion strongly supports the existence of an endogenous mechanism for brain repair. However, these physiological processes are not as effective as they appear to be at a first glance. Actually, neurogenesis seems to be an unproductive process. Few new neurons that are able to successfully migrate and differentiate, survive for longer than a month (Lledo *et al.* 2006). It is likely that endogenous regenerative processes after brain injury are not sufficiently activated and/or inhibitory programs sufficiently activated. Therefore, it seems critical to clearly

understand the balance between pro and anti-neurogenic factors to design new efficient brain repair strategies.

1.3 - RETINOIC ACID

Retinoic acid (RA) is a metabolic product of retinol (vitamin A). Its name origin is derived from the retina, the region where the class of retinoids were first described in association to eye development (Wald 1968). RA plays an important role in the developing mammalian nervous system and it is essential for anteroposterior patterning and development of the spinal cord and hindbrain structures (Maden 2002). RA also regulates both neural development and plasticity, long-term potentiation (LTP) and long-term depression (LTD) (Chiang *et al.* 1998), neurite outgrowth (Corcoran *et al.* 1999), axon outgrowth (Maden 2007), and neuronal differentiation (Crandall *et al.* 2004; Sakai *et al.* 2004).

In the nucleus, retinoid signal is transduced by heterodimers formed between the retinoic acid receptors (RAR) and the retinoid X receptors (RXR), both members of the nuclear receptor superfamily (Kastner *et al.* 1997; Krezel *et al.* 1999). Each receptor consists of three isotypes (α, β and γ) encoded by separate genes (A, B and G). For each isotype, at least two isoforms are generated by differential promoter usage and alternative splicing (Gutierrez-Mazariegos *et al.* 2014). These receptors heterodimerize and bind to a DNA sequence called retinoic acid-response element (RARE), activating gene transcription upon ligand binding (Bastien *et al.* 2004) (Figure 1.5). The most abundant RAR isotypes are RARα and RARγ. In the entire human genome obtained from breast cancer cell line MCF-7, approximately 4,000 RARγ and more than 7,000 RARα binding sites were detected by chromatin immunoprecipitation. Noteworthy, more than 3,000 binding sites were shared by both receptors, indicating that RARα has more exclusive DNA binding sites than RARγ (Hua *et al.* 2009). Many genes have been reported to increase or decrease expression after RA signaling. These genes include metabolic enzymes, ionotropic receptors, transporters and signaling molecules, among others (reviewed by (Lane *et al.* 2005)) (Figure 1.5).
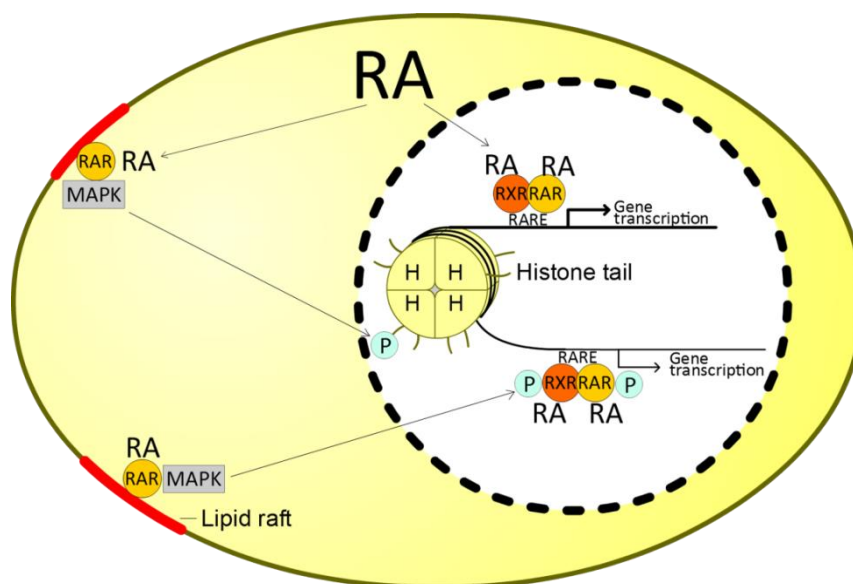
Figure 1.5 - Retinoic acid (RA) mechanisms of action. RA acts primarily *via* its nuclear receptors retinoic acid receptor (RAR) and retinoid X receptor (RXR). These receptors heterodimerize and bind to a specific DNA sequence called retinoic acid response element (RARE) activating gene transcription upon ligand binding. RAR is also present in membrane lipid rafts. Upon binding to RA, these receptors activate mitogen-activated protein kinases (MAPK). MAPK are recruited do the nucleus were they, among other actions, phosphorylate histone tails and RA receptors. Phosphorylation induces conformational changes that enable RA to activate the transcription of a distinct subset of genes.

Ligands can bind to both monomeric and dimeric receptors and each subunit can independently bind to its agonist. RAR is activated by *all-trans* retinoic acid and its 9-*cis* isomer, while RXR is only activated by 9-*cis* RA. Although RAR agonists can autonomously activate transcription through a RAR–RXR heterodimer, RXR is unable to respond to RXR-selective agonists in the absence of a RAR ligand *in vitro* (Gilardi *et al.* 2014; le Maire *et al.* 2014). This phenomenon is referred to as RXR subordination or silencing. The significance of this subordination is presumably to avoid interference between multiple RXR-partner signaling pathways. However, recent *in vivo* data is contradictory. RXRα homodimers were shown to regulate the transcription of inflammatory cytokines responsible for leukocyte recruitment by myeloid cells, unveiling a novel role for RXRα in the regulation of innate immunity (Núñez *et al.* 2010).

It was recently established that RAR also regulates non-nuclear and non-transcriptional effects, namely the activation of kinase cascades (Al Tanoury *et al.* 2013) (Figure 1.5). Accordingly, non-nuclear RARα was found in membrane lipid rafts (Piskunov *et al.* 2012). This pool of RA interacts with Gαq proteins or PI3K to activate the p38 or p42/p44 (Erk) MAPK pathways, respectively in a cell type-dependent fashion (Masiá *et al.* 2007; Piskunov *et al.* 2012). Once activated, these MAPK translocate to the nucleus, and phosphorylate nuclear factors, including histone tails and nuclear RAR (Bruck *et al.* 2009). Noteworthy, RARα1 phosphorylation by protein kinase A (PKA) was described to be required for RA-induced parietal endodermal differentiation of F9 mouse embryonal carcinoma cells (Rochette-Egly *et al.* 2000). Additionally, RA-induced neuronal differentiation of mouse embryonic stem cells requires nuclear RARγ2 phosphorylation. Phosphorylation controls the recruitment of RARγ2 to a small subset of gene promoters by binding an unusual RARE consisting of two direct repeats separated by seven base-pairs (Al Tanoury *et al.* 2014).

To activate gene expression, RA receptors have to compete with repressive heterochromatin structures to allow the recruitment of transcription machinery. In this regard, receptors bound to RARE are subjected to ligand-induced conformational changes that cause the dissociation of corepressors and the recruitment of coactivators. Upon association with larger complexes that involve chromatin-modifying and -remodeling activity, heterochromatin is uncondensed into euchromatin. Consequently, RNA polymerase II and general transcription factors (GTFs) are directed to the promoter to initiate gene transcription (Dilworth *et al.* 2001). It is also hypothesised that the non-nuclear kinase-dependent RA effect aids the recruitment of RAR to inaccessible RARE by phosphorylating histone tails. This process loosens chromatin and exposes new RARE binding sites (Piskunov *et al.* 2014). Additionally, nuclear RA action further increases histone modifications. Kashyap and colleagues reported extensive histone modifications in response to RA, such as H3K27me3, H3K4me3 and H3 acetylation (acH3) levels at the Hoxa cluster response (Kashyap *et al.* 2011).

The involvement of RA on adult neurogenesis is evident. Rats with Vitamin A deficiency show downregulated RAR expression, depression of LTP and severe defects in spatial learning and memory, suggesting that RA is required for the maintenance of memory mechanisms and

neuronal plasticity in the hippocampus (reviewed by (Maden 2007)). Moreover, depletion of RA in adult mice leads to decreased neuronal differentiation and cell survival within the SGZ (Jacobs *et al.* 2006). Similarly, administration of disulfiram (RA synthesis inhibitor) to neonatal mice decreased cell proliferation in the SVZ. Regarding the same study, the authors also demonstrated that electroporation of dominant-negative RARα and RXRα into the SVZ of mouse sagittal slice cultures blocked neuroblast migration to the olfactory bulb and altered the morphology of neuronal progenitors (Wang *et al.* 2005). Importantly, defective RA signaling has been implicated in the onset of brain diseases. In AD, co-administration of RAR and RXR agonists effectively reduced insoluble Aβ peptides and improved cognitive deficits in an animal model of the disease (Kawahara *et al.* 2014). In post-mortem brains of Parkinson's disease (PD) patients, retinaldehyde dehydrogenases (Raldh1/Aldh1a1) mRNA levels, a RA-synthesizing enzyme, were down-regulated in *substantia nigra* dopaminergic neurons (Anderson *et al.* 2011). Accordingly, RA was able to prevent dopaminergic neuronal death in a mouse model of PD (Esteves *et al.* 2015). Moreover, RA has also been shown to promote neurological functional recovery in rats subjected to stroke (Li *et al.* 2008). Retinyl palmitate, a derivate of RA, demonstrated neuroprotective effects in the mouse hippocampus following stroke (Shimada *et al.* 2013). One of the few studies that have examined the effects of RA in stroke-induced neurogenesis reported that RA-enriched diet further increases SVZ neurogenesis after transient MCAO in rats (Plane *et al.* 2008) (Figure 1.6).

However, RA-based therapies are unsettled, in a sense that this molecule is rapidly metabolized by cells, has poor water solubility and requires a defined range of concentrations to exert its positive effects (Szuts *et al.* 1991; McCaffery *et al.* 2006) posing difficulties in the delivery of therapeutic doses. Therefore, the use of nanoparticles (NP) is a powerful strategy to overcome these limitations by ensuring protection and intracellular delivery of RA.
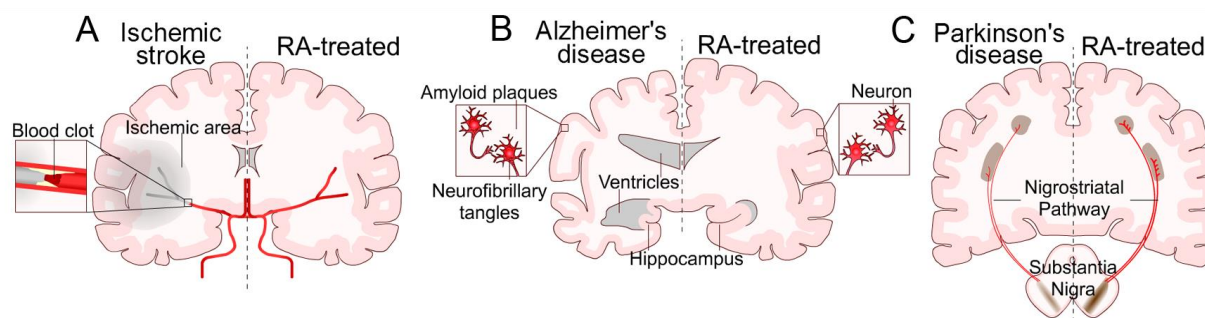
Figure 1.6 - Therapeutic potential of retinoic acid (RA). Scheme summarizing the regenerative effects of RA signaling in animal models of neurodegenerative diseases. . (A) RA promotes neurological functional recovery and neuroblast migration towards the ischemic area in ischemic stroke models. (B) RA protects against ventricular enlargement, shrinking of the hippocampus and accumulation of amyloid plaques and neurofibrillary tangles in Alzheimer's disease models. (C) RA protects against degeneration of dopaminergic neurons in the *substantia nigra* in Parkinson´s disease models Given its neuroprotective and neurogenic activities, RA-based therapies are a promising platform for brain regenaration.

1.4 - TYPES OF MICRO- AND NANOCARRIERS TO MODULATE THE ACTIVITY OF ENDOGENOUS NSC

The potential of stem cells to differentiate into almost any kind of cell type within their germinal layer, allied to their unlimited expansion ability, has opened up room for their use in regenerative medicine strategies. Nevertheless, until stem cell-based therapies can be considered as a reliable clinical strategy, several challenges will need to be overcome, such as the control over stem cell self-renewal, the control over differentiation into specific cell lineages, the *in vivo* delivery, and the integration into the host milieu (Hwang *et al.* 2008). Micro- and nanoparticles may be a platform to modulate the differentiation and activity of endogenous NSC and to manipulate and track exogenous NSC transplanted into the brain (Ferreira *et al.* 2008b; Ferreira 2009). Regardless of their composition, materials should display basic characteristics: high stability to protect the incorporated biomolecules, biodegradability to allow them to be removed or excreted after cargo delivery, and biocompatibility. These advanced materials may be engineered to incorporate multiple features providing simultaneous targeting and tracking capabilities in a single biomaterial (Ferreira *et al.* 2008a; Santos *et al.* 2012b; Srikanth *et al.* 2012). In addition, these materials might be conjugated with multiple

protein ligands to enable control over multivalent interactions (Conway *et al.* 2014). For this purpose it is important to use biopolymers that are present throughout the human body and have multiple attachment points such as hyaluronic acid. In case of intracellular delivery, the nanostructured materials should further include the capacity to efficiently cross the cellular membrane, escape the endosomal compartment and accumulate in the cell cytoplasm (Maia *et al.* 2011). But the role of these formulations may not be only related to the efficient delivery of biomolecules.

Several micro- and nanomaterials have been developed in the last twenty years to release drugs into the brain, and hence, these formulations may be used in NSC research. These include liposomes, polymeric micro- and nanoparticles (e.g. formed by synthetic polymers including poly(lactic acid), poly(glycolic acid), poly[lactide-co-glycolide], poly(alkylcyanoacrylate), polyanhydride, poly[bis(p-carboxyphenoxy) propane-sebacic acid], polyethyleneimine (PEI) or natural polymers including chitosan, alginate, gelatin, dextran sulfate), inorganic nanoparticles (e.g. silica, gold), solid lipid nanoparticles (i.e., solid lipid matrices stabilized by surfactants), micelles and dendrimers (reviewed by (Orive *et al.* 2009)). Diameter ranges from 10 to 1,000 nm for nanoparticles and 1 μm to 200 μm for microparticles. The optimal size changes according to the final application, route of administration and type of drug to administer. Additionally, the surface of the carriers can be functionalized in order to enhance brain uptake through the blood-brain barrier (BBB) and to target specific cell populations in the brain. The selection of the optimal formulation depends on the concentration of drug to be released, hydrophilicity/hydrophobicity, the need for functionalization, intracellular/extracellular targeting, among others.

The majority of proneurogenic modulators identified so far act through membrane receptors, which simplifies the design and complexity degree of the delivery systems. However, neuronal differentiation inductive agents have strikingly different physico-chemical characteristics, which range from complex to simple proteins and to small molecules. Therefore, the design of a controled release strategy will have to contemplate an architecture that delivers neuronal differentiators in a successful and timely fashion under the most appropriate concentration ranges. The purpose of intracellular *versus* membrane targeting

presents an additional challenge. An intracellular drug delivery system must pass through the cellular membrane; subsequently escape the endosomal degradation fate, before finally addressing the target organelle, which might comprise another barrier, such as the mitochondrial or nuclear membrane. Target localization can help define the necessary dimensions of the drug delivery vehicle, since uptake of foreign material by cells is size-dependent.

1.4.1 - BRAIN DELIVERY

Drug delivery to brain tissue can be achieved either through systemic, intranasal or local administration. Delivery of systemically-administered bioactive agents to the brain is highly restricted by the BBB. Several studies have shown a clear inverse relationship between NP size and BBB penetration. Low diameter gold NP (15 nm) tend to accumulate more in the mouse brain than large NP (3 fold increase for 100 nm and 250 times for the 200 nm NP) after intravenous administration. However, it is unclear whether smaller NP (bellow 15 nm) are advantageous for BBB permeation since 4 nm NP might be taken up by the reticuloendothelial system or incorporated by the endothelial cells before reaching the brain (Sonavane *et al.* 2008). Therefore, the majority of studies describing brain delivery use NP with sizes between 10 to 20 nm. A similar inverse relationship between NP size and BBB penetration was also observed with silica NP *in vitro* (Hanada *et al.* 2014). Importantly, NP shape also influences the rate of cellular uptake and body distribution. Shapes can vary from spherical, disk-like, cubic, rod-like, among other forms (Figure 1.7). Rod-shaped particles, for example, were described to be more efficient in knocking down a therapeutic target for AD when infused into the lateral ventricles of mice (Shyam *et al.* 2015). However, most of the studies have been performed with spherical NP since they are relatively easy to prepare (Guerrero *et al.* 2010).

To maximize the ability of NP to cross the BBB, they can be coated with ligands or antibodies that are recognized by receptors/transporters or epitopes on brain endothelial cells. For example, NP coated with transferrin peptide, glucose, insulin or apolipoprotein E can cross the BBB and accumulate in the brain. Additionally, NP can be coated with molecules that specifically adsorb molecules from the blood which are recognized by the endothelial cells

from the BBB. For example, a polysorbate 80 (Tween 80)-coating on poly(butyl cyanoacrylate) NP leads to the adsorption of apolipoprotein E3 which enables them to cross the BBB (Michaelis *et al.* 2006). Enhanced permeability through the BBB is also achieved by coating NP with anti-fouling molecules such as poly(ethylene glycol) (PEG) (Alyautdin *et al.* 2014) (Figure 1.7). Few reports explore the biodistribution of NP injected i.v. in distinct brain regions (that can be specifically affected by neurodegenerative diseases) and the ability of NP to escape from the vasculature into the brain parenchyma (Sousa *et al.* 2010; Wohlfart *et al.* 2012; Wiley *et al.* 2013). Therefore, it is imperative to test the ability of these nanoformulations to cross the BBB with reliable *in vitro* and *in vivo* experimental models.
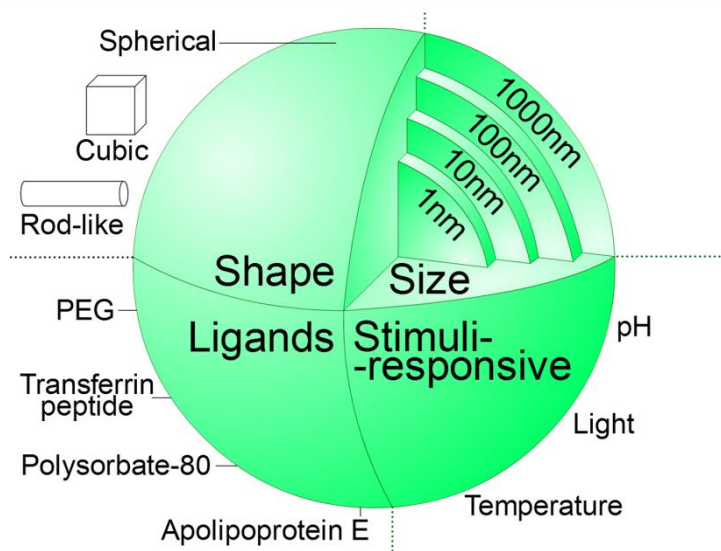
Figure 1.7 - Main tunable nanoparticle (NP) features. NP shape (e.g. spherical, cubic, rod-like) and size (1-1000 nm) can vary. NP can be coated with ligands to, for example, improve blood circulation or facilitate BBB crossing (e.g. polyethylene glycol (PEG), transferrin peptide, polysorbate-80, apolipoprotein E). Additionally, NP can be remotely disassembled by stimuli such as pH, light and temperature.

The intranasal approach is a promising platform for brain delivery. This route was used for the administration of NP containing basic fibroblast growth factor (bFGF) in hemiparkinsonian rats, demonstrating therapeutic relevance (Zhao *et al.* 2014). Since growth factors are important modulators of neurogenesis, it would be of particular interest to evaluate this type of administration with other unstable molecules with clinical relevance (Figure 1.8).

Finally, the local administration (e.g. intracerebroventricular (i.c.v.) injection) is more invasive, but it also allows a precise delivery in high therapeutic doses for extended periods of time. Therefore, to successfully reach the neural stem/progenitor cell niches, invasive approaches are often used. VEGF for example, which is known to have neuroprotective and neurogenic properties, was injected continuously for 3 days by the i.c.v. route, after induction of focal cerebral ischemia (Sun *et al.* 2003). Despite the aggressiveness of this strategy, animals recovered and demonstrated promising outcomes in parameters such as infarct size, neurological performance and survival of newborn neurons in DG and SVZ (Sun *et al.* 2003) (Figure 1.8).
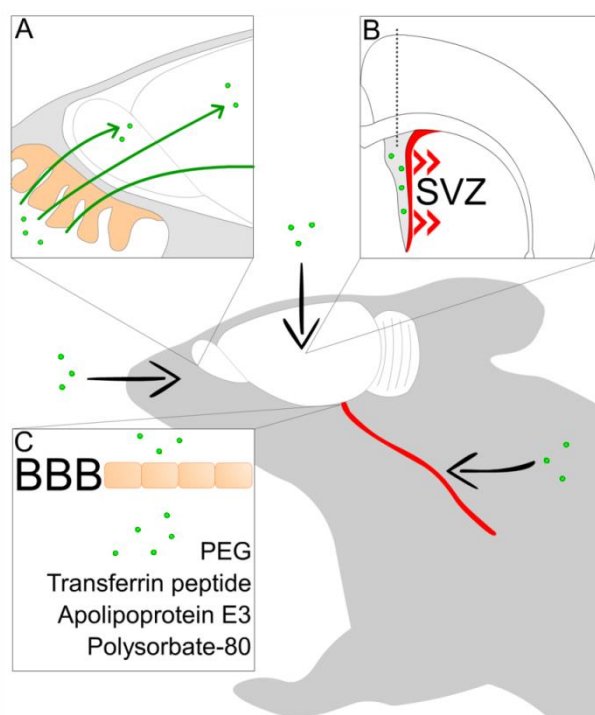
Figure 1.8 – Route of administration of nanostructured materials to target the brain. Nanomaterials delivered by the intranasal route (A) target several brain regions, including neurogenic and non-neurogenic regions. Intracerebral injections (B) maximize the amount of materials and their cargo that interact locally with cellular components of the neurogenic niche, such as the subventricular zone (SVZ). The intravenous or intraperitoneal administration (C) may require surface coating of nanoparticles to allow an efficient passage through the BBB (e.g. polyethylene glycol (PEG), transferrin peptide, polysorbate-80, apolipoprotein E3). Nanomaterials are shown in green.

With the rapid development of nanomedicine, a demand for biomaterials able to remotely disassemble by an exogenous stimulus is urging. By doing so, such systems would provide a spatial and temporal control of drug release while diminishing severe side effects on healthy organs. Such stimuli include pH, specific enzymes, temperature, ultrasound, and light (Delcea *et al.* 2011). However, few stimuli-responsive biomaterials have been developed to target neural stem cells for brain repair. The stimulation of drug delivery by pH alterations is a suitable strategy for pathologies such as tumors, ischemia and other conditions where pH is altered by the accumulation of lactic acid. Accordingly, a pH-sensitive copolymer composed by poly (urethane amino sulfamethazine) (PUASM) was designed for the controled release of stromal cell-derived factor-1α (SDF-1α) in stroke. Targeted delivery of SDF-1α enhanced both neurogenesis and angiogenesis, but did not influence cell survival or inflammation in a rat model of MCAO (Kim *et al.* 2015).

Among the exogenous stimuli, light is particularly attractive as it can be remotely applied with high spatial and temporal precision at a specific wavelength (ultraviolet, visible or near-infrared (NIR) regions) in a non-invasive fashion. This strategy enables the development of a one-time or repeatable drug release systems. However, the downside of light-responsive materials is the low tissue penetration of visible and ultraviolet regions of the spectrum (Mura *et al.* 2013). Nevertheless, NIR light (700-1000nm) covers the tissue-transparency window of the spectrum with low absorbance by water and biological tissues (Konig 2000). Thus, NIR-responsive materials are extremely promising for clinical applications. The NIR absorbing capacity of nanomaterials such as carbon nanotubes and gold nanoshells has been used to trigger the release of therapeutic cargo. Accordingly, Oct4 siRNA-loaded gold nanoshells were used to differentiate human embryonic stem cells *in vitro*. Upon femto-second pulses of NIR, siRNA was released to cellular cytosol and initiated the expression of differentiation markers. Importantly, this approach did not demonstrate any evident adverse side effects. This study provides proof of concept for the manipulation of stem cell differentiation by siRNA with potential application in adult NSC-based therapy (Huang *et al.* 2015).

1.5 - NANOMEDICINE TO ENHANCE ENDOGENOUS NEUROGENESIS

The application and development of nanomaterial-based therapies will be next presented in key examples of brain injury and/or degeneration as a means to boost neurogenesis and brain regeneration.

In the human brain, stroke stimulates neurogenesis and neuroblast migration to the site of injury. However, the number of neurons generated from the SVZ of post-ischemic brain is insufficient (about 0.2% of the striatal cells lost), and the survival of these new neurons is minimal. Due to the inherent repair potential of NSC, targeting the endogenous niche provides a promising platform for the treatment of stroke. Biomolecule delivery by NP offers a promising strategy to manipulate endogenous NSC niche after stroke. For example, polymeric NP containing epidermal growth factor (EGF, which stimulates NSC proliferation) or erythropoietin (EPO, which reduces cell apoptosis of the differentiated cells from NSC) have been encapsulated in a hyaluronan methylcellulose hydrogel which was implanted in the epicortical region of the brain (2-3 mm from the SVZ region). In these conditions, EGF was completely released within the first week while EPO was released for three weeks. The sequential release of both molecules induced the regeneration in the peri-infarct region, which was correlated with the increase of NSC proliferation observed at the SVZ region (Wang *et al.* 2013).

A promising therapeutic approach to PD involves the modulation of NSC from the SVZ niche in order to obtain new dopaminergic neurons able to repopulate the lesioned striatum of PD patients. One of the approaches is to induce the mobilization of NSC from the niche. For example, the combination of hepatocyte growth factor (HGF)-loaded hydrogels with leukemia inhibitory factor (LIF)-loaded NP significantly mobilized human NSC *in vitro* (Li *et al.* 2012). Both molecules induce NSC migration according to their release profile, i.e., HGF and LIF induced migration for approximately 2 and 5 weeks, respectively. A separate study has shown that a multifunctional biomaterial comprising an injectable multifunctional gelatin-hydroxyphenylpropionic acid hydrogel and dextran sulfate/chitosan polyelectrolyte complex NP

containing stromal cell-derived factor 1α (SDF-1α) is very promising to treat cavitary brain lesions to recruit endogenous NSC and enhance neural tissue regeneration (Lim *et al.* 2013).

NSC are ideal donor-cell sources for AD patients. The transplantation of NSC, genetically altered or stimulated with proneurogenic factors such as BDNF, were able to rescue spatial and memory deficits in several AD animal models (Park *et al.* 2012; Park *et al.* 2013; Zhang *et al.* 2014b). Moreover, cell replacement in AD might also be achieved through the induction of endogenous NSC from SGZ. The demonstration that NP containing bioactive agents are capable of inducing neurogenesis and consequently reverse learning and memory impairments in a rat model of AD has been recently reported (Tiwari *et al.* 2014).

Polymeric conjugates (100 nm) based on hyaluronic acid conjugated with multiple molecules of ephrin-B2 and sonic hedgehog *per* polymer chain have been successfully used to stimulate neurogenesis in normally quiescent regions of the brain (Conway *et al.* 2014). These engineered multivalent ligands were developed to increase the half-life of proteins and efficiency compared to corresponding monovalent ligands (spacing between ligands has an important effect in modulating conjugate activity) (Conway *et al.* 2013). It was shown that hyaluronic acid conjugated with 22 molecules of ephrin-B2 *per* polymer chain enhanced neuronal differentiation. The multivalent ligand induced a six-fold increase in the fraction of newly-divided cells expressing the early neuronal marker doublecortin in the adult rat striatum. The main risk factor for developing AD is ageing. Noteworthy, the multivalent ligand partially restored neurogenesis in geriatric rats (Conway *et al.* 2014).

1.6 - POTENTIAL USE OF BIOMATERIALS IN NEURODEGENERATIVE DISEASES: NEW PERSPECTIVES

The modulation of NSC activity such as the control of their proliferation and differentiation by nanotechnologies, would represent a significant step towards the development of new therapeutic approaches for brain repair. However, several issues remain to be solved for the clinical translation of this approach. An important issue is to identify NSC

epitopes to specifically target this cell population *in vivo*. This will increase the specificity and likely the efficiency of the nanomedicine platforms while reducing potential side effects. Some peptides able to target NSC have been identified (Schmidt *et al.* 2007) and their use should be explored in the near future. Another important issue is to better understand the NSC niche in order to further manipulate adult NSC. In addition, an understanding of the pathology and involved signaling pathways are critical elements to consider when selecting an appropriate nanomaterial for brain repair therapy.

Although in many studies reported so far, the nanostructured materials acted in neurogenic regions, in particular at the NSC niche, the materials might also boost neurogenesis in non-neurogenic regions (e.g. striatum, cortex). In this case, the biomaterials should first recruit NSC or neural progenitor cells to the non-neurogenic region, for example by the delivery of SDF-1α (Conway *et al.* 2014), and then induce neuronal differentiation by the delivery of neurogenic factors. The accomplishment of this goal requires the development of biomaterials that can release multiple bioactive molecules at different times and dosages. In some cases, this might require the release of the biomolecule for several weeks until a specific neuronal phenotype is obtained, and the differentiated cell integrates in the existing neuronal circuitry.

1.7 - OBJECTIVES

Currently, there are no efficient and broad-spectrum therapies for neurodegenerative diseases, a group of brain disorders that are increasingly impacting on society. Their main common trait is the loss of neuronal tissue followed by cognitive and/or motor impairment. In this sense, NSC-based therapy relies on a potent endogenous source of new neurons that not only can replace dead cells but can restore neuronal circuits. This approach has encountered some limitations in the past: insufficient number of new neurons reach the lesion site and the ones that survive this hostile environment cannot efficiently differentiate and become mature and functional. A well-known powerful inducer of neuronal differentiation is retinoic acid

(RA), however, this molecule is rapidly metabolized by cells and has low solubility in aqueous solutions. Hence, we have designed a new approach to overcome this obstacle by developing nanoparticles as a suitable strategy to ensure its intracellular delivery. We have previously demonstrated that this formulation efficiently induces the differentiation of adult neural stem cells from the subventricular zone *in vitro* (Maia *et al.* 2011). However, we did not explore its mechanisms or its cellular and molecular *in vivo* applicability.

Our aim is to evaluate the therapeutic potential of RA-loaded nanoparticles (RA-NP) for brain regeneration. For that reason, we will take the following specific objectives:

1) To disclose the NSC differentiation mechanisms triggered by RA-NP. For that purpose, we will compare the dynamics of initial stages of stem cell differentiation, upon exposure to either RA-NP or free solubilized RA.

2) To assess the neurogenic capability of RA-loaded NP *in vivo*. We will deliver RA-NP intracerebroventricularly in a mouse model and evaluate neurogenic gene expression. The successful demonstration of RA-NP neurogenic potential *in vivo* establishes the basis for the next objective.

3) To use light-responsive nanoparticles (LR-NP) to control RA stability and solubility and deliver this molecule with high spatial and temporal precision. In particular, we will test a formulation able to efficiently deliver a pro-neurogenic drug (RA) upon an external stimulus, which is a major innovation of this work.

CHAPTER 2

Materials and Methods

All experiments were performed in accordance with European Community Council Directives (2010/63/EU) and the Portuguese law (DL nº 129/92) for the care and use of laboratory animals.

2.1 - PREPARATION OF NANOPARTICLES

2.1.1 - RA-loaded nanoparticles (RA-NP)

Nanoparticles (NP) were prepared by adding dropwise 0.6 mL of RA (2% w/v, in dimethyl sulfoxide (DMSO)) into 12 mL of polyethylenimine PEI (1% w/v, in pH 8.0 borate buffer). The formation of complexes between RA-PEI occurred immediately and was allowed to proceed for 30 min with intense magnetic stirring. Then, 2.4 mL of dextran sulphate (DS) solution (1% w/v) was added dropwise and stirred for another 5 min. Finally, 1.2 mL of ZnSO4 aqueous solution (1 M) was added and stirred for 30 min. Nanoparticles were centrifuged 3 times in 5% mannitol solution at 14,000 g for 20 min. Supernatants from each step were collected to determine PEI and DS amounts in nanoparticles. Resulting nanoparticles were frozen and lyophilized for 4 days to obtain a dry powder. Lyophilized nanoparticles were stored at 4 ºC. Void nanoparticles (blank) were prepared using the same procedure in the absence of RA.

2.1.2 - Light-responsive RA-loaded nanoparticles (LR-NP)

For the preparation of LR-NP, a RA solution (24 μL, 50 mg/mL, in DMSO) and a solution of PEI and 4,5-dimethoxy-2-nitrobenzyl chloroformate (PEI-DMNC) (66.7 μL, 150 mg/mL respectively, in DMSO) were added simultaneously to an aqueous solution of DS (5 mL, 0.4 mg/mL) and stirred for 5 min. Then, an aqueous solution of ZnSO4 (120 μL, 1 M) was added and stirred for 30 min. The nanoparticle suspension was dialyzed (Spectra/Por® 1 Regenerated Cellulose dialysis membrane, MWCO 6000-8000 Da, Spectrum) for 24 h, in the dark, against an aqueous solution of mannitol (5 %, w/v), lyophilized and stored at 4 ºC before use.

2.2 – SUBVENTRICULAR ZONE CELL CULTURE

Subventricular zone (SVZ) cells were obtained from 1-3 day-old C57BL/6 mice. Animals were euthanized and brains placed into calcium- and magnesium-free Hank's balanced salt solution supplemented with 100 U/mL penicillin and 100 μg/mL streptomycin (all from Life Technologies, Carlsbad, CA, USA). Fragments of SVZ were dissected out of 450 μm-thick coronal brain sections using a McIlwain tissue chopper and SVZ fragments were digested in 0.025% trypsin, 0.265 mM EDTA (all from Life Technologies) (10 min, 37 ºC), followed by mechanical dissociation. Cell suspension was diluted in medium composed by Dulbecco's modified eagle medium [(DMEM)/F12 + GlutaMAXTM-I)] supplemented with 100 U/ml penicillin, 100 μg/ml streptomycin, 1% B27 supplement, 10 ng/ml epidermal growth factor (EGF) and 5 ng/ml basic fibroblast growth factor-2 (FGF-2) (all from Life Technologies). Cells were then plated on uncoated Petri dishes at a density of 3,000 cells/cm^2 and allowed to develop in an incubator with 5% CO_2 and 95% atmospheric air, at 37 ºC.

2.3 - CELL TREATMENTS

Six-day-old neurospheres were allowed to adhere for 2 days onto poly-D-lysine (0.1 mg/mL)-coated 6-well plates for western blots, qChIP and qRT-PCR and 24-well plates, for all remaining experiments in Chapter 3; and 96-well plates for ROS quantification and 12-well μ-chamber slides (IBIDI, Martinsried, Germany) for all remaining experiments in Chapter 4. SVZ cells were then allowed to develop in growth factor (EGF, FGF-2)-devoid medium for different time frames in the presence of nanoparticles. Regarding laser experiments, cells were also treated with the combination of LR-NP for 24 h followed by laser treatment (405 nm, 800 mW/cm^2) treatment. Laser aperture was set to cover the area of one well. During laser treatments, cell media was reduced to 80 μL/well to allow enhanced light penetration and reduced dispersion. The distance between laser source and cells was kept constant in all treatments (5 cm).

To disclose the involvement of retinoic acid receptors in the proneurogenic effect exerted by RA-NP, cultures were co-exposed to RA-NP and 2 μM BMS493 (inverse pan-RAR agonist; Tocris, Missouri, USA) for 7 days. BMS493 treatment was renewed every 2 days. All the inhibitors used were added to cell media 1 h before treatments, namely apocynin (5 μM, Sigma, St. Louis, MO, USA), a broad nicotinamide adenine dinucleotide phosphate oxidase (Nox) inhibitor and IWR-1-endo (5 μM, Santa Cruz Biotechnology, Santa Cruz, CA, USA), a Wnt pathway inhibitor *via* proteasomal degradation of β-catenin. Controls including void nanoparticles (blank) and DMSO (1:10,000) were also tested.

2.4 - HYPERSPECTRAL SCAN FROM CYTOVIVA

The Hyperspectral imaging system from CytoViva (CytoViva Inc., Auburn, AL) was used to identify the presence of RA-NP within SVZ cell cytoplasm. The CytoViva hyperspectral imager captures the unique reflectance spectra for each high resolution image pixel (down to 64 nm), enabling data to be presented as a spectral curve and RGB image. First, reference spectral signatures were collected from multiple pixels of RA-NP dissolved and vortexed in aqueous solution (water). Then the reference spectrum was compared to those obtained in cells treated for 18 h with 10 μg/mL of RA-NP, or untreated cells (control). On our untreated sample, no RA-NP spectrum was mapped.

2.5 - SINGLE CELL CALCIUM IMAGING

SVZ cultures treated for 7 days with 100 ng/mL RA-NP were loaded for 40 min at 37 ºC with 5 μM Fura-2 AM (Life Technologies), 0.1% fatty acid-free bovine serum albumin (BSA), and 0.02% pluronic acid F-127, in Krebs buffer (132 mM NaCl, 1 mM KCl, 1 mM $MgCl_2$, 2.5 mM $CaCl_2$, 10 mM glucose, 10 mM HEPES, pH 7.4). After a 10 min post-loading period at room temperature (RT), the coverslips were mounted on a RC-25 chamber in a PH3 platform (Warner Instruments, Hamden, CT, USA) on the stage of an inverted Axiovert 200 fluorescence

microscope (Carl Zeiss, Göttingen, Germany). Cells (approximately 100 cells *per* field) were continuously perfused with Krebs and stimulated with 100 μM histamine or high-potassium Krebs solution (containing 50 mM KCl, isosmotic substitution with NaCl) by the mean of a fast pressurized (95% air, 5% CO^2 atmosphere) system (AutoMate Scientific Inc., Berkeley, CA, USA). Intracellular calcium concentration ($[Ca^{2+}]_i$) was evaluated by quantifying the ratio of the fluorescence emitted at 510 nm following alternate excitation (750 milliseconds) at 340 and 380 nm, using a Lambda DG4 apparatus (Sutter Instrument, Novato, CA, USA) and a 510 nm longpass filter (Carl Zeiss) before fluorescence acquisition with a 40x objective and a CoolSNAP digital camera (Roper Scientific, Tucson, AZ, USA). Acquired values were processed using MetaFluor software (Universal Imaging, Downingtown, PA, USA). KCl and histamine peaks given by the normalized ratios of fluorescence at 340/380 nm were used to calculate the ratios of response. Percentage of cells displaying a neuronal-like profile was calculated on the basis of the Histamine/KCl ratio (Agasse *et al.* 2008b) (Figure 2.1)
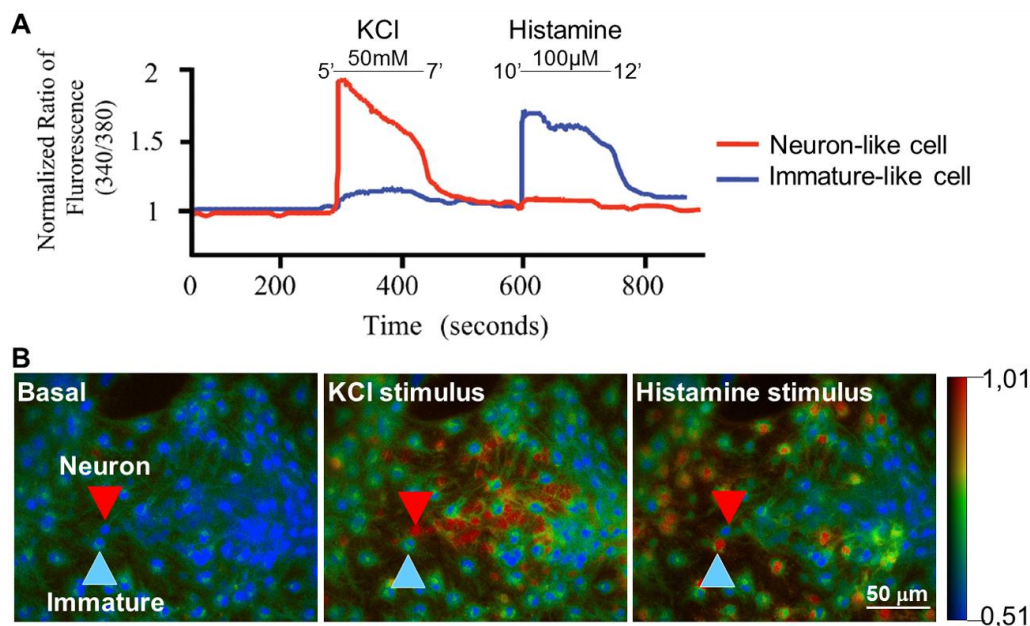
Figure 2.1 - Single cell calcium imaging experimental protocol. (A) SVZ cells were continuously perfused with Krebs during 15 min and stimulated with KCl 50 mM and histamine 100 μM for 2 min. Neuron-like cells increase intracellular calcium concentration ($[Ca^{2+}]_i$) upon KCl stimulus (representative profile of response shown in red) whereas immature-like cells increase $[Ca^{2+}]_i$ when stimulated with histamine (representative profiles of response shown in blue). $[Ca^{2+}]_i$ were determined by changes in the 340/380 nm ratio of Fura-2 AM fluorescence. (B) Representative fluorescence images depict a neron (red arrowhead) and an immature cell (blue arrowhead) during KCl and histamine stimulus. Scale of non-normalized ratio of fluorescence intensity is indicated at the right; blue and red indicate low and high ratios, respectively. Adapted from (Agasse *et al.* 2008b).

2.6 - WESTERN BLOT

SVZ cells were washed with 0.15 M phosphate-buffered saline (PBS) and incubated in Radioimmunoprecipitation assay (RIPA) lysis buffer [0.15 M NaCl , 50 mM Tris-Base, 1 mM EGTA, 5 mM EDTA, 1% Triton X-100, 0.5% sodium deoxycholate, 0.1% sodium dodecyl sulfate (SDS), 10 mM dithiothreitol containing a cocktail of proteinase inhibitors (Roche, Basel, Switzerland)] at 4 ºC. Lysates were collected and protein concentration determined by BCA assay (Thermo Scientific, Braunschweig, Germany). Samples were boiled for 5 min at 95 ºC with Laemmli buffer and stored at -20 ºC until use. Proteins (40 µg of total protein) were resolved in 10% SDS polyacrilamide gels at 120V and then transferred to Amersham Hybond PVDF membranes (GE Healthcare, Buckinghamshire, UK) with 0.45 µm pore size in the following conditions: 300 mA, 90 min at 4 ºC in a solution containing 10 mM CAPS and 20% methanol, pH 11). Membranes were blocked in Tris-buffer (TBS) containing 0.1% porcine gelatin (Sigma) for 30 min at RT and incubated overnight at 4 ºC with primary antibodies diluted in blocking solution (Table 2.1). After rinsing three times with TBS, membranes were incubated for 1 h, at RT, with secondary antibodies (Table 2.1) in blocking solution. GAPDH or β-actin was used as endogenous control. Protein immunoreactive bands were visualized in a ChemidocTMMP imaging system (Bio-Rad Laboratories, CA, USA), following membrane incubation with NZY supreme ECL reagent (NZYTech, Lisbon, Portugal). Densitometric analysis was performed using ImageJ software.

Table 2.1 – Primary (top) and secondary (bottom) antibodies used for western blot.

REACTIVITY	SPECIES	DILUTION	COMPANY
Dvl2	Mouse monoclonal	1:250	Santa Cruz
GAPDH	Mouse monoclonal	1:500	Millipore
GFAP	Rabbit monoclonal	1:20,000	Sigma
Nox1	Goat polyclonal	1:250	Santa Cruz
Nox4	Goat polyclonal	1:250	Santa Cruz

NRX	Goat polyclonal	1:250	Santa Cruz
Rac1	Rabbit polyclonal	1:250	Santa Cruz
RARα	Rabbit polyclonal	1:1,000	St. John's Lab.
β-actin	Mouse monoclonal	1:20,000	Sigma
β-catenin (active)	Mouse monoclonal	1:1,000	Millipore
β-catenin (total)	Rabbit polyclonal	1:4,000	Abcam
βIII-tubulin	Mouse monoclonal	1:1,000	Cell Signaling
SECONDARY ANTIBODIES (HRP-CONJUGATED)			
Anti-goat	Chicken	1:5,000	Santa Cruz
Anti-mouse	Goat	1:5,000	Santa Cruz
Anti-rabbit	Chicken	1:5,000	Santa Cruz

Legend: Dvl2: Dishevelled 2; GAPDH: Glyceraldehyde 3-phosphate dehydrogenase; Nox: Nicotinamide adenine dinucleotide phosphate (NADPH) oxidase; NRX: Nucleoredoxin; Rac1: Rho Family, Small GTP Binding Protein Rac1; RARα: Retinoic acid receptor alpha; HRP: Horseradish peroxidase. Companies: Santa Cruz Biotechnology, Santa Cruz, CA, USA; Millipore, Billeria, MA, USA; Sigma, St. Louis, MO, USA; St. John's Laboratory, London, UK; Abcam, Cambridge, UK; Cell Signaling Technology, Beverly, MA, USA.

2.7 - IMMUNOSTAINING

2.7.1 - IMMUNOCYTOCHEMISTRY

Cells were fixed with 10% formalin solution, neutral buffered. After washing three times with PBS, unspecific binding was blocked and cells permeabilized for 30 min, at room temperature (RT) with a solution containing 3% BSA, 0.3% Triton X-100. Cells were kept overnight at 4 ºC in primary antibody solution (Table 2.2), then washed with PBS and incubated for 1 h at RT with the corresponding secondary antibody (Table 2.2) together with Hoechst 33342 (2 µg/ml; Life Technologies) for nuclear staining. Preparations were mounted in Dako fluorescent medium (Dakocytomation Inc., Carpinteria, CA, USA) and images acquired using a confocal microscope (LSM 710 or LSM 510 Meta confocal microscopes; Carl Zeiss).

2.7.2 - IMMUNOHISTOCHEMISTRY

In order to detect the presence of RA-NP in the subventricular zone, intracerebroventricularly injected mice (see section 2.15) were sacrificed after 24 h and the brains removed and frozen with freezer spray (Thermo Scientific). Coronal brain sections were cut on a freezing cryostat (-18 ºC) at a thickness of 50 μm and mounted on Superfrost Plus slides (Thermo Scientific). After sectioning, the preparations were fixed in Methanol/Acetone (1:1 v/v) for 20 min at -20 ºC. After washing three times with PBS, unspecific binding was prevented by incubating with 3% BSA in PBS for 30 min, at RT. Slices were kept overnight at 4 ºC with anti-FITC antibody (Table 2.2) in PBS containing 0.5% BSA solution. In the next day, brain slices were washed with PBS and then incubated for 1 h, at RT, with Alexa Fluor 594 secondary antibody (Table 2.2). For nuclear labeling, cell preparations were stained with Hoechst 33342 (2 μg/ml) in PBS for 5 min, at RT, and mounted in Dako fluorescent medium. Fluorescent images were acquired using a confocal microscope (LSM 510 Meta, Carl Zeiss).

Table 2.2 – Primary (top) and secondary (bottom) antibodies used for immunostaining.

REACTIVITY	SPECIES	DILUTION	COMPANY
8-oxo-dG	Mouse monoclonal	1:100	Trevigen
DCX	Goat polyclonal	1:100	Santa Cuz
Dlx2	Rabbit polyclonal	1:200	Abcam
FITC	Mouse monoclonal	1:100	Sigma
GFAP	Mouse monoclonal	1:200	Cell Signaling
Nestin	Mouse monoclonal	1:200	Abcam
NeuN	Mouse monoclonal	1:100	Millipore
P-JNK	Rabbit monoclonal	1:100	Cell Signaling
Sox2	Goat polyclonal	1:200	Santa Cruz
Tau	Mouse polyclonal	1:200	Cell Signaling
β-catenin (active)	Mouse monoclonal	1:100	Millipore
β-catenin (total)	Rabbit polyclonal	1:500	Abcam

SECONDARY ANTIBODIES (ALEXA-CONJUGATED)			
Anti-goat	Donkey / Alexa 594	1:200	Life Technologies
Anti-goat	Donkey / Alexa 488	1:200	Life Technologies
Anti-mouse	Donkey / Alexa 594	1:200	Life Technologies
Anti-mouse	Donkey / Alexa 488	1:200	Life Technologies
Anti-rabbit	Donkey / Alexa 594	1:200	Life Technologies
Anti-rabbit	Donkey / Alexa 488	1:200	Life Technologies

Legend: 8-oxo-dG: 8-oxo-7,8-dihydro-2-deoxyguanosine; DCX: doublecortin; Dlx2: distal-less homeobox 2; FITC: fluorescein isothiocyanate; GFAP: glial fibrillary acidic protein; NeuN: neuronal nuclei; P-JNK: phospho-c-Jun N-terminal kinase; Sox2: sex determining region Y-box 2. Companies: Trevigen, Gaithersburg, MD, USA; Santa Cruz Biotechnology, Santa Cruz, CA, USA; Abcam, Cambridge, UK; Sigma, St. Louis, MO, USA; Cell Signaling Technology, Beverly, MA, USA; Millipore, Billeria, MA, USA; Life Technologies, Carlsbad, CA, USA

2.8 – PROPIDIUM IODIDE INCORPORATION

Propidium iodide (PI; 3 µg/mL, Sigma) was added to cell media 10 min before the end of the 48 h treatments. Cells were fixed using 10% formalin solution, neutral buffered, rinsed with PBS, stained with Hoechst-33342 (2 µg/mL), and mounted in Dako fluorescent medium. Images of PI uptake labeling were acquired using a fluorescent microscope (Axioskope 2 Plus; Carl Zeiss).

2.9 - SOX2 CELL PAIR ASSAY

Dissociated SVZ cell suspension obtained from freshly dissected SVZ explants were plated onto poly-D-lysine coated glass coverslips at a density of 6400 cells/cm^2. After seeding, SVZ cells were grown in SFM containing 5 ng/ml EGF and 2.5 ng/ml FGF-2 (low EGF/FGF-2) supplemented or not (control) with 100 ng/mL RA-NP for 24 h. Cells were then fixed in ice cold methanol for 15 min at -20 ºC and processed for immunocytochemistry against Sox2 and Dlx2 (Table 2.2).

2.10 - SELF-RENEWAL ASSAY

SVZ cells were seeded at 2500 cells *per* well in 24-well cell culture plates in SFM containing 5 ng/ml EGF and 2.5 ng/ml FGF-2 (low EGF/FGF-2) and supplemented or not (control) with 100 ng/mL RA-NP. After 6 days, the number of primary neurospheres was determined. Then, neurospheres were collected, dissociated as single cells using the Neurocult dissociation kit (Stem Cell Technology, Grenoble, France) and seeded in low EGF/FGF-2 medium without any treatment. After 6 days, the number of secondary neurospheres was determined. Data was obtained from counting the number of primary and secondary neurospheres in each well, in quadruplicate, *per* independent cell culture.

2.11 - QUANTITATIVE CHROMATIN IMMUNOPRECIPITATION (QCHIP)

After treatment of SVZ cells with 100 ng/mL RA-NP for 1 and 2 days, cells were washed with 0.15 M PBS and the chromatin was crosslinked to proteins by incubating cells with 1% formaldehyde in PBS containing 50 mM MgCl^2, for 15 min, at 37 ºC. SVZ cells were then incubated with 125 mM glycine, for 10 min at RT, washed twice with sterile 0.15 M PBS and incubated with lysis buffer [1% SDS, 10 mM EDTA, 50 mM Tris pH 8.1, containing a cocktail of proteinase inhibitors (Roche)], for 5 min. Samples were sonicated repeatedly on ice (using Sonics & Materials, Model Vibra Cell™ VC 50, Parameters: power 20, time 10 x 30 sec with 30 sec intervals), to cleave genomic DNA. After the analysis of the genomic DNA fragments in a 1% agarose gel, cell suspension was centrifuged at 10 000xg, for 5 min, at 4 ºC. The supernatant was diluted ten-fold in ice-cold dilution buffer [0.01% SDS, 1% Triton, 1.2 mM EDTA, 16.7 mM Tris pH 8.1, 167 mM NaCl and a cocktail of protease inhibitors (Roche)]. Then, samples were pre-cleared with 30 μL of 50% blocked protein G-sepharose beads (Sigma) in 0.15 M PBS, for 30 min at 4 ºC, with rotation. Beads were afterwards eliminated by centrifugation at 10 000xg, for 5 min, at 4 ºC. While 1/10 was kept as the input, the remaining portion, for each sample, was incubated with 10 μg mouse monoclonal antibody against

Histone H3 tri-methylated on lysine 4 (H3K4me3; Abcam, Cambridge, UK), at 4 ºC, overnight. A negative control was done by incubating half of the respective sample with 10 µg of an unrelated antibody [rabbit polyclonal anti-tumor necrosis factor receptor 1 (TNFR1); Santa Cruz Biotechnology]. Immune complexes were captured by 1 h incubation with 40 µL of 50% blocked protein G sepharose beads, at 4 ºC. Then, protein G-sepharose beads were rinsed 7 times, for 10 min, in washing buffer (TE containing 150 mM NaCl and 0.5% nonyl phenoxypolyethoxylethanol-40) and incubated with 50 µg/mL RNaseA/TE, for 30 min, at 37 ºC. The input-lysate was prepared in the same way. Proteinase K (1 mg/mL) and SDS (0.5%) were added to samples which were left overnight at 37 ºC, before being incubated at 65 ºC for 3 h for reverse crosslinking. After a centrifugation at 1,000 g, for 5 min, beads were discarded and the DNA samples were purified by phenol-chloroform extraction and precipitated with 1 µg glycogen, plus sodium acetate and ethanol. The DNA pellets were suspended in nuclease-free water and DNA was then subjected to qPCR analysis with SybrGreen (iQ SYBR Green Supermix; Bio-Rad).

For gene expression analysis, 2 µL of sample DNA or 1 µL of the respective input were added to 10 µL SYBR Green Supermix, and the final concentration of each primer was 0.2 µM in 20 µL total volume. The thermocycling reaction was initiated with activation of Taq DNA polymerase by heating at 95 ºC during 3 min, followed by 40 cycles of a 10 sec denaturation step at 95 ºC, a 30 sec annealing and elongation step at 64 ºC. The fluorescence was measured after the extension step by the iQ5 Multicolor Real-Time PCR Detection System (Bio-Rad). After the thermocycling reaction, a melting curve was performed with slow heating, starting at 55 ºC and with a rate of 0.5 ºC *per* 10 sec, up to 95 ºC, with continuous measurement of fluorescence, allowing detection of possible nonspecific products. The assay included a non-template control (sample was substituted by RNase- DNase-free sterile water) and a standard curve (in 10-fold steps) of DNA for assessing the efficiency of each set of primers. All reactions were run in duplicates. Primers used in real-time analysis were as follows: GAPDH: forward primer 5'-CAA GGC TGT GGG CAA GGT-3' and reverse primer 5'-TCA CCA CCT TCT TGA TGT CAT CA-3' (Lim *et al.* 2009); Mash1: forward primer 5'-CCC TGG CCA GAA GTG AGA-3' and reverse primer 5'-CTG GGT GTC CCA TTG AAA AG-3'; Neurogenin1

(Ngn1) forward primer 5'-ATT ACG GGC ACG CTC CAG-3', reverse primer 5'-CAG CTC CTG TGA GCA CCA AG- 3' (Wu *et al.* 2009). The threshold cycle (Ct) was measured in the exponential phase and therefore was not affected by possible limiting components in the reaction. Data analysis was performed with Bio-Rad iQ5 software. Recovery of genomic DNA as a percentage input was calculated as the ratio of copy numbers in the precipitated immune complexes to the input control. The relative expression of each gene was normalized against GAPDH.

2.12 - cDNA SYNTHESIS AND QUANTITATIVE RT-PCR ANALYSIS

For cDNA synthesis, 1 µg of total RNA was mixed with 2.5 µM anchored-oligo-p(dT)18 primers, 1x PCR reaction buffer, 20 U RNase inhibitor, dNTPs (1 mM each) and 10 U AMV Reverse Transcriptase in a 20 µl final volume (Roche). The reaction was performed at 55 ºC for 30 min and stopped by 85 ºC for 5 min step. The samples were then stored at -80 ºC until further use. For gene expression analysis, 2 µL of sample cDNA were added to 10 µL of Evagreen Supermix (SsoFast Evagreen Supermix; Bio-Rad), and the final concentration of each primer was 1/10 of total volume according to primers datasheet. The thermocycling reaction was initiated with activation of Taq DNA polymerase by heating at 94 ºC during 3 min, followed by 40 cycles of a 15 sec denaturation step at 94 ºC, and a 30 sec annealing and elongation step at 60 ºC for Mash1 and 64 ºC for Ngn1. Validated primer sets for use in real-time RT-PCR were obtained from selected QuantiTect Primer Assays (Qiagen, Austin, Texas). The fluorescence was measured after the extension step by the iQ5 Multicolor Real-Time PCR Detection System (Bio-Rad). After the thermocycling reaction, the melting step was performed with slow heating, starting at 55 ºC and with a rate of 0.5 ºC *per* 10 sec, up to 95 ºC, with continuous measurement of fluorescence, allowing detection of possible nonspecific products. The assay included a non-template control and a standard curve (in 10-fold steps) of DNA for assessing the efficiency of each set of primers. All reactions were run in duplicates. Ct values were measured in the exponential phase. Data analysis was performed with Bio-Rad iQ5 software (Bio-Rad). The relative expression of each gene was normalized against GAPDH,

using the comparative Ct method as described by Pfaffl's formula (Pfaffl 2001). The PCR products were subjected to electrophoresis in a 1 % agarose gel stained with ethidium bromide. Photographs were taken in a Gel-Doc Imaging System (Bio-Rad).

2.13 - CO-IMMUNOPRECIPITATION

Dvl2 co-immunoprecipitation experiments were performed as described elsewhere (Sandieson *et al.* 2014). SVZ cells were treated with laser alone and protein lysates were collected 1 h after in nonyl phenoxypolyethoxylethanol-40 lysis buffer containing 50 mM Tris pH 7.2, 100 mM NaCl, 0.1% NP-40, 10% glycerol, 1 mM EDTA containing a cocktail of proteinase inhibitors (Roche) at 4 ºC. Protein concentration was determined by BCA assay (Thermo Scientific) and 300 µg of total protein from each lysate was pre-cleared using 10 µl of sepharose beads (Preotein A/G PLUS Agarose Immunoprecipitation Reagent, Santa Cruz) during 1 h at 4 ºC in a microtube rotator. Then, 1/10 of total volume from each sample was stored as input for later processing and the remaining volume was split into two equal parts and treated overnight at 4 ºC with either 1 µg of anti-Dvl2 antibody or 1 ug of IgG normal mouse serum as control (both from Santa Cruz). Antibody-protein complexes were immobilized on 30 µL of sepharose beads for 2 h at 4 ºC in a microtube shaker. Bound protein was washed thrice with NP-40 lysis buffer before being boiled during 5 min at 95 ºC with Laemmli buffer. SDS-polyacrylamide gel separation, transfer and signal detention was perfomed as described in the section "2.6 - Western Blot".

2.14 - INTRACELLULAR ROS QUANTIFICATION

SVZ cells plated on 96-well plates were culture in DMEM/F-12 medium devoid of phenol red and supplemented with 100 U/mL penicillin, 100 µg/mL streptomycin and 1% B27 supplement (all from Life Technologies). Cells were treated with laser alone for different time points and 10 min before the end of the experiment, 2',7'-dichlorodihydrofluorescein diacetate

(DCFDA) or MitoSOX red (both from Life Technologies) was added to cell media in order to reach a final concentration of 50 μM and 5 μM respectively. DCFDA is a fluorogenic dye that allows the measurement of cellular peroxide levels, while MitoSOX detects mitochondrial superoxide species. After 10 min, cells were washed with warm medium and the emitted fluorescence was read in a microplate spectrophotometer plate reader at Ex/Em(DCFDA): 485/530 nm and Ex/Em(MitoSOX): 510/580 nm.

2.15 - *IN VIVO* EXPERIMENTS

Adult male mice (8-10 weeks old) were anesthetized with intraperitoneal injection of 2,2,2-tribromoethanol (avertin; 240 mg *per* gram of mice weight). After reaching full anaesthesia, mice were placed on the stereotaxic frame (Stoelting 51600, Dublin, Ireland). Scalp was disinfected with Betadine™ and an incision was made along the midline with a scalpel. With the skull exposed, scales were taken after setting the zero at the bregma point (X, AP: +0.70; Y, ML: -0.75; corresponding to the right lateral ventricle). The skull was drilled and the syringe was lowered until the target (Z, DV: -2.85). The intracerebroventricular injection of 100 ng/mL RA-NP or void nanoparticles (blank), dissolved in 0.15 M PBS, was performed with a Hamilton syringe (Hamilton, Reno, NV, USA) at a speed of 0.5 μL/min during 5 minutes. After the needle was removed and the incision sutured, mice were kept warm during recovery (37 ºC). Three, four or seven days after injection, mice were sacrificed and the brains were removed and frozen with freezer spray (Thermo Scientific). Coronal brain sections were cut on a freezing cryostat (-18 ºC) at a thickness of 10 μm and mounted on polyethylene naphthalate (PEN)-membrane slides (Carl Zeiss) which were previously treated by UV irradiation for 30 min at 254 nm. After sectioning, the slides were fixed using ethanol 90% (v/v). Laser microdissection and pressure catapulting (LMPC) of SVZ region was carried out using a PALM MicroBeam IP system featuring a 337 nm nitrogen laser (Carl Zeiss), and a 20x LD-PlanNeoFluar objective (Carl Zeiss). A total of 6 mm^2 of tissue sample was collected directly in the cap of microfuge tubes. The same stereotaxic coordinates were always used to circumscribe

the SVZ region by LMPC analysis. After LMPC, the tissue sample was immediately process for mRNA extraction and the protocol followed was as described previously for qRT-PCR analysis.

2.16 - STATISTICAL ANALYSIS

All experimental conditions were performed in triplicate from 3 independent cell cultures, unless stated otherwise. For SCCI experiments and NeuN immunocytochemistry, measurements were performed in the pseudomonolayer of cells surrounding the seeded SVZ neurospheres. The percentage of neuronal-like responding cells (Hist/KCl ratio <0.8) was calculated on the basis of one microscopic field *per* coverslip, containing approximately 100 cells (40x magnification).

For the cell pair assay, 60 cell pairs *per* condition were counted, in triplicates from 5 independent cultures. Number of neurospheres in self-renewal assays were measured counting the total number of neurospheres *per* well (from a 24-well plate) in quadruplicate of 5 independent cultures. Quantification of the number of neuritic ramifications, as well as the total neuritic length positive for P-JNK, *per* neurosphere, was performed in 3 culture preparations, in approximately 20 non-overlapping fields *per* coverslip (in triplicate, 20x magnification). The analysis software used was ImageJ (NIH Image, Bethesda, MD, USA). For qChIP and qRT-PCR *in vitro* experiments, samples were pooled from a 6-well plate, *per* experimental condition. For *in vivo* experiments, a minimum of 3 animals were used *per* experimental condition.Immunocytochemistry counting was performed in 5 random fields *per* replicate from 3 independent cultures. A minimum of 1500 cells *per* culture were counted. All experiments included untreated controls or treatment with void nanoparticles whenever nanoparticles were used. Data are expressed as mean ± standard error of mean (SEM). Statistical significance was determined with GraphPad Prism 5 (Graph pad, San Diego, CA, USA) by using ANOVA followed by Dunnet's, Bonferroni's or unpaired two-tailed Student's t test, with $P < 0.05$ considered to represent statistical significance.

CHAPTER 3

Polymeric Nanoparticles to Control the Differentiation of Neural Stem Cells in the Subventricular Zone of the Brain

Awarded with the Pulido Valente Science Prize 2013

3.1 - INTRODUCTION

The subventricular zone (SVZ) represents the main germinal neurogenic niche in the adult mammalian brain. Within this region there are self-renewing and multipotent neural stem cells (NSC) which can ultimately give rise to new neurons, astrocytes and oligodendrocytes (Doetsch *et al.* 1999a; Ming *et al.* 2011a). Therefore, driving SVZ stem/progenitor cell differentiation towards the desired cell phenotype may be a promising platform to influence brain regenerative capacities in the setting of diseases such as Parkinson's (PD), Alzheimer's (PD) and Huntington's (HD) diseases (Sanai *et al.* 2011).

A potential approach to drive the differentiation of SVZ cells *in vivo* involves the efficient delivery of proneurogenic biomolecules into the brain (Santos *et al.* 2012b). Yet the lack of sustained bioavailability is a major issue in these platforms. The efficacy of these approaches is limited likely due to the poor effect in inducing and controlling the differentiation of SVZ cells. Therefore, the development of new nanoparticle formulations able to release proneurogenic factors and provide a sustainable therapeuric effect in the SVZ cell niche is an utmost need.

Central nervous system injury is accompanied by an increased activity of retinaldehyde dehydrogenase. This enzyme is responsible for the conversion of retinaldehyde to retinoic acid (RA) (Maden 2007). In this context, RA represents a molecule of great importance to modulate neurogenesis, specially the *all-trans* RA isoform. Retinoid signaling is transduced by heterodimers formed between the retinoic acid receptors (RAR), and the retinoid X receptors (RXR), which are members of the nuclear receptor superfamily. These receptors heterodimerize and bind to a DNA sequence called retinoic acid-response element (RARE), thereby activating gene transcription upon agonist-binding (le Maire *et al.* 2014). RA is capable of inducing neurite outgrowth and neuronal differentiation from various cell sources, such as embryonic stem cells (ESC) (Rochette-Egly 2015), NSC (Janesick *et al.* 2015) and dorsal root ganglia (Paschaki *et al.* 2012). Regardless of its referred effects, RA is rapidly metabolized by

cells, has low solubility in aqueous solutions and requires a fine tuning of concentration window to achieve its results, posing difficulties in the delivery of therapeutic doses.

Nanoparticles (NP) can be a powerful strategy to overcome these limitations by ensuring controled release of RA. Recently, we reported that the intracellular delivery of retinoic acid-loaded NP (RA-NP) was effective in driving the neuronal differentiation of SVZ neural stem cells *in vitro* (Maia *et al.* 2011). However, it was unclear the molecular mechanisms of RA action following intracellular delivery were unclear and the *in vivo* proneurogenic potential of the formulation was not demonstrated. Here, we show that RA reduces SVZ cell self-renewal while inducing the expression of proneurogenic genes and functional neuronal differentiation *in vitro*. Importantly, RA-NP injected into the brain of an animal model contributes to the successfull commitment of NSC present in the SVZ niche towards neuronal progenitors expressing Mash1 and Neurogenin1 (Ngn1). The NP formulation described herein is a very promising agent to drive the neuronal commitment of SVZ cells both *in vitro* and *in vivo* for brain regenerative therapies.

3.2 - RESULTS AND DISCUSSION

3.2.1 - RA-NP INDUCE NEURONAL DIFFERENTIATION *VIA* NUCLEAR RAR ACTIVATION

NP were prepared by the electrostatic interaction of polyethylenimine (PEI, polycation) complexed with RA and dextran sulfate (DS, polyanion) according to a methodology reported previously by us (Maia *et al.* 2011). RA-NP have a DS/PEI ratio of 0.2, an approximate diameter of 220 nm and positive net charge (zeta potential of ~16 mV) (Figure 3.1A). Moreover, RA-NP are not cytotoxic when used in concentrations equal or below 10 μg/mL and do not impact SVZ cell proliferation (Maia *et al.* 2011). NP (10 μg/mL) conjugated with fluorescein isothiocyanate (FITC) are internalized by SVZ cells after 18 h of exposure and accumulate in cell cytoplasm, as confirmed by immunocytochemistry and by hyperspectral imaging system (CytoViva) analysis (Figure 3.1B to G). These results are in line with previous
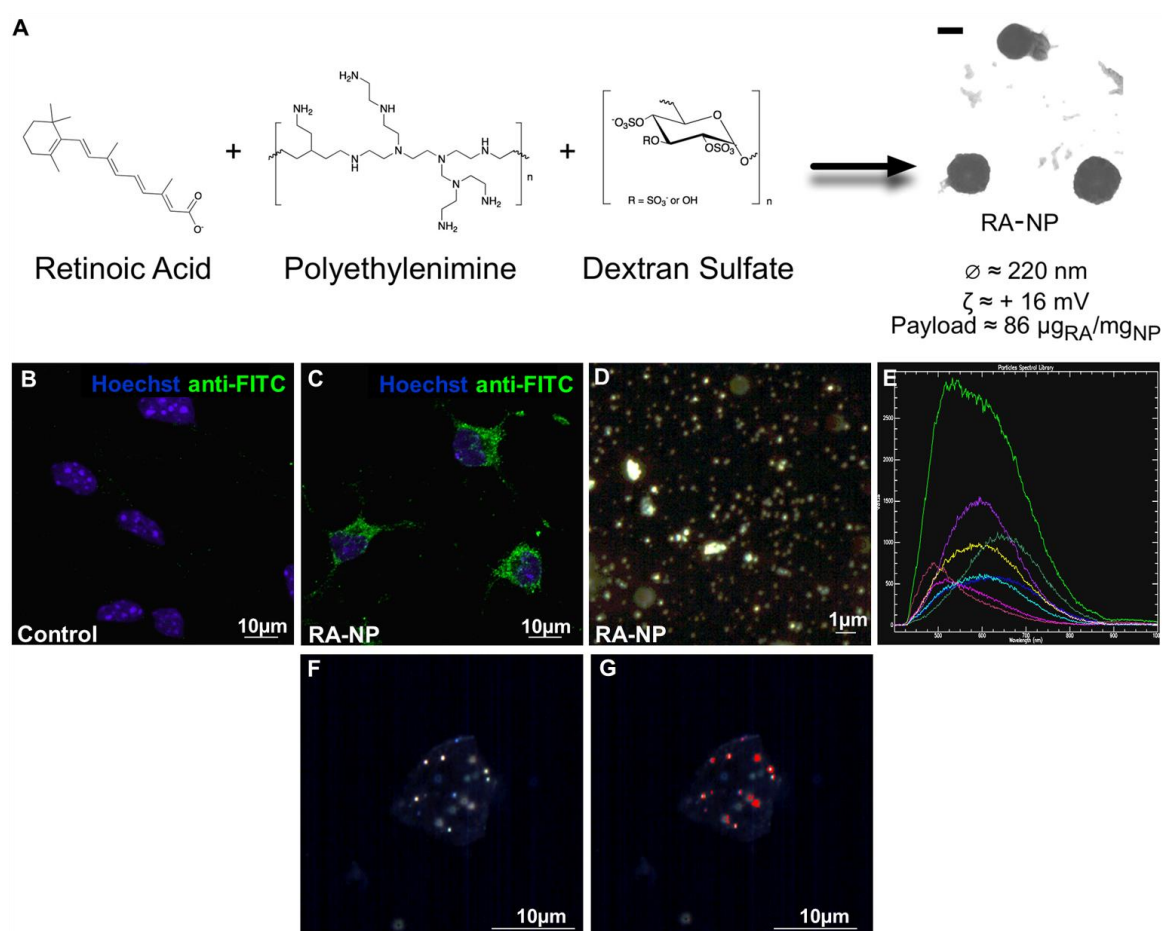
Figure 3.1. SVZ neural stem/progenitor cells internalize RA-NP. (A) Composition and physical properties of RA-NP. Representative confocal digital images of untreated (control; B) or 10 µg/mL FITC-labeled RA-NP-treated SVZ cells for 24 h (C; FITC labeling in green and Hoechst in blue). Hyperspectral scanned image of RA-NP in solution (D) and correspondent reference spectra library of the signatures of each detected NP (E). Hyperspectral scan of one SVZ cell with internalized RA-NP (F) and the same photo revealing each pixel matching the nanoparticle library reference spectra in red (G).

findings, demonstrating that that RA-NP are efficiently internalized by SVZ cells and escape endo-lysosomal fate. NP were detected by confocal microscopy as soon as 1 h after treatment and continued accumulating throughout 24 h, were they reached its maximum internalization (Maia *et al.* 2011).

Several reports have suggested the involvement of RA in the modulation of both neural plasticity and neurogenesis in the adult brain (reviewed in (Maden 2007)). In fact, we have recently demonstrated that a formulation of polymeric RA-loaded NP could be used *in vitro* to control the differentiation of NSC (Maia *et al.* 2011). We showed that NP concentrations above 100 ng/mL (RA payload of 4 nM RA) and bellow 1 µg/mL of nanoparticles (40 nM RA

payload) promoted a robust neuronal differentiation as detected by neuronal nuclei (NeuN, mature neuron marker) immunocytochemistry (Figure 3.2A). Remarkably, the RA concentration present in 100 ng/mL of nanoparticles (4 nM RA), was not able to induce SVZ differentiation; this was only achieved with 10 μM of free RA. This meant that this formulation offered a significant advantage by achieving a proneurogenic effect with a RA concentration ~2500-fold lower than the one needed with free RA (Figure 3.2A). The lowest concentration of RA-NP required to differentiate SVZ cells (100 ng/mL) was used throughout this study together with the equivalent RA concentration they carry (4 nM) and a neurogenic concentration (10 μM) to compare the initial stage dynamics of differentiation between RA-NP and free solubilized RA.

The process of neuronal differentiation is mediated by the interaction of RA with its receptors. For that reason, we evaluated whether RA delivered intracellularly by RA-NP was acting *via* its functional receptor, RAR, in the process of neuronal differentiation. For this purpose, SVZ cells were cultured in differentiation conditions for 7 days, in the presence of 100 ng/mL RA-NP. At this concentration, NP have no cytotoxic effect (Maia *et al.* 2011). As shown in Figure 3.2B, 100 ng/mL RA-NP significantly increased the number of NeuN-positive mature neurons (20.2 ± 1.9% *versus* Control: 11.2 ± 1.2%; P < 0.005) and its proneurogenic effect was completely prevented by 2 μM BMS493, an inverse agonist of RAR (10.4 ± 1.4; P < 0.005). BMS493 binding induces analogous conformational changes in all three RAR subtypes, inhibiting their action (Germain *et al.* 2009). In accordance with our data, Yu and colleagues reported that RA-induced transition of stem cells into neuronal progenitors is RAR dependent in P19 stem cells. Curiously, these authors further demonstrated that only at a later stage, during the maturation process of neuronal progenitors into mature neurons, RA shifts its action through the activation of another nuclear receptor able to heterodimerize with RXR, the peroxisome, proliferator-activated receptor (PPAR) (Yu *et al.* 2012).

Next, we evaluated the functionality of the newly differentiated neuronal cells by single cell calcium imaging (SCCI) analysis. For that purpose, we measured the variations of intracellular calcium concentration ($[Ca^{2+}]_i$) in single SVZ cells, following KCl and histamine (Hist) stimulations, where Hist/KCl ratios below 0.8 are characteristic of SVZ-derived

neuronal-like cells (Agasse *et al.* 2008b). As shown in Figure 3.2C, RA-NP induced a significant increase in the percentage of cells presenting Hist/KCl ratios below 0.8 and this effect was also mediated by nuclear RAR activation (Control: $7.9 \pm 2.1\%$; RA-NP: $36.9 \pm 3.4\%$; RA-NP+BMS493: $6.8 \pm 2.0\%$; $P < 0.001$). An increased expression of βIII-tubulin, a microtubule element expressed exclusively in neurons, was also found increased in RA-NP treated cultures but not in cultures co-treated with BMS493 (Figure 3.2D).
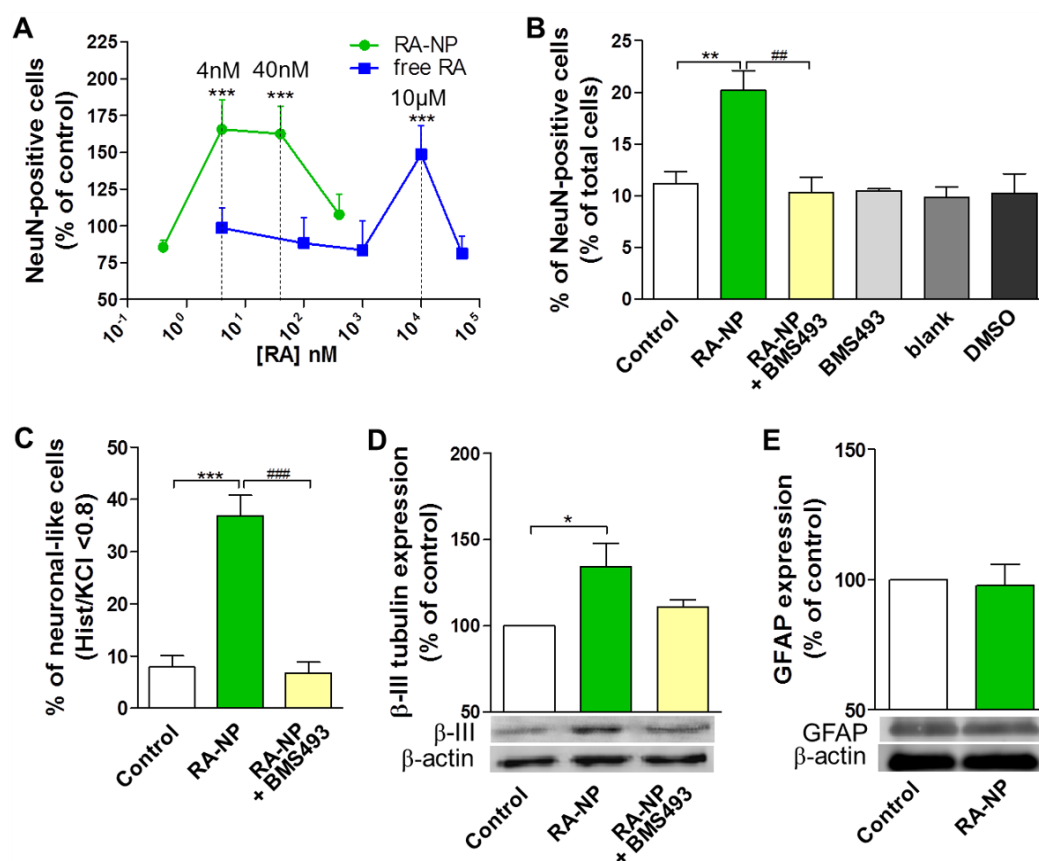

Figure 3.2. RA-NP induce functional neuronal differentiation *via* nuclear RAR activation. SVZ cultures were treated for 7 days and the following parameters were evaluated: (A) Percentage of NeuN-positive neurons using varying concentrations of RA-NP or free RA. Data are expressed as mean percentage of control ± SEM (n=6). ***$P < 0.001$ *vs.* control using Bonferroni's multiple comparison test. Adapted from (Maia *et al.* 2011). (B) Percentage of NeuN-positive neurons as a percentage of the total number of cells. SVZ cells were exposed for 7 days to 100 ng/mL RA-NP and/or to the inverse agonist BMS493 (2 µM). Data are expressed as mean ± SEM (n=6). **,##$P < 0.01$ using Bonferroni's multiple comparison test. (C) Percentage of neuronal-like responding cells (Hist/KCl below 0.8). Data are expressed as mean ± SEM (n=17 coverslips from 6 independent cultures). ***,###$P < 0.001$ using Bonferroni's multiple comparison test. (D) Percentage relative to control of 50 kDa βIII-tubulin protein expression, a neuronal marker, and (E) 55 kDa GFAP protein expression, an astrocytic marker, both normalized to 42 kDa β-actin. Below each graph, a representative Western blot is shown. Data are expressed as mean ± SEM (n=5). Control values were normalized to 100%. *$P < 0.05$ using paired Student's t test.

Additionally, RA-NP-derived neuronal differentiation did not affect astrocytic differentiation (Figure 3.2E). This is in accordance with other results showing that rat NSC treated with free RA (1 μM) for 7 days increased neurogenesis without affecting astrocytic differentiation (Chu *et al.* 2015). Importantly, BMS493, void nanoparticles (blank) or DMSO *per se* (at the dilution used to prepare the free RA) had no effect on neuronal differentiation (Figure 3.2B). Altogether, our results suggest that RA-NP, acting *via* RAR binding, induce a robust proneurogenic effect in SVZ cell cultures.

3.2.2. - RA-NP SUSTAIN STEM/PROGENITOR CELL COMMITMENT

Mammalian neural stem/progenitor cells can divide symmetrically or asymmetrically, either retaining their undifferentiated character or undergoing differentiation, and this decision can be modulated by extrinsic signals (Shitamukai *et al.* 2012). To investigate the effect of RA released from NP in the symmetry of cellular divisions, single SVZ cells were plated for 24 h in the presence of 100 ng/mL RA-NP and 4 nM or 10 μM of solubilized RA. After treatment, cells were immunostained for Sox2 and Dlx2. Sox2 is a transcription factor expressed in self-renewing and multipotent NSC (Episkopou 2005), whereas immunodetection of Dlx2 labels SVZ-derived progenitors (Doetsch *et al.* 2002). Therefore, we quantified the pattern of Sox2 expression in Dlx2-positive SVZ cell divisions (Figure 3.3A). Uncommitted stem/progenitor cells divide symmetrically into two positive NSC daughter cells (Sox2 +/+), whereas cells committed to differentiate divide asymmetrically into a stem/progenitor and a committed cell (Sox2 +/-), or terminally into two equally committed cells (Sox2 -/-). Noteworthy, after RA-NP exposure, we observed a shift in the type of cell divisions towards terminal symmetric divisions (Sox2 -/-; Control: $26.7 \pm 1.6\%$; RA-NP: $40.8 \pm 3.1\%$; $P < 0.001$) in parallel with a significant reduction in the number of Sox2 +/+ cell divisions (Control: $51.1 \pm 3.8\%$; RA-NP: $29.6 \pm 1.9\%$; $P < 0.001$; Figure 3.3B). These data indicate that RA-NP increased progenitor cell commitment and reduced NSC self-renewal capacity. In accordance, it was shown that RA derived from the meninges is essential for corticogenesis by inducing the switch from symmetric to asymmetric divisions of radial glia during development (Siegenthaler *et al.* 2009).
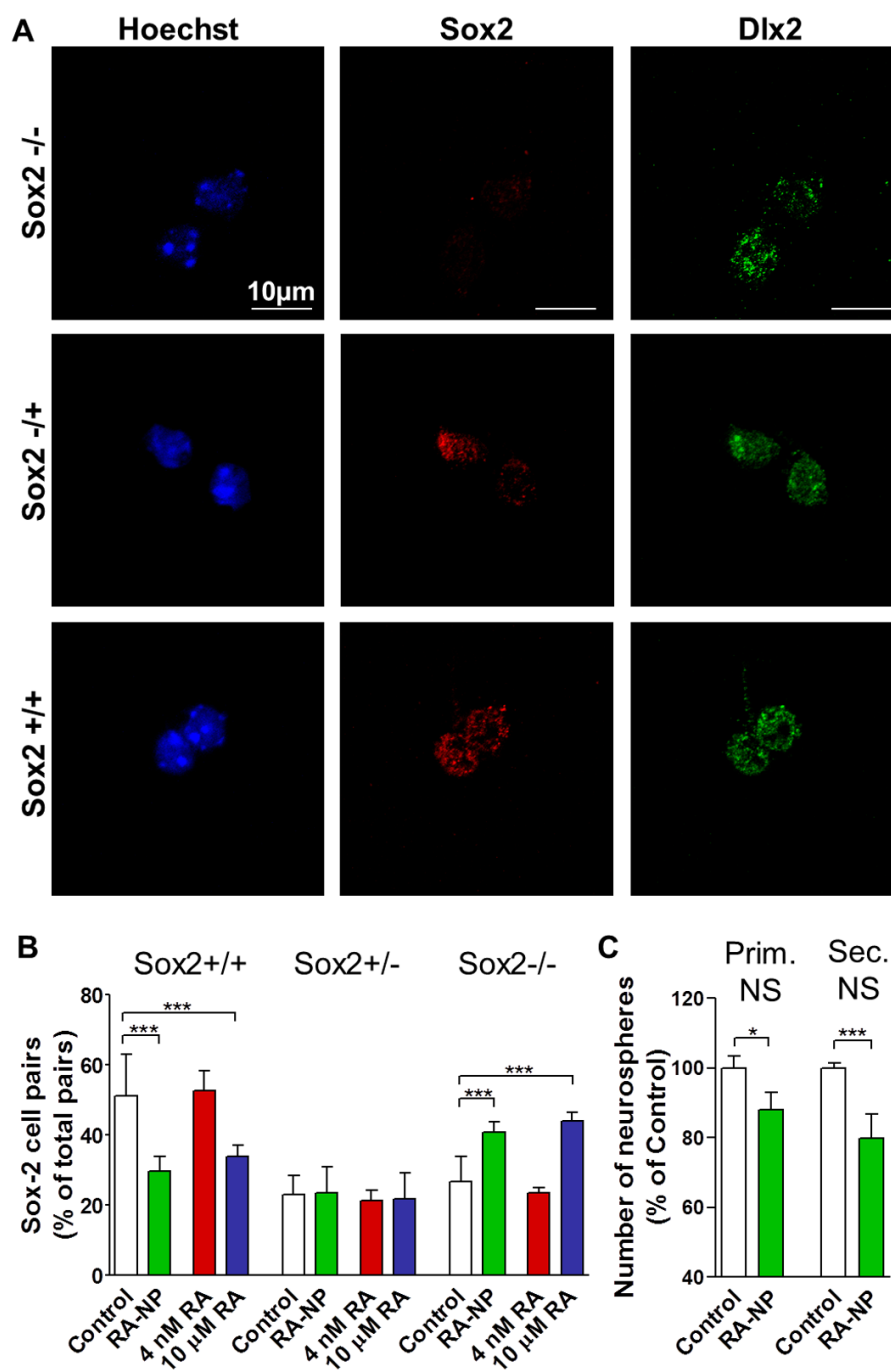
Figure 3.3. RA-NP induce the commitment of SVZ NSC. A) Representative confocal digital images of Sox2 -/-, +/-, +/+ cell pairs revealed by Sox2 (red), Dlx2 (green) and Hoechst (blue) labeling. (B) Bar graph demonstrates the percentage of Sox2 +/+, +/-, -/- daughter cells *per* total cell pairs after treatment with 100 ng/mL RA-NP, 4 nM RA or 10 μM RA for 24 h. Data are expressed as mean ± SEM (n=5); ***P < 0.001 using Bonferroni´s multiple comparison test; (C) Bar graph shows the percentage of primary neurospheres (NS) generated upon 100 ng/mL RA-NP exposure and the resultant secondary NS cultured in untreated medium. Control values were normalized to 100%. Data are expressed as mean ± SEM (n = 4); *P < 0.05, ***P < 0.001 using paired Student's t test.

A similar result was obtained with 10 μM RA, although 4 nM RA was not able to shift cell divisions towards a commited state. Further reinforcing these observations, SVZ neurospheres exposed to 100 ng/mL RA-NP generated a lower number of primary neurospheres ($88.0 \pm 5.0\%$; $P < 0.05$) and less secondary neurospheres ($79.8 \pm 6.9\%$; $P < 0.001$) as compared to control (set to 100%). Secondary neurospheres were obtained from cells dissociated from the primary neurospheres untreated or treated with RA-NP (Figure 3.3C). This result is consistent with a loss of self-renewal induced by RA. In summary, our data indicates that RA-NP reduces stemness and direct early immature stem/progenitor cells towards a committed progenitor fate, ultimately leading to the expansion of late precursors and neuronal differentiation. Our results further emphasize that the biological efficacy of RA-NP requires a concentration of 4 nM of encapsulated RA, a concentration that is 2500-fold lower than the one required with soluble RA.

3.2.3 - RA-NP PROMOTE AXONOGENESIS

A newborn neuron must be able to sprout a single axon and multiple neurites in order to integrate a pre-existing neuronal circuitry. c-Jun N-terminal kinase (JNK) pathway, also referred to as stress-activated kinase (SAPK), appears to play an important role in neuronal differentiation and maturation. Indeed, the JNK pathway is involved in neurite outgrowth and axonogenesis (Oliva *et al.* 2006; Bernardino *et al.* 2012). To evaluate the role of RA released by NP in the axonogenesis, neurospheres were exposed to RA-NP for 6 h and the phosphorylation of JNK was evaluated by immunocytochemistry. According to Figure 3.4, RA-NP induced a robust increase in the phosphorylation of JNK (P-JNK: active form) in growth cone-like projections and in axons emerging out of the neurospheres, while control cultures showed a diffuse or faint P-JNK staining. Moreover, RA-NP treatment increased by approximately 3-fold the total number (Control: $0.80 \pm 0.05\%$; RA-NP: $1.95 \pm 0.31\%$ $P < 0.05$; Figure 3.4A) and length (Control: $357.2 \pm 29.7\%$; RA-NP: $948.1 \pm 327.6\%$ $P < 0.005$; Figure 3.4B) of P-JNK-positive ramifications.

In line with previous studies from our group (Agasse *et al.* 2008a; Bernardino *et al.* 2008; Bernardino *et al.* 2012), the results obtained with RA-NP also show that P-JNK

immunoreactivity co-localized with Tau, a microtubule-associated protein mainly present in new differentiating axons (Figure 3.4C). In addition, this short-timed effect suggests that RA is acting in a non-nuclear and non-transcriptional way. In fact it was recently established that non-nucler RAR are present in membrane lipid rafts and can activate kinase cascades (Piskunov *et al.* 2012). Accordingly, RA was reported to stimulate neurite outgrowth in murine SH-SY5Y neuroblastoma cells in a non-genomic way *via* the activation of JNK and p38 MAPK (Fujibayashi *et al.* 2015). Altogether, our results suggest that RA-NP promote axonogenesis and axon outgrowth through the JNK pathway activation in Tau-positive axons.
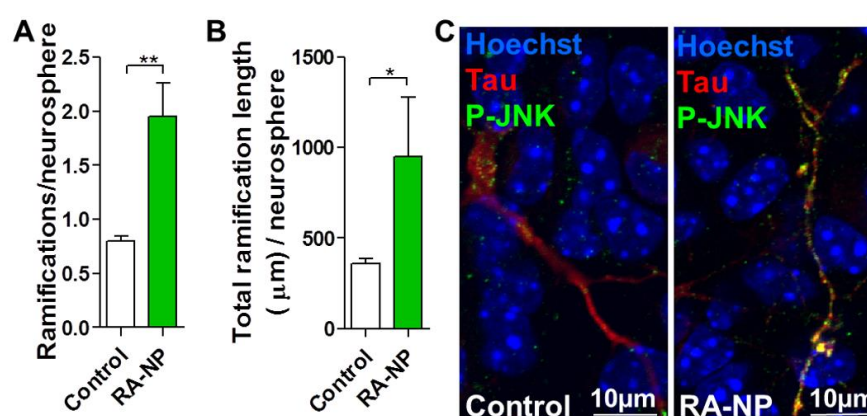
Figure 3.4. RA-NP activate the JNK pathway in Tau-positive axons. Bar graphs depict (A) number of ramifications and (B) total length (µm) of ramifications *per* neurosphere. Data are expressed as a mean ± SEM (n = 3). *P < 0.05, **P < 0.01, using paired Student's t test. (C) Representative confocal digital images of the P-JNK (green), Tau (red) and Hoechst staining (blue), in control cultures and in cultures exposed to 100 ng/mL RA-NP for 6 h. Double-labeling of P-JNK and Tau in growth cone-like structures and axons was seen in RA-NP treated cultures.

3.2.4 - RA-NP SUSTAIN THE EXPRESSION OF MASH1 AND NGN1 PRONEUROGENIC GENES *IN VITRO*

RA induces conformational changes in the nuclear receptors bounded to RARE, causing the dissociation of co-repressors and the recruitment of co-activators that comprise histone modifiers, RNA polymerase II and general transcription factors (Gudas 2013). Histone modifiers are capable of covalent modifications like acetylation, phosphorylation and methylation on the N-terminal tails of core histones (Tyssowski *et al.* 2014). Methylation of histone lysine residues is a critical determinant of active and silent gene expression states.

Histone 3 tri-methylated on lysine 4 (H3K4me3) correlates strongly with active transcription (Santos-Rosa *et al.* 2002). Therefore, we performed quantitative chromatin immunoprecipitation (qChIP) studies to monitor the presence of H3K4me3 at Mash1 and Neurogenin1 (Ngn1) promoter regions. Mash1 (also recognized as Ascl1) and Ngn1 are two basic helix-loop-helix (bHLH) proteins that are strongly associated with neuronal differentiation (Oh *et al.* 2013; Imayoshi *et al.* 2015). Basic helix-loop-helix (bHLH) proteins exist in most stages of neural lineage, which play crucial roles in determining cell fates and are essential in neurogenesis (Huang *et al.* 2014). Accordingly, we observed an increase in H3K4me3 recruitment to Mash1 promoter region one day after RA-NP treatment (3.4 ± 1.3 fold; $P < 0.05$), whereas the enhancement of H3K4me3 associated with the Ngn1 promoter region was only detected on the second day after treatment (2.7 ± 0.8 fold; $P < 0.05$; Figure 3.5A). These observations suggested that RA-NP treatment enhances the transcriptional activity of Mash1 and Ngn1 promoters, thus we further examined Mash1 and Ngn1 mRNA expression through quantitative RT-PCR (qRT-PCR). In line with qChIP results, Mash1 and Ngn1 mRNA levels were increased three days after cell treatment with 100 ng/mL RA-NP (Mash1: 1.9 ± 0.5 fold; Ngn1: 3.5 ± 1.2 fold; $P < 0.05$; Figure 3.5B). Surprisingly, solubilized RA at 10 μM increased Ngn1 (1.9 ± 0.5 fold; $P < 0.05$), but not Mash1 mRNA levels. Additionally, the expression of both Mash1 and Ngn1 genes was also evaluated 2 days after cell treatment; however, no effect was observed in all conditions tested (Figure 3.5B). As expected, 4 nM RA was not able to induce the overexpression of both proneurogenic genes.

The epigenetics behind RA-induced neuronal differentiation seem to be different between free RA and RA-NP. NSC are a heterogeneous population of cells comprising immature multipotent cells and commited progenitors which have a variable epigenetic signature and genetic profile. For example, Mash1 is expressed predominantly in transit amplifying C cells (GFAP-negative, Nestin-,EGFR- and Ki67-positive) but also in a small subset of slow-dividing B stem cells (GFAP- and Nestin-positive) (Kim *et al.* 2007; Kim *et al.* 2011). Adittionally, Ngn1 is higly expressed in proliferating progenitors undergoing late cell divisions (Lundell *et al.* 2009). Based on these data, we postulate that RA-NP may be targeting a broader population of cells than free RA. Moreover, it cannot be excluded that the intracellular machinery involved

in the Mash1 and Ngn1 expression may respond differently to the continuous release of RA by RA-NP *versus* one-time treatment of free RA. Thus, SVZ cells may be differentially responsive to distinct platforms of RA delivery (NP *versus* free RA), ultimately resulting in distinct dynamics of gene expression. Of note, it was recently described that RAR/RXR binding sites redistribute to different gene *loci* during RA-induced differentiation of F9 mouse embryonal carcinoma cells (Chatagnon *et al.* 2015). This event leads to differentially expressed genes when in the presence of ligand. Thus, it is conceivable that the continuous release of RA by NP can activate redistributed RAR/RXR resulting in the transcription of additional genes compared to one-time treatment with free RA.

Altogether, our data suggest that RA-NP increase a robust commitment of mouse SVZ cells towards the neuronal lineage by epigenetic modifications and subsequent mRNA expression of proneurogenic genes (Ngn1 and Mash1).
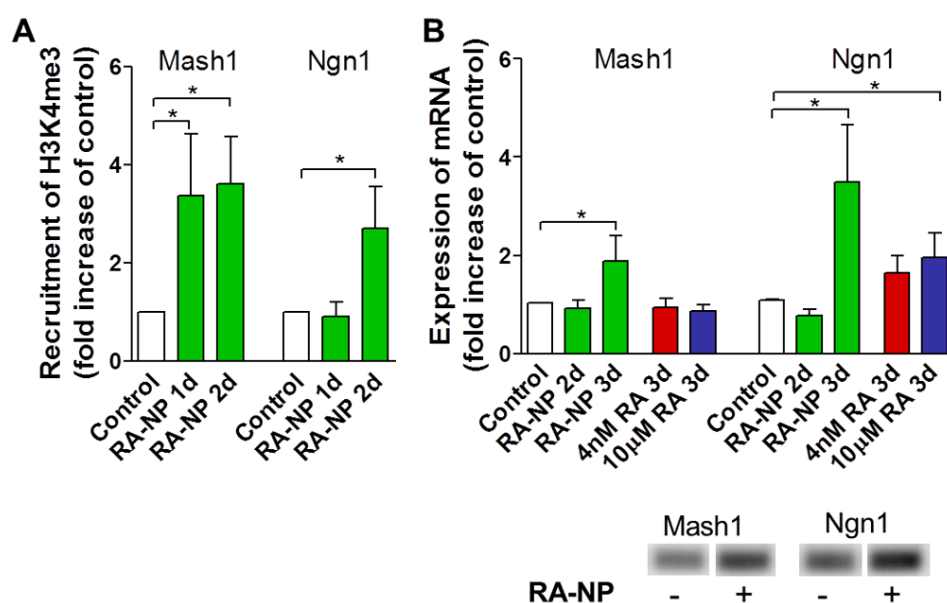
Figure 3.5. RA-NP promote the expression of proneurogenic genes *in vitro*. (A) Bar graphs show the fold increase of H3K4me3 associated with the promoter regions of Mash1 and Ngn1 assessed by qChIP and (B) the fold increase of the respective mRNA expression for both genes, measured by qRT-PCR, in control, 100 ng/mL RA-NP, 4 nM RA and 10 µM RA-treated cell cultures for 1 and 2 days (qChIP) or 2 and 3 days (qRT-PCR). Data are expressed as fold increase relative to control (set to 1), mean ± SEM (n=5-7); *P < 0.05 using Bonferroni's multiple comparison test. A representative agarose gel for Mash1 and Ngn1 qRT-PCR amplicons in control (-) and RA-NP treated (+) cells for 3 days is shown bellow the graph.

3.2.5 - RA-NP MODULATE THE EXPRESSION OF PRONEUROGENIC GENES IN THE *IN VIVO* SVZ NEUROGENIC NICHE

Next, we evaluated the proneurogenic potential of RA-NP *in vivo,* at the SVZ cell niche. We delivered RA-NP intracerebroventricularly (i.c.v.), directly into the ventricular lumen. As shown in Figure 3.6A, internalized FITC-labelled RA-NP were easily detected, lining the lateral ventricle (LV) of the SVZ in treated mice but not in saline-injected animals. *In vivo*, SVZ cellular progeny is mainly derived from quiescent type B stem cells that give origin to rapidly dividing transit-amplifying C cells, which ultimately generate newly born neurons (Figure 3.7). These type B stem cells expand a cilium through the monolayer of ependymal layer surrounding the ventricles in order to contact the cerebrospinal fluid (CSF) (Doetsch *et al.* 1999b). Therefore, RA-NP can affect the neurogenic microenvironment by contacting with ependymal cells (paracrine effect) or by the direct contact with the cilium displayed by SVZ GFAP-positive stem cells (type B cells) that contact the ventricle lumen.

Later on, SVZ was collected by laser microdissection (Figure 3.6B) and mRNA levels of Mash1 and Ngn1, were quantified by qRT-PCR. Similarly to *in vitro* results, the SVZ of animals treated with RA-NP overexpressed both Mash1 and Ngn1. However, Mash1 and Ngn1 revealed different timings of expression: Mash1 mRNA levels only increased after 7 days post-injection (1.9 ± 0.4 fold; $P < 0.05$), while Ngn1 mRNA levels increased after 3 days (1.5 ± 0.1 fold; $P < 0.05$) and were maintained up to 7 days after injection (1.4 ± 0.2 fold; $P < 0.05$; Figure 3.6C). No changes were detected in animals injected with DMSO or blank for Mash1 (DMSO: 1.0 ± 0.1; blank: 0.9 ± 0.2) and Ngn1 (DMSO: 1.1 ± 0.0; blank: 1.0 ± 0.1) expression levels. Differences between the *in vitro* and *in vivo* kinetics might be ascribed to differences in cellular composition. *In vitro,* SVZ progeny is mostly derived from the highly mitotic transit-amplifying C cells and not the quiescent stem cells such as type B cells *in vivo* (Figure 3.7). The cells exposed to epidermal growth factor (EGF) grow to form neurospheres that are multipotent and self-renewing (Doetsch *et al.* 2002).
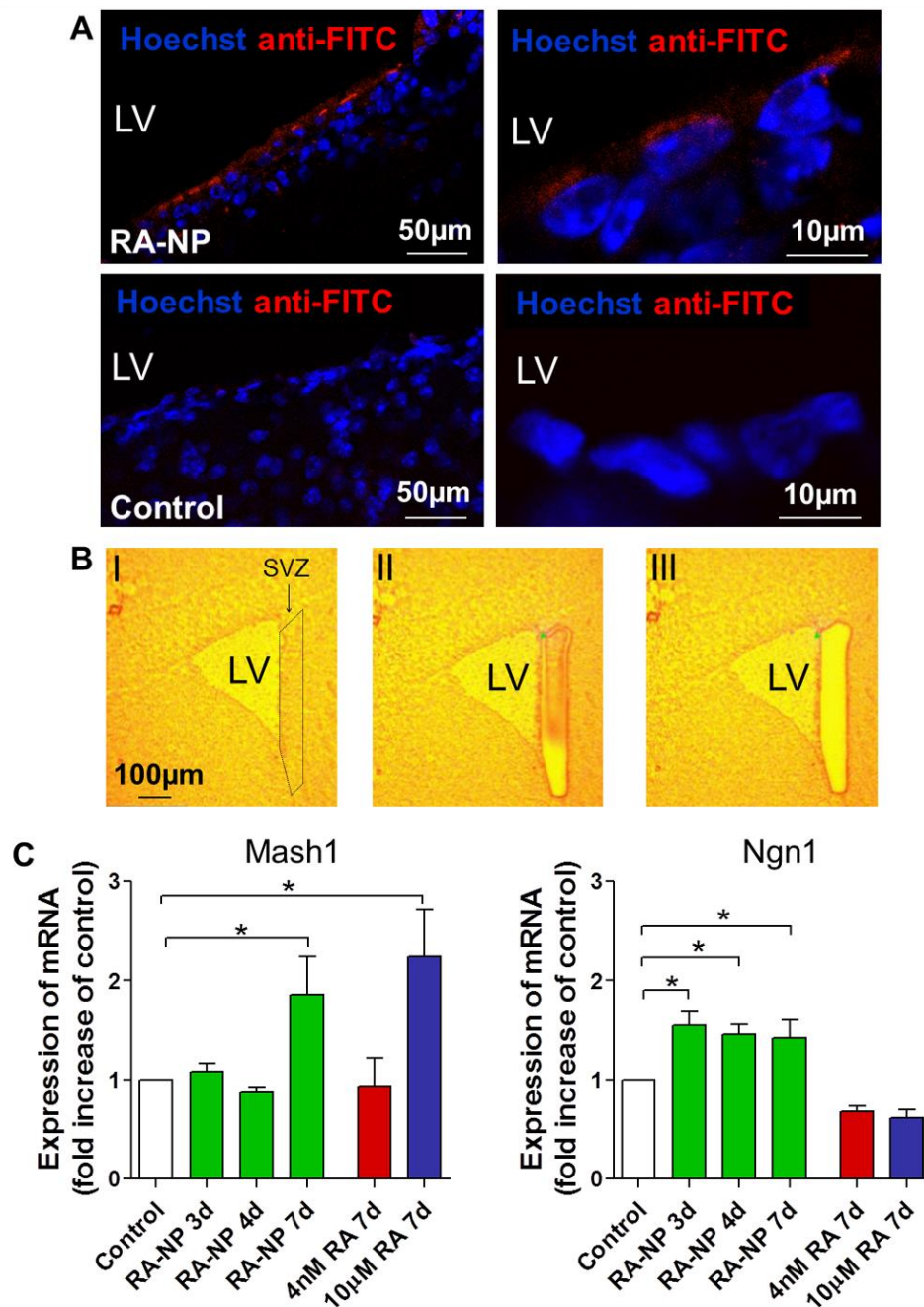
Figure 3.6. RA-NP induce the expression of proneurogenic genes in the SVZ neurogenic niche *in vivo*. (A) Confocal digital images indicating the presence of FITC-labeled RA-NP (red) lining the lateral ventricles 1 day after i.c.v. injection with RA-NP, but not in saline-injected animals (control). (B) Representative digital images of the laser microdissection procedure depicting a mouse brain slice containing the lateral ventricle; I: Identification of the SVZ region; II: SVZ was circumscribed and separated from unwanted cells; III: Laser shots catapulted the SVZ tissue into a lid of a PCR tube. (C) Bar graphs indicate the fold increase of mRNA expression for Mash1 and Ngn1, measured by qRT-PCR, in control, 100 ng/mL RA-NP, 4 nM RA and 10 μM RA-treated animals, for 3, 4 or 7 days after i.c.v. injection. Data are expressed as fold increase relative to control (set to 1), mean ± SEM (n=5-10); *$P < 0.05$ using Bonferroni's multiple comparison test.

It should be noted that differences in gene expression of SVZ cells *in vivo* and *in vitro* (neurospheres) have been also described in the setting of stroke (Liu *et al.* 2007). These changes end up being complementary, but the genes triggered are not the same. Seven days after stroke, only 8 out of the 23 genes upregulated *in vitro* were also upregulated *in vivo* (Liu *et al.* 2007).

The delivery of high (10 µM), but not low (4 nM), concentrations of soluble RA into the ventricular lumen had a different impact in gene expression than *in vitro*. In line with *in vitro* results, 4 nM RA was ineffective in inducing the *in vivo* expression of Mash1 and Ngn1 (Figure 3.6C). However, in contrast with *in vitro* results, 10 µM RA induced a robust increase in the expression of Mash1, 7 days post-injection (2.2 ± 0.5 fold; $P < 0.05$), but had no effect on Ngn1 mRNA levels. Importantly, it has been demonstrated that the expression of Mash1 alone is sufficient to induce neuronal differentiation (Vierbuchen *et al.* 2010; Voronova *et al.* 2011). These results highlight existing differences in the differentiation dynamics of SVZ cells in *in vivo* and *in vitro* conditions likely because of their intrinsic composition (see above). Furthermore, given the fact that the CSF is being constantly filtered and renewed by the *choroid plexus* (Johanson *et al.* 2011), it is possible that this could interfere with the free RA injected. Therefore, one can assume that cells were exposed to different kinetics of RA exposure *in vitro* and *in vivo*.

Overall, our results indicate that SVZ cells treated with RA-NP or solubilized RA have clearly different dynamics of neuronal differentiation between *in vitro* and *in vivo*. These differences are likely ascribed to variances in phenotypic composition of SVZ, but also in changes related to the uptake and intracellular delivery of RA when solubilized *versus* encapsulated in a NP formulation as described in the previous section. Our results further indicate that, similarly to *in vitro* results, RA-NP are more efficient in differentiating SVZ cells than solubilized RA since a lower amount of RA is needed (4 nM *versus* 10 µM) and the epigenetic events are more robust.

3.3 - CONCLUSIONS

In conclusion, this work reports three important findings. First, we demonstrate the differentiation mechanism mediated by RA released from a polymeric NP within NSC. NP were used to facilitate cellular internalization, intracellular positioning and concentration of RA above its solubility limit (approximatelly 63 ng/mL) at physiologic pH (Szuts *et al.* 1991). Our results show that RA released from NP interacted with RAR, activated JNK signaling pathway, and induced the methylation of histone lysine residues which in turn induced the expression of proneurogenic genes such as Ngn1 and Mash1. Second, we successfully demonstrated that a NP formulation could be used *in vivo* to control the differentiation of NSC. Although a previous study has shown that NP formulations may be an efficient platform to transfect SVZ cells *in vivo* with plasmid DNA expressing the nucleus-targeting fibroblast growth factor receptor type 1 (Bharali *et al.* 2005), to the best of our knowledge this was the first study to demonstrated the ability to control *in vivo* the neuronal differentiation of SVZ cells by small molecules delivered by NP. Notably, our formulation offers a significant advantage over free solubilized RA, by circumventing the use of solvents like DMSO, and by achieving a proneurogenic effect with a RA concentration ~2500-fold lower than the one needed with free RA. Third, our study is the first to show the dynamics of initial stages of stem cell differentiation both *in vitro* and *in vivo* after exposure to a NP formulation containing a biomolecule or a solubilized biomolecule. The study of the differentiation profile of stem cells in both conditions is important to design more effective formulations to modulate the stem cell niche. Our results show that RA-NP were more robust in maintaining the signature of gene expression (although with different kinetics) both *in vitro* and *in vivo* than solubilized RA (Figure 3.7). Although not explored, the NP formulation described herein can be engineered at surface level to display stem cell targeting sequences in order to maximize its location and effect. Following recent advances in the use of RA for AD (Szutowicz *et al.* 2015), hippocampal memory deficits (Kawahara *et al.* 2014), PD (Esteves *et al.* 2015) and stroke (Kong *et al.* 2015) therapy, our results provide the foundations for the use of RA-NP to modulate *in vivo* the differentiation of neural stem cells and open new perspectives for the treatment of neurodegenerative diseases.
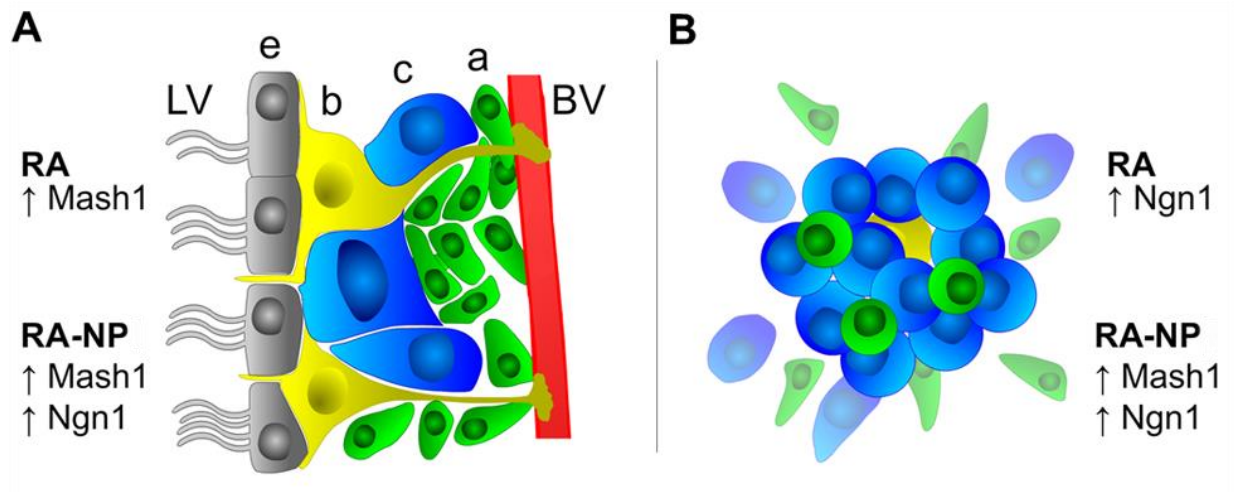
Figure 3.7. Dynamics of initial stages of differentiation between SVZ cells treated with RA-NP and solubilized RA. (A) *In vivo*, the SVZ contains a subpopulation of neural stem cells, or type B cells (b; yellow), that contact with ependymal cells (e; gray), the ventricular lumen and blood vessels (BV; red). Type B cells originate rapidly dividing transit-amplifying C cells (c; blue), which in turn generate neuroblasts, or type A cells (a; green). These neuroblasts will ultimately differentiate into mature neurons. Upon i.c.v. injection with solubilized RA or RA-NP, the SVZ population overexpresses Mash1 and Mash1/Ngn1, respectively. (B) *In vitro*, SVZ cells form neurospheres, mainly composed by EGF-responsive type C cells (blue). Under differentiation conditions, neurospheres give rise to a mixed population of progenitors in different stages of differentiation, neurons, oligodendrocytes and astrocytes. Upon treatment with solubilized RA or RA-NP, the SVZ population overexpresses Ngn1 and Mash1/Ngn1, respectively.

CHAPTER 4

Enhanced Neuronal Differentiation of Neural Stem Cells by Blue Light-Responsive Retinoic Acid-Loaded Polymeric Nanoparticles

In preparation for submission

4.1 - INTRODUCTION

RA-based therapies are unsettled, in a sense that this molecule is rapidly metabolized by cells, has poor water solubility and requires a defined range of concentrations to exert its positive effects, posing difficulties in the delivery of therapeutic doses. Therefore, the use of nanoparticles (NP) is a powerful strategy to overcome these limitations by ensuring protection and intracellular delivery of RA. In fact, we have recently demonstrated that a formulation of polymeric RA-loaded NP could be used to control the differentiation of NSC (Maia *et al.* 2011; Santos *et al.* 2012a). Despite the neurogenic properties of RA, this biomolecule is also known for its teratogenicity and for affecting numerous systems of the body including the CNS (Maden 2002). Therefore, the development of synthetic nanocarriers that can be remotely disassembled by light and release the RA in specific CNS cell populations in the right time could be of high value. Light is a promising trigger for remote activation since it allows high spatial and temporal resolution (Fomina *et al.* 2010; Yavlovich *et al.* 2010). Even if light-responsive NP distribute to other tissues, they will only release their content upon light stimulation (Mura *et al.* 2013). Herein, we propose to use light-responsive RA-loaded nanoparticles (LR-NP) to control the differentiation of NSC. The stimulus used to trigger RA release from nanoparticles was a blue light (405 nm laser), which demonstrated neurogenic capabilities by itself and increased RA receptor alpha (RARα) levels, thereby enhancing the neurogenic effect obtained from nanoparticle-released RA. Therefore, using our combinatory therapy we obtain an amplified neurogenic effect. Moreover, our light-responsive formulation offers great advantages regarding temporal and spatial control of RA release and efficiently induces SVZ neurogenesis. The successful development of this platform will provide innovative and efficient applications for brain regenerative therapies by inducing neurogenesis from the resident endogenous NSC present in neurogenic niches of the adult brain.

4.2 - RESULTS AND DISCUSSION

4.2.1 - LIGHT-RESPONSIVE RA-LOADED NP

The light-responsive polymeric NP were prepared by reacting poly(ethyleneimine) (PEI) with 4,5-dimethoxy-2-nitrobenzyl chloroformate (DMNC), a light-responsive photochrome, and then precipitating the PEI-DMNC conjugate (with or without RA) against an aqueous solution of dextran sulfate (DS). NP were formed due to the hydrophobicity of PEI-DMNC conjugate and the electrostatic interaction of PEI-DMNC (polycation) with DS (polyanion). To stabilize the NP formulation, zinc sulfate was added (Tiyaboonchai *et al.* 2001; Maia *et al.* 2011). NP with a diameter of 110 nm and a zeta potential of 25 mV were prepared. PEI was selected as initial NP block because it facilitates the cellular internalization of NP and subsequent escape from endosomes (Boussif *et al.* 1995; Maia *et al.* 2011) while DMNC was selected because it responds rapidly to light and the degradation products are relatively non-cytotoxic (Dvir *et al.* 2010). RA-loaded NP were tested by exposing them to a blue laser (405 nm, 80 mW) for few minutes, and confirming the presence of released RA by photo-disassembled NP to the aqueous solution (Boto *et al.* in preparation).

4.2.2 - CELL VIABILITY STUDIES

We first evaluated light- and light-responsive RA-loaded NP (LR-NP)-induced cytotoxicity by propidium iodide (PI) uptake. PI is a cell death marker incorporated by necrotic and late-apoptotic cells. To establish proof of concept of our strategy, an energetic wavelength was required to maximize the release of RA from NP. The wavelength used (405 nm) is within the most energetic section of the visible light spectrum. We performed a single laser treatment with increasing duration. Using our protocol of light exposure, 60 sec of 405 nm exposure at 300 mW/cm^2 (60s), which corresponds to a fluence of 18 J/cm^2, was the longest exposure time that did not affect cell viability (Figure 4.1A). Regarding LR-NP, no significant effect on cell death was observed for all the experimental groups tested with nanoparticle concentrations up to 20 µg/mL, including blank nanoparticles and the conjugation of LR-NP followed by 60 sec

of laser exposure (Figure 4.1B). This highest non-toxic concentration (20 µg/mL) was selected for LR-NP cellular internalization studies. DMNC (4,5-dimethoxy-2-nitrobenzyl chloroformate), the photo-cleavable compound used to trigger RA release has fluorescent properties, enabling NP detection by confocal microscopy. Visualization of cytoplasmic NP was obtained within 4 h of incubation and reached its maximum after 24 h (Figure 4.1C). No signal was detected in untreated control cells.
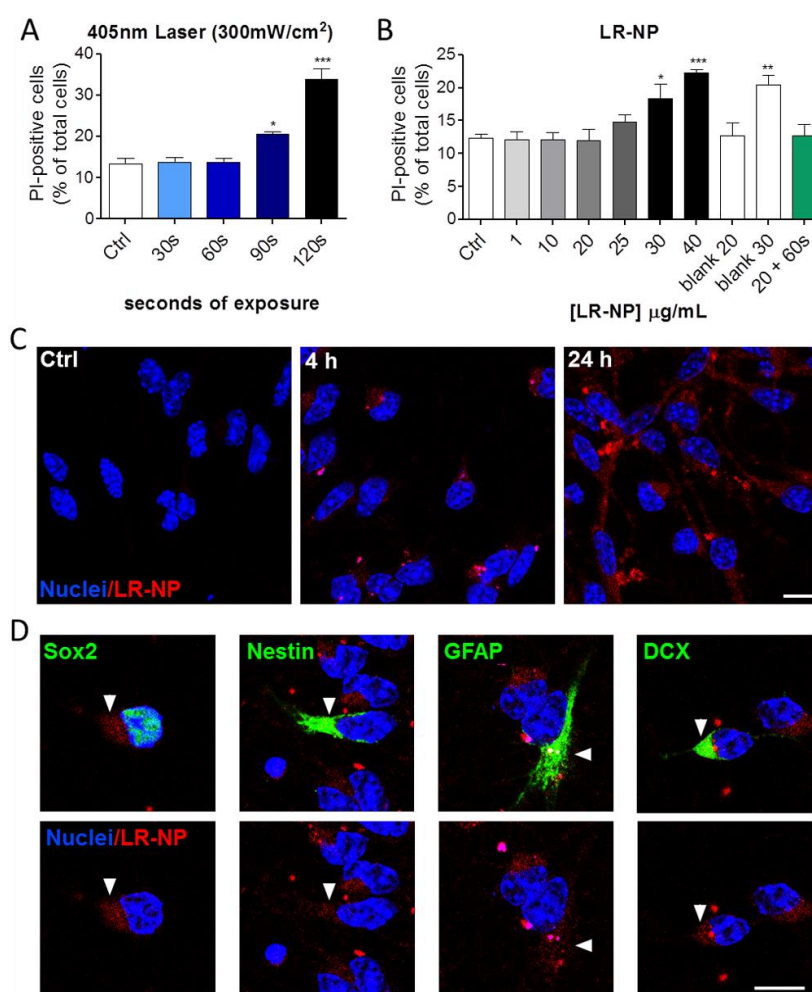
Figure 4.1. Cell viability and tracking studies of light-responsive RA-loaded nanoparticles (LR-NP) in SVZ cells. Percentage of propidium iodide (PI)-positive cells in cultures exposed to (A) 405 nm laser and/or (B) LR-NP 2 days after treatment. Data are expressed as percentage of total cells (mean ± SEM; n = 3). *$P < 0.05$, **$P < 0.05$, ***$P < 0.001$ vs. control using Bonferroni's Multiple Comparison Test. (C) Representative confocal digital images of internalized LR-NP (20 µg/mL; red). (D) Representative confocal images of LR-NP internalization by different subventricular zone cell phenotypes, namely (sex determining region Y)-box 2 (Sox2), nestin, glial fibrillary acidic protein (GFAP) and doublecortin (DCX) 24 h post treatment. All phenotypic markers are shown in green and nuclei in blue. Scale bars = 10µm.

This is in line with our previous studies (Maia *et al.* 2011) and others (Varkouhi *et al.* 2011; Benjaminsen *et al.* 2013) where PEI-based nanoparticles were associated to a rapid escape from endo-lysosomal fate. The effect through which PEI-based NP escape endolysosomes is still debatable. The "proton sponge" effect is thought to be the main responsible mechanism for endosome rupture and NP escape (Varkouhi *et al.* 2011). However, this mechanism was recently questioned since no lysosomal pH alterations happen when PEI is present (Benjaminsen *et al.* 2013). Nevertheless, PEI buffering capacity is thought to facilitate its interaction with the endo-lysosome membrane, creating tension and opening pores (Bieber *et al.* 2002). By escaping into the cytoplasmic compartment, NP and their cargo evade the acidic pH-induced degradation. In the present work, LR-NP internalization was homogenous throughout the cell culture, indicating that no preferential cellular uptake was occurring, similarly to the results obtained with our previous polymeric formulation (Maia *et al.* 2011). This was confirmed by co-labeling different SVZ cell phenotypes after 24 h, namely (sex determining region Y)-box 2 (Sox2)-positive self-renewing and multipotent cells, nestin-positive progenitor cells, glial fibrillary acidic protein (GFAP)-positive astrocytic cells and doublecortin (DCX)-positive neuronal precursor cells/neuroblasts (Figure 4.1D). Noteworthy, our target population, the self-renewing multipotent stem/progenitors, internalize LR-NP.

4.2.3 - NEURONAL DIFFERENTIATION ANALYSIS

Based on the previous results, LR-NP concentration up to 20 µg/mL and laser exposure time up to 60 sec were then used to evaluate the neurogenic potencial of our formulation (Figure 4.2). Remarkably, 60 sec of laser alone significantly increased the number of NeuN-positive mature neurons 7 days after a single treatment ($312.9 \pm 8.3\%$; $P < 0.001$). This neurogenic effect was further enhanced when cells were pre-treated with 0.6 µg/mL LR-NP before 60 sec of laser exposure ($443.2 \pm 36.4\%$; $P < 0.05$) but not when 0.6 µg/mL blank NP were used ($307.2 \pm 9.1\%$). The enhancement of neurogenesis detected upon 0.6 µg/mL LR-NP in combination with 60 sec is attributed to laser-induced release of RA. Noteworthy, neuronal differentiation was less evident when using higher concentrations of LR-NP, indicating that RA-induced neurogenesis is dose dependent. Accordingly, we have previously reported that RA

has an optimal concentration window to drive the neuronal commitment of SVZ cells (Maia *et al.* 2011). A minor increase in NeuN-positive cells was detected for LR-NP alone treatment (no laser exposure; 0 sec), meaning that some RA might be leaking from LR-NP. However, these results are not statistically significant. Interestingly, 30 sec of laser exposure required a higher concentration of LR-NP (2 μg/mL) to achieve an amplified neurogenic effect (234.8 ± 34.5%; P < 0.01). By repeating the 30 sec laser treatment 24 h after the first stimulation, no differences in neuronal differentiation were detected (245.7 ± 39.2%; P < 0.01; data not shown). For that reason, and to avoid repeated exposure-induced cytotoxicity, we proceeded with our established protocol of one single 405 nm laser treatment.
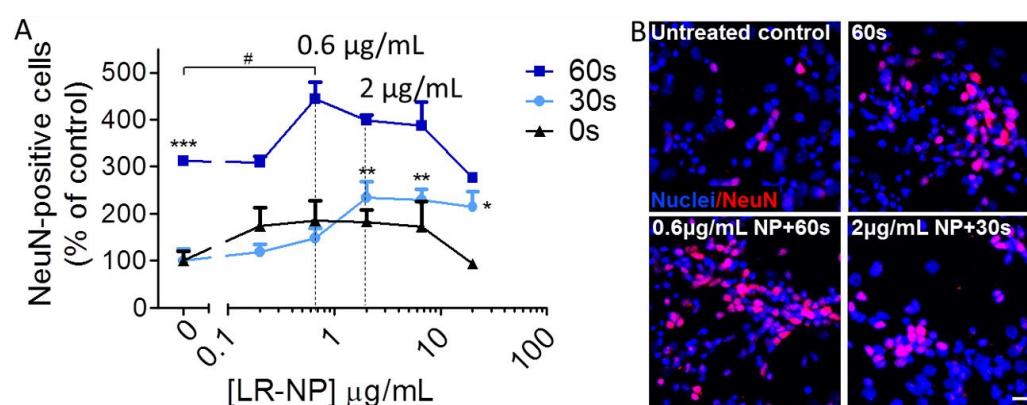
Figure 4.2. Light-responsive RA-loaded nanoparticle (LR-NP) treatment and 405 nm laser shining induce neuronal differentiation. (A) SVZ cells were treated with LR-NP (0.2-20uM) alone (0s; no laser exposure) or in combination with a single 405 nm laser treatment for 30 or 60 sec. Percentage of NeuN-positive neurons relative to untreated control cells was determined by immunocytochemistry 7 days after treatment (mean ± SEM; n = 3). *P < 0.05, **P < 0.05, ***P < 0.001 vs. control and #P < 0.05 vs. 60s alone using Bonferroni's Multiple Comparison Test. (B) Representative confocal digital images of NeuN (red) immunocytochemistry (nuclei in blue). Scale bar = 20μm.

To the best of our knowledge, there are no reports describing blue light-induced neuronal differentiation of NSC. However, blue light-induced differentiation was reported for other types of stem cells. As an example, one single exposure to UVB was reported to activate hair follicle melanocyte precursors and originate epidermal melanocytes *via* cell extrinsic mechanisms involving growth factor release (Ferguson *et al.* 2015). Moreover, a separate study reported that epidermal keratinocytes and epidermal melanocytes secrete Wnt7 upon UVB exposure.

Secreted Wnt7 was then responsible for melanocyte stem cell differentiation through the activation of Wnt/β-catenin signaling pathway (Yamada *et al.* 2013). Additionally, recent data using low-level laser therapy revealed that near-infrared (NIR) light (700-1400nm) improves neurological performance in traumatic brain injury (Huang *et al.* 2012b; Xuan *et al.* 2013; Xuan *et al.* 2014). In fact, 18 J/cm^2 of NIR, the same fluence we obtain with 60 sec, was able to increase the number of new neurons in a mouse model of traumatic brain injury (Xuan *et al.* 2014). Additionally, NIR was also reported to differentiate human dental pulp stem cells both *in vitro* and *in vivo* through the activation of endogenous latent transforming growth factor–beta 1 (TGF-β1) (Arany *et al.* 2014).

4.2.4 - EVALUATION OF NSC COMMITMENT

To better understand the effect of 405 nm laser alone or in combination with LR-NP on the initial steps of cell commitment, Ki67-positive proliferating cells were co-labeled for different neural phenotypes 2 days after treatment. For that reason, treatments were narrowed to 60 sec of laser, 0.6 µg/mL of LR-NP or the combination of both. This concentration of LR-NP was chosen based on the neurogenic potential demonstrated in combination with 60 sec of laser treatment (Figure 4.2). Albeit not significantly, a decreased number of proliferating cells when using light alone or in combination with LR-NP was detected (Figure 4.3A), possibly due to UV-induced G2/M delay (Bulavin *et al.* 2001). G2/M is a DNA repair checkpoint that prevents damaged cells from entering mitosis. There were no alterations detected in the number of proliferative Nestin- and Sox2-positive cells, meaning that the stem-like population of self-renewing and multipotent cells is not affected in detriment to neuronal differentiation (Figure 4.3B, C). This result has high therapeutic relevance considering that SVZ neurogenic niche can be mobilized without exhausting its stem population. As expected, the number of proliferating DCX-positive neuroblasts was significantly increased in both 60 sec laser (65.3 ± 11.0%; P < 0.05) and LR-NP+60s (80.7 ± 5.1%; P < 0.01) comparing to control (40.7 ± 6.6%), but not in LR-NP alone condition (Figure 4.3D). In contrast to neuronal differentiation results (Figure 4.2A), there was no statistical significance in neuroblast proliferation between 60s laser and LR-NP+60s treatments, although an increasing trend for LR-NP+60s was detected. One

possibility is that some neural stem/progenitor cells are undergoing conversion into neurons without cell division. Direct differentiation of stem cells was recently described and it is accompanied by a decrease of the NSC pool (Barbosa *et al.* 2015).
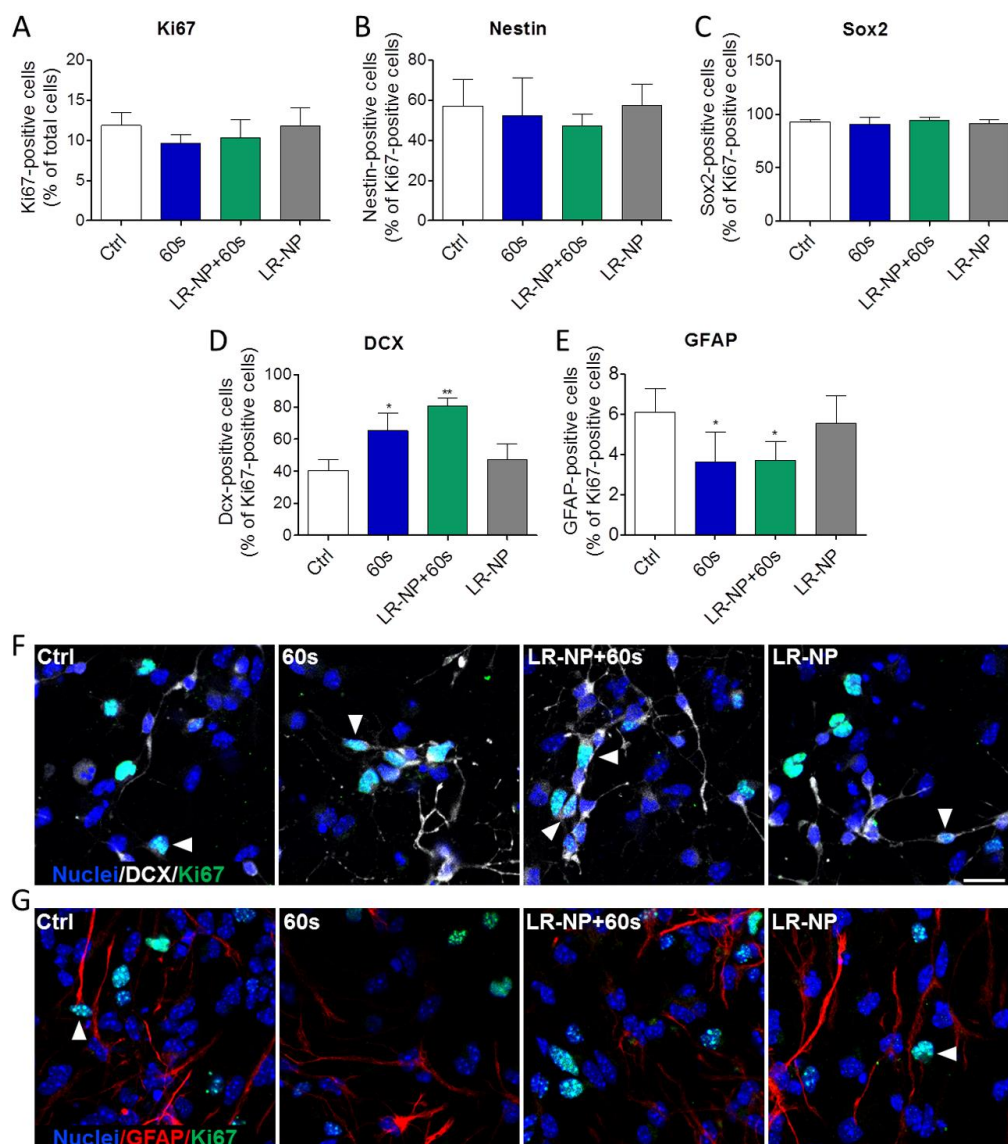
Figure 4.3. Light (405 nm laser) and light-responsive RA-loaded nanoparticles (LR-NP) induce neuronal commitment. (A) Percentage of Ki67-positive cells 2 days after treatment with 60 sec of 405 nm laser, 0.6 µg/mL LR-NP+60s or 0.6 µg/mL LR-NP. Within Ki67-positive cells, different phenotypes were co-labeled, namely (B) nestin, (C) (sex determining region Y)-box 2 (Sox2), (D) doublecortin and (E) glial fibrillary acidic protein (GFAP) (mean ± SEM; n = 3). *P < 0.05, **P < 0.05 vs. control using two-tailed unpaired Student t-test. Representative confocal digital images of (F) DCX/Ki67 and (G) GFAP/Ki67 immunostainings. White arrowheads depict double-positive cells. Scale bar = 20µm.

Accordingly, there is a decreasing trend for proliferating Nestin-positive cells in LR-NP+60s-treated cells that, if derived from direct conversion, might contribute to the statistical difference found 7 days after treatment (LR-NP+60s vs 60s; Figure 4.2A). The observed increase in proliferating neuroblasts was accompanied by a decrease in GFAP-positive astrocytic cell proliferation (Figure 4.3E). In this case there were no differences between the significance of 60s laser treatment ($3.7 \pm 1.5\%$; $P < 0.05$) and LR-NP+60s laser ($3.7 \pm 1.0\%$; $P < 0.05$) *versus* control ($6.1 \pm 1.2\%$). Since we have previously reported that RA-loaded polymeric nanoparticles do not affect astrocytic differentiation (Santos *et al.* 2012a), this result might indicate that decreased astrocytic proliferation is a characteristic restricted to laser-induced differentiation.

4.2.5 - LIGHT INDUCES TRANSIENT MITOCHONDRIAL OXIDATIVE STRESS

To disclose the mechanisms behind the neuronal differentiation induced by blue light, we focused our study using laser treatments alone. High energy wavelengths can induce mitochondrial DNA (mDNA). mDNA damage leads to mitochondrial dysfunction, resulting in higher levels of superoxide production (Raha *et al.* 2000). Accordingly, we observed a significant increase in mitochondrial superoxide 30 min after 60s ($152.7 \pm 7.1\%$; $P < 0.05$), reaching its maximum at 1 h ($158.9 \pm 7.2\%$; $P < 0.05$) and decreasing back to basal levels at 7h (Figure 4.4A). Treatment with 30 sec of laser exposure was not capable of inducing significant superoxide alterations. Mitochondrial superoxide dismutes into hydrogen peroxide (H_2O_2) spontaneously or enzymatically by manganese superoxide dismutase (MnSOD), the main dismutase in mitochondria (Finkel 2011). In opposition to the negatively charged superoxide anion, hydrogen peroxide readily permeates biological membranes, thus escaping mitochondria. For that reason we also evaluated cytosolic H_2O_2 levels and found a significant increase 3 h after 60s ($258.7 \pm 17.8\%$; $P < 0.05$) reaching its peak at 7 h ($288.6 \pm 31.2\%$; $P < 0.01$). After 36 h, basal peroxide levels were rescued (Figure 4.4B). In fact, tightly regulated mROS transiently shift as part of cellular processes. Physiologically, low levels of mROS work as signaling pathways in processes such as differentiation, autophagy, metabolic adaptation and immune cell activation (Sena *et al.* 2012). Rharass and colleagues demonstrated that the primary trigger

for neuronal differentiation upon growth factor depletion in human neural progenitor cells is the generation of Ca^{2+}-mediated mROS. Interestingly, they reported that after growth factor depletion mROS reached a maximum increase of ~200% at 1 h and this increase was significantly but not completely restored at 3 h (no further time points were tested) (Rharass *et al.* 2014). Xavier and colleagues also corroborate our findings by reporting a transient increase in superoxide mROS 1 h after the induction of NSC differentiation (Xavier *et al.* 2014). These results are in line with the ones obtained by us when using 60 sec, indicating that 405 nm laser exposure is capable of triggering processes occurring at early stages of NSC differentiation.
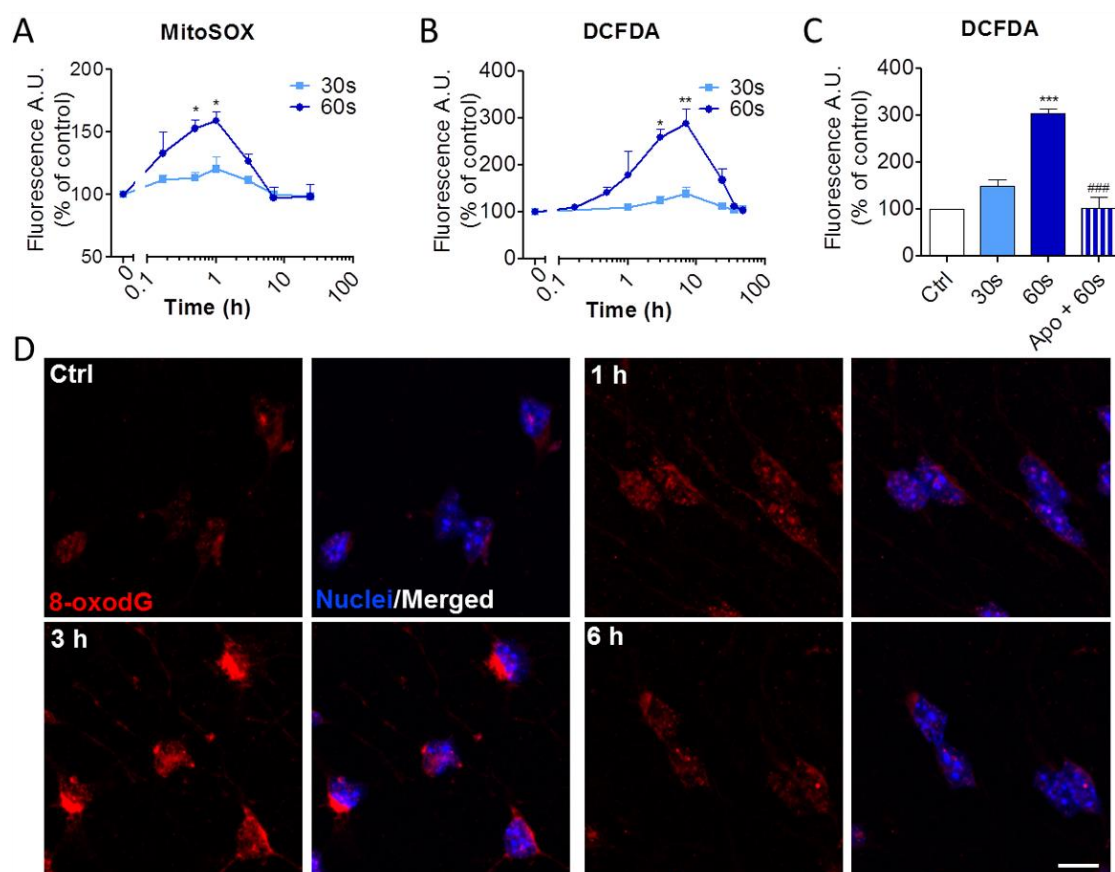
Figure 4.4. Light (405 nm laser) induces transient mitochondrial ROS production and DNA damage. Graph depicts (A) mitochondrial superoxide levels or (B) cytosolic peroxide levels throughout time after 30 or 60 sec of laser exposure (mean ± SEM; n=3). *P < 0.05, **P < 0.05, ***P < 0.001 vs. control using Bonferroni's Multiple Comparison Test. (C) Graph depicts cytosolic peroxide levels 7 h after treatments; Apo – Apocynin; Data are expressed as percentage of control (mean ± SEM; n = 3). ***P < 0.001 vs control, ###P > 0.001 vs. 60 sec using two-tailed unpaired Student t-test. (D) Representative confocal digital images of 60 sec laser treated cells labeled for 8-oxo-7,8-dihydro-2-deoxyguanosine (8-oxodG; red). Scale bar = 10μm.

Nicotinamide adenine dinucleotide phosphate (NADPH) oxidases (Nox) are superoxide-generating enzymes that participate in several biological processes such as host defense, protein post-translational processing, cellular signaling, gene expression regulation, and cell differentiation. Increased activity of Nox enzymes is also associated with pathological conditions such as cardiovascular and neurodegenerative diseases (reviewed by Bedard *et al.*) (Bedard *et al.* 2007). To evaluate Nox participation in this process, we have selected the 7 h time point, in which we have found the highest increase in cellular ROS, to pre-treat cells with apocynin (Apo), a routinely used Nox inhibitor (Figure 4.4C). Apo-pre-treated cells presented peroxide levels similar to untreated control and statistically different from 60 sec of laser treatment alone (Apo+60s: $101.8 \pm 24.4\%$; 60s: $303.2 \pm 9.8\%$; $P < 0.001$).

Oxidative DNA lesions such as the induction of 8-oxo-7,8-dihydro-2-deoxyguanosine (8-oxodG) also occur upon UV exposure in both nuclear and mitochondrial DNA (Besaratinia *et al.* 2005). This type of lesion was transiently detected 3 h after 60 sec of laser treatment (Figure 4.4D). However, 8-oxodG was primarily detected in cytoplasm rather than the cell nucleus, indicating that mitochondrial DNA (mDNA) is more vulnerable to laser-induced damage than nuclear DNA. This singularity is in accordance with other reports describing mDNA to be more susceptible to lesions during oxidative stress events associated or not with ageing (Raha *et al.* 2000). As a matter of fact, mDNA damage was reported to be a reliable UV-induced oxidative stress marker (Birch-Machin *et al.* 2013). Nevertheless, in our setup the increase in 8-oxodG is transient and completetly reversed 6 h after treatment.

4.2.6 - INVOLVEMENT OF THE NOX FAMILY IN ROS GENERATION

Our results demonstrated that upon light exposure, mROS are increased and mDNA is affected. Mitochondrial sources of ROS include complexes I and III and Nox4. Nox4 is the only constitutively active Nox isoform. This enzyme is also implicated in processes generated by damage signals (Tang *et al.* 2014). Western blot results demonstrated that Nox4 is upregulated 1 h after 60 sec ($263.3 \pm 31.0\%$; $P < 0.05$; Figure 4.5A). Nox4 was reported to be the only Nox enzyme involved in fate determination and differentiation of neural crest stem

cells during embryogenesis (Lee *et al.* 2014). Moreover, Nox4-derived ROS promote embryonic stem cell differentiation into smooth muscle cells (Xiao *et al.* 2009) or cardiac cells (Li *et al.* 2006). For cardiovascular differentiation of embryonic stem cells by mechanotransduction, the involvement of both Nox4 and Nox1 enzymes are critical in early stages of differentiation (Sauer *et al.* 2008). Other Nox isoforms can also be activated. In fact, it was described that mROS trigger Nox1 action by stimulating phosphoinositide 3-kinase (PI3K) and Rho GTPase Rac1 (Lee *et al.* 2006). Active Rac1 induces the activation of the Nox complex. Accordingly, we have detected an increase in both Rac1 (167.9 ± 20.0; P < 0.05) and Nox1 (230.0 ± 71.1%; P < 0.05) expression at 3 h (Figure 4.5C). Noteworthy, other processes occurring during DNA repair can also activate Rac1. The enzyme 8-oxoguanine DNA glycosylase-1 (OGG1), responsible for 8-oxodG excision, together with free 8-oxodG base pairs released during DNA repair also activate Rac1, leading to increased Nox-derived ROS levels (Hajas *et al.* 2013). DNA damage also induces phosphorylation of histone H2AX, activating Rac1 GTPase and Nox1, resulting in increased ROS (Kang *et al.* 2012).
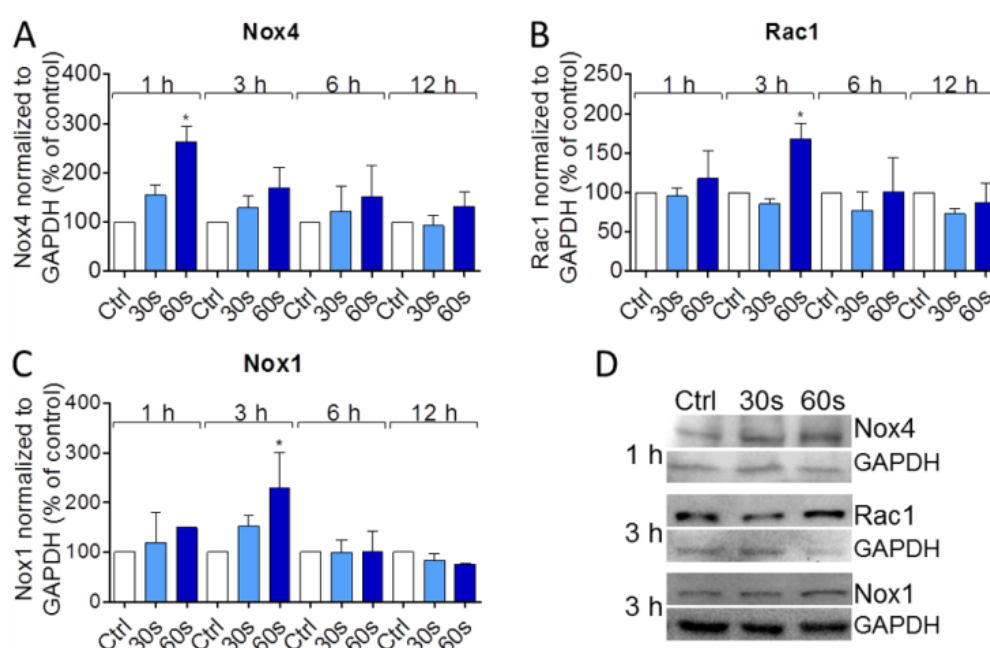
Figure 4.5. Light (405 nm laser) treatment increases NADPH oxidase (Nox) and Rac1 expression. Graph depicts the percentage relative to control of (A) Nox4, (B) Rac1 and (C) Nox1 protein expression normalized to GAPDH in cultures exposed to 405 nm laser (30 or 60 sec) after 1, 3, 6 and 12 h. Data are expressed as percentage of control ± SEM (n = 3-4). *P < 0.05 vs control using two-tailed unpaired Student t-test. (D) Representative Nox4 (65 kDa), Rac1 (20 kDa), Nox1 (65 kDa) and GAPDH (37 kDa) western blots.

Importantly, all the processes described here activate Rac1. This enzyme is also implicated in neurogenic processes occurring in both adult neurogenic niches, the SVZ and subgranular zone (SGZ) of the hippocampus. Rac1 is required for normal proliferation, survival and differentiation of SVZ progenitors in the developing forebrain (Leone *et al.* 2010) and synaptic plasticity, dendritic spine structure, hippocampal spatial memory and learning-evoked neurogenesis in the SGZ (Haditsch *et al.* 2009; Haditsch *et al.* 2013).

4.2.7 - DISSOCIATION OF DVL FROM NRX ACTIVATES β-CATENIN

Mitochondrial superoxide-derived cytosolic hydrogen peroxide is considered the primary type of signaling ROS, acting mainly *via* the oxidation of proteins containing thiol groups (Sena *et al.* 2012). Examples of such proteins include glutathione, protein phosphatases, peroxiredoxin, thioredoxin (TRX) and nucleoredoxin (NRX). NRX is a TRX-like protein that interacts with Dishevelled (Dvl), a key player downstream from Wnt receptors (Funato *et al.* 2006). During Wnt signaling activation, Dvl stabilizes β-catenin that, in turn, translocates to the nucleus and induces neurogenic gene transcription through the activation of T cell factor (TCF) and/or lymphoid enhancer factor (LEF) (Reya *et al.* 2005). In the absence of ROS, NRX is bound do Dvl inactivating its functions. However, increased ROS levels oxidize NRX thiol groups leading to structural changes that result in Dvl dissociation. Free Dvl is then capable of activating Wnt/β-catenin signaling pathway (Funato *et al.* 2006). This pathway is divided into canonical (β-catenin-dependent) and noncanonical (β-catenin-independent) Wnt signaling pathways. Both are essential in the developing and adult brain and are activated distinctly depending on the ligands and receptors involved. Wnt signaling can drive neural stem cell self-renewal, expansion, asymmetric cell division, maturation and differentiation (reviewed by (Bengoa-Vergniory *et al.* 2015)). During the process of NSC neuronal differentiation, Dvl2 was reported to dissociate from NRX after 1 h of growth factor depletion (Rharass *et al.* 2014). Accordingly, our co-immunoprecipitation studies confirmed that 60 sec of laser treatment induces the dissociation between Dvl2 and NRX after 1 h (Figure 4.6A). Again, 30 sec revealed to be insufficient to trigger mechanisms associated with neuronal differentiation. Moreover, this redox sensitive dissociation of Dvl2 was accompanied by an increase in β-catenin levels.

Active β-catenin was detected as soon as 2 h after 60s (Figure 4.6B). Importantly, our data is in accordance with the processes reported to occur at early stages of NSC differentiation, namely Dvl dissociation and β-catenin activation (Rharass *et al.* 2014). Quantification by western blot confirmed a significant increase in β-catenin activation (196.2 ± 42.0%; P < 0.05; Figure 4.6C). Noteworthy, this effect was not detected when cells were pre-incubated with apocynin (120.5 ± 15.9%).
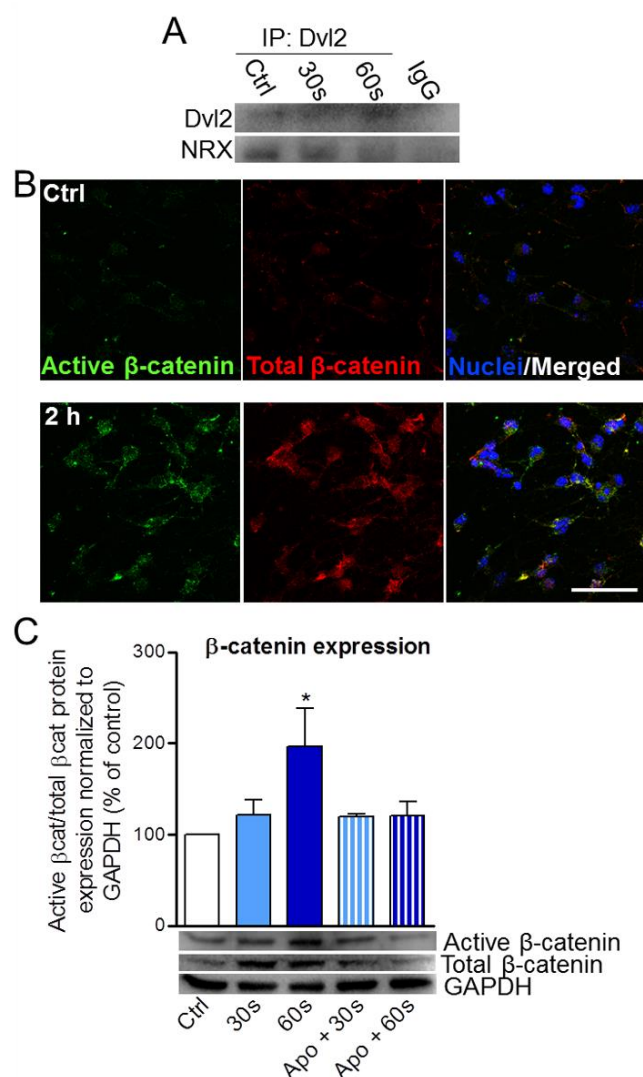
Figure 4.6. Light (405 nm laser) dissociate Dvl2 from NRX and activate β-catenin. (A) Anti-Dvl2 co-immunoprecipitation of neural stem cell lysates 1 h after treatment with 405 nm laser (30 or 60 sec) or IgG as control; Dvl2 (92 kDa), NRX (55 kDa). (B) Representative confocal images of active β-catenin (green), total β-catenin (red) and nuclei (blue) in control cultures and in cultures 2 h after exposure to 60 sec. Scale bar = 50μm. (C) Graph depicts the ratio of active β-catenin to total β-catenin levels normalized to GAPDH 2 h after treatment. Apo – Apocynin; Data are expressed as percentage of control (mean ± SEM n=3-4). *P < 0.05 *vs.* control, using Bonferroni's Multiple Comparison Test. A representative western blot of active β-catenin (95 kDa), total β-catenin (95 kDa) and GAPDH (37 kDa) is shown below the graph.

4.2.8 - RETINOIC ACID RECEPTOR ALPHA (RARα) UPREGULATION ENHANCES NEURONAL DIFFERENTIATION

To confirm the above-mentioned proposed mechanisms, neuronal differentiation was evaluated by NeuN (mature neuronal marker) expression in the presence of Apo (Nox inhibitor) and IWR-1-endo (IWR; inhibitor of β-catenin action). As predicted, both inhibitors were able to independently suppress 60s-induced neuronal differentiation. However, pre-treatment with Apo or IWR generated different outcomes in combination with LR-NP (0.6 µg/mL) and 60s. IWR+LR-NP+60s-induced differentiation (290.8 ± 19.2%) was significantly higher than Apo+LR-NP+60s (194.0 ± 14.0%; P < 0.05). By dissecting the proposed mechanism of differentiation, we may suggest that IWR acts downstream of Apo. While Apo inhibits the initial formation of ROS, IWR only inhibits the later-stage β-catenin action. These results indicate that LR-NP+60s treatment includes another variable affecting neuronal differentiation that was not present using laser alone. When cells are exposed to LR-NP-released retinoic acid, ROS also activate additional mechanisms that may enhance RA-induced neuronal differentiation. One of which, particularly relevant, was recently reported by Cao and colleagues demonstrating that moderate ROS stabilize RARα through NF-κB signaling (Cao *et al.* 2015). In turn, increased levels of RARα enhance RA-induced differentiation. We confirmed this hypothesis by western blotting. Notably, increased protein levels of RARα were detected 12 h after 60s treatment (248.3 ± 62.8%; P < 0.05; Figure 4.7B).
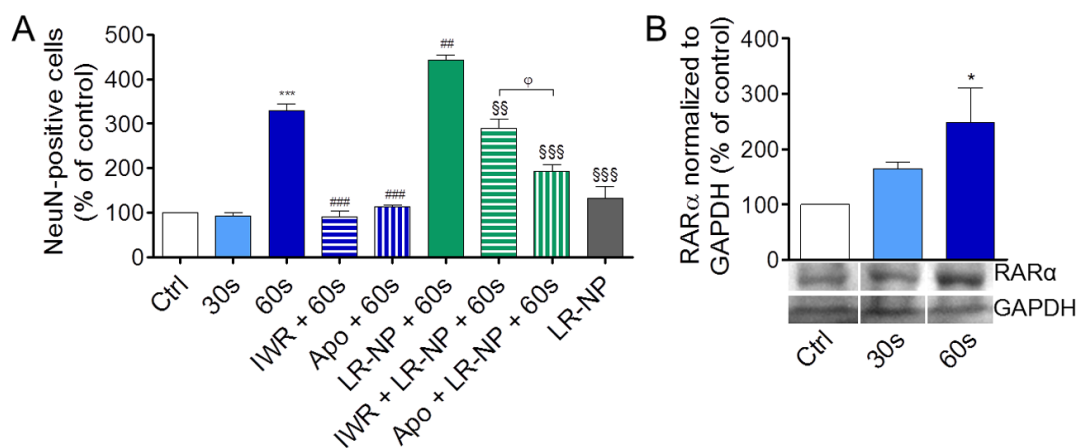
Figure 4.7. Light (405 nm laser)-induced ROS increase retinoic acid receptor alpha (RARα) levels resulting in enhanced neurogenesis from light-responsive RA-loaded nanoparticles (LR-NP). (A) SVZ cells were treated with LR-NP (0.6 µg/mL) and/or 405 nm laser (30 or 60 sec) alone or in combination with apocynin (Apo) or IWR-1-endo (IWR).

Percentage of NeuN-positive neurons relative to untreated control cells was determined by immunocytochemistry 7 days after treatment (mean ± SEM; n=3-4).*P < 0.05, ***P < 0.001 vs. control; ##P < 0.005, ###P < 0.001 vs. 60s alone; §§P < 0.005, §§§P < 0.001 vs. LR-NP+60s using Bonferroni's Multiple Comparison Test. φP < 0.05 using two-tailed unpaired Student t-test (B) Graph depicts percentage relative to control of RARα protein expression normalized to GAPDH in cultures exposed to 405 nm laser (30 or 60 sec) (mean ± SEM; n = 3). *P < 0.05 vs control using two-tailed unpaired Student t-test. A representative western blot of RARα (51 kDa) and GAPDH (37 kDa) is shown below the graph.

4.3 - CONCLUSIONS

We report an innovative and efficient platform to differentiate adult neural stem cells by using light-responsive RA-loaded nanoparticles (Figure 4.8). The main finding we report is that LR-NP can efficiently induce neurogenesis upon light (405 nm laser) exposure by enabling the intracellular delivery of RA, therefore offering great advantages regarding temporal and spatial control of RA release. Additionally, we demonstrated the mechanisms by which light alone has neurogenic properties. In fact, one single pulse of 60 sec (300 mW/cm^2, 18 J/cm^2 fluence) transiently induces the generation of mitochondrial Nox-derived ROS to levels similar to the ones found during earlier stages of induced neuronal differentiation (Rharass *et al.* 2014; Xavier *et al.* 2014). Cytoplasmic ROS dissociate Dvl2 from NRX, resulting in β-catenin-induced neurogenesis. Based on the capacity to induce mitochondrial ROS other wavelengths such as NIR might act *via* similar mechanisms, demonstrating that, when finely tuned, light is capable of triggering ROS-involved physiological processes. Other major finding is that laser-induced ROS up-regulate the expression of retinoic acid receptor alpha (RARα), which enhances RA-induced neurogenesis, further highlighting the relevance of our combinatorial treatment for brain regenerative therapies. In this sense, our approach relying on the modulation of SVZ endogenous stem cells for the generation of new neurons is very promising and may potentially replace dead cells and restore neuronal circuits in neurodegenerative diseases such as Huntingtons's disease, PD and stroke. Additionally, another neurogenic niche is affected in AD, the SGZ of the dentate gyrus in the hippocampus. It is known that stimulating neurogenesis in this region is beneficial to halt AD progression. By aiming LR-NP treatment and targeting laser stimulus to the NSC of the hippocampus, our therapy is also expected to delay disease progression and/or promote reversion, further highlighting its broad applicability. The

successful development of this platform may provide innovative and efficient therapeutic applications for a large spectrum of brain repair strategies.
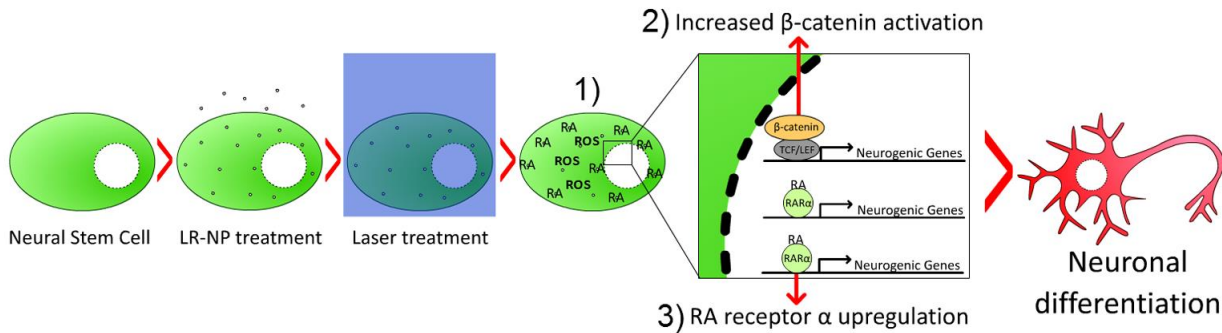
Figure 4.8. Combinatorial treatment of light-responsive retinoic-acid loaded nanoparticles (LR-NP) and light (405 nm laser) induces neural differentiation. Treatment is summarized in the present scheme. Neural stem cells were treated with LR-NP (black dots) and light (blue). Light is capable of 1) inducing the production of reactive oxygen species (ROS) and the release of retinoic acid (RA) from LR-NP, 2) increasing β-catenin activity, leading to the expression of neurogenic genes, and 3) increasing retinoic acid receptor alpha expression, sensitizing the cell for RA-induced expression of neurogenic genes. Altogether, LR-NP together with light induces a neuronal differentiation increase of approximately 450%.

CHAPTER 5

General Conclusions

The innovation of the work herein presented resides in the efficient induction of neuronal differentiation *in vivo* and efficient delivery of a pro-neurogenic drug upon an external stimulus by nanoparticulate systems. RA is one powerful pro-neurogenic molecule when delivered intracellularly, and nanoparticles provide the perfect platform to ensure this task. Noteworthy, in Chapter 3 we reported the use of RA-loaded polymeric nanoparticles to induce the neuronal differentiation of subventricular zone neural stem cells. The intracellular delivery of RA *via* nanoparticles activated nuclear retinoic acid receptors, decreased stemness, and increased a more robust proneurogenic gene expression than free RA. Additionally, we described for the first time a nanoparticle formulation able to modulate *in vivo* the subventricular zone neurogenic niche.

However, the *in vivo* use of biomaterials and differentiating factors must be well established, since bioaccumulation and concomitant toxicity can originate undesired side-effects. For that reason, in Chapter 4 stimuli-responsive RA-loaded nanoparticles were developed. The stimulus used was light (405nm laser) which demonstrated neurogenic capabilities through the transient induction of NADPH oxidase-mediated ROS and β-catenin activation improving the neurogenic potential of RA *via* its receptor RARα. Therefore, an amplified neurogenic effect was obtained when using this combinatory therapy. Nevertheless, to prove the feasibility of this approach, *in vivo* studies still need to be conducted. With the successful demonstration of *in vivo* applicability, RA-loaded nanoparticles can be further optimized. Using a near-infrared (NIR)-responsive molecule such as 2-diazo-1,2-naphthoquinones (DNQ) to trigger the release of RA, it would be possible to bypass the invasive implantation of fiber-optic required for blue light treatments. NIR has high clinical relevance since it covers the tissue transparency window of the spectrum while sharing similar biological effects with blue light, namely the induction of neurogenesis and mitochondria-derived ROS. Thus, it is conceivable that the combinatorial effect of light- and RA-induced neurogenesis can be also observed with this wavelength. Nonetheless, further studies still need to be conducted to confirm this premise.

Therefore, our work covers key aspects essential for the development of a new brain regenerative therapy based on the controlled delivery of RA and opens new perspectives for the treatment of brain injury and neurodegenerative diseases.

CHAPTER 6

References

Abbott, A. (2011). "Dementia: a problem for our age." *Nature* 475(7355): S2-4.

Agasse, F., Bernardino, L., Kristiansen, H., Christiansen, S. H., Ferreira, R., Silva, B., Grade, S., Woldbye, D. P. D. and Malva, J. O. (2008a). "Neuropeptide Y Promotes Neurogenesis in Murine Subventricular Zone." *Stem Cells* 26(6): 1636-1645.

Agasse, F., Bernardino, L., Silva, B., Ferreira, R., Grade, S. and Malva, J. O. (2008b). "Response to Histamine Allows the Functional Identification of Neuronal Progenitors, Neurons, Astrocytes, and Immature Cells in Subventricular Zone Cell Cultures." *Rejuvenation Res* 11(1): 187-200.

Akerblom, M., Sachdeva, R. and Jakobsson, J. (2012). "Functional Studies of microRNAs in Neural Stem Cells: Problems and Perspectives." *Front Neurosci* 6: 14.

Al Tanoury, Z., Gaouar, S., Piskunov, A., Ye, T., Urban, S., Jost, B., Keime, C., Davidson, I., Dierich, A. and Rochette-Egly, C. (2014). "Phosphorylation of the retinoic acid receptor RARgamma2 is crucial for the neuronal differentiation of mouse embryonic stem cells." *Journal of Cell Science* 127(Pt 9): 2095-2105.

Al Tanoury, Z., Piskunov, A. and Rochette-Egly, C. (2013). "Vitamin A and retinoid signaling: genomic and nongenomic effects: Thematic Review Series: Fat-Soluble Vitamins: Vitamin A." *Journal of Lipid Research* 54(7): 1761-1775.

Alvarez-Buylla, A., García-Verdugo, J. M., Mateo, A. S. and Merchant-Larios, H. (1998). "Primary Neural Precursors and Intermitotic Nuclear Migration in the Ventricular Zone of Adult Canaries." *The Journal of Neuroscience* 18(3): 1020–1037.

Alyautdin, R., Khalin, I., Nafeeza, M. I., Haron, M. H. and Kuznetsov, D. (2014). "Nanoscale drug delivery systems and the blood-brain barrier." *Int J Nanomedicine* 9: 795-811.

Anderson, D. W., Schray, R. C., Duester, G. and Schneider, J. S. (2011). "Functional significance of aldehyde dehydrogenase ALDH1A1 to the nigrostriatal dopamine system." *Brain Research* 1408: 81-87.

Arany, P. R., Cho, A., Hunt, T. D., Sidhu, G., Shin, K., Hahm, E., Huang, G. X., Weaver, J., Chen, A. C., Padwa, B. L., Hamblin, M. R., Barcellos-Hoff, M. H., Kulkarni, A. B. and D, J. M. (2014). "Photoactivation of endogenous latent transforming growth factor-beta1 directs dental stem cell differentiation for regeneration." *Sci Transl Med* 6(238): 238ra269.

Arvidsson, A., Collin, T., Kirik, D., Kokaia, Z. and Lindvall, O. (2002). "Neuronal replacement from endogenous precursors in the adult brain after stroke." *Nature Medicine* 8(9): 963.

Ashton, R. S., Conway, A., Pangarkar, C., Bergen, J., Lim, K. I., Shah, P., Bissell, M. and Schaffer, D. V. (2012). "Astrocytes regulate adult hippocampal neurogenesis through ephrin-B signaling." *Nature Neuroscience* 15(10): 1399-1406.

Barbosa, J. S., Sanchez-Gonzalez, R., Di Giaimo, R., Baumgart, E. V., Theis, F. J., Gotz, M. and Ninkovic, J. (2015). "Neurodevelopment. Live imaging of adult neural stem cell behavior in the intact and injured zebrafish brain." *Science* 348(6236): 789-793.

Bastien, J. and Rochette-Egly, C. (2004). "Nuclear Retinoid Receptors and the Transcription of Retinoid-Target Genes." *Gene* 328: 1-16.

Bedard, K. and Krause, K. H. (2007). "The NOX family of ROS-generating NADPH oxidases: physiology and pathophysiology." *Physiological Reviews* 87(1): 245-313.

Bengoa-Vergniory, N. and Kypta, R. M. (2015). "Canonical and noncanonical Wnt signaling in neural stem/progenitor cells." *Cellular and Molecular Life Sciences*.

Benjaminsen, R. V., Mattebjerg, M. A., Henriksen, J. R., Moghimi, S. M. and Andresen, T. L. (2013). "The Possible "Proton Sponge" Effect of Polyethylenimine (PEI) Does Not Include Change in Lysosomal pH." *Molecular Therapy* 21(1): 149-157.

Bernardino, L., Agasse, F., Silva, B., Ferreira, R., Grade, S. and Malva, J. O. (2008). "Tumor Necrosis Factor-alpha Modulates Survival, Proliferation, and Neuronal Differentiation in Neonatal Subventricular Zone Cell Cultures." *Stem Cells* 26(9): 2361-2371.

Bernardino, L., Eiriz, M. F., Santos, T., Xapelli, S., Grade, S., Rosa, A. I., Cortes, L., Ferreira, R., Bragança, J., Agasse, F., Ferreira, L. and Malva, J. O. (2012). "Histamine Stimulates Neurogenesis in the Rodent Subventricular Zone." *Stem Cells* 30(4): 773-784.

Besaratinia, A., Synold, T. W., Chen, H. H., Chang, C., Xi, B., Riggs, A. D. and Pfeifer, G. P. (2005). "DNA lesions induced by UV A1 and B radiation in human cells: comparative analyses in the overall genome and in the p53 tumor suppressor gene." *Proc Natl Acad Sci U S A* 102(29): 10058-10063.

Bharali, D. J., Klejbor, I., Stachowiak, E. K., Dutta, P., Roy, I., Kaur, N., Bergey, E. J., Prasad, P. N. and Stachowiak, M. K. (2005). "Organically Modified Silica Nanoparticles: a Nonviral Vector for *In Vivo* Gene Delivery and Expression in the Brain." *Proc Natl Acad Sci USA* 102(32): 11539-11544.

Bieber, T., Meissner, W., Kostin, S., Niemann, A. and Elsasser, H. P. (2002). "Intracellular route and transcriptional competence of polyethylenimine-DNA complexes." *J Control Release* 82(2-3): 441-454.

Birch-Machin, M. A., Russell, E. V. and Latimer, J. A. (2013). "Mitochondrial DNA damage as a biomarker for ultraviolet radiation exposure and oxidative stress." *British Journal of Dermatology* 169 Suppl 2: 9-14.

Boekhoorn, K., Joels, M. and Lucassen, P. J. (2006). "Increased proliferation reflects glial and vascular-associated changes, but not neurogenesis in the presenile Alzheimer hippocampus." *Neurobiol Dis* 24(1): 1-14.

Boussif, O., Lezoualc'h, F., Zanta, M. A., Mergny, M. D., Scherman, D., Demeneix, B. and Behr, J. P. (1995). "A versatile vector for gene and oligonucleotide transfer into cells in culture and in vivo: polyethylenimine." *Proc Natl Acad Sci U S A* 92(16): 7297-7301.

Brill, M. S., Snapyan, M., Wohlfrom, H., Ninkovic, J., Jawerka, M., Mastick, G. S., Ashery-Padan, R., Saghatelyan, A., Berninger, B. and Gotz, M. (2008). "A dlx2- and pax6-dependent transcriptional code for periglomerular neuron specification in the adult olfactory bulb." *J Neurosci* 28(25): 6439-6452.

Bruck, N., Vitoux, D., Ferry, C., Duong, V., Bauer, A., de The, H. and Rochette-Egly, C. (2009). "A coordinated phosphorylation cascade initiated by p38MAPK/MSK1 directs RAR[alpha] to target promoters." *EMBO J* 28(1): 34-47.

Bulavin, D. V., Higashimoto, Y., Popoff, I. J., Gaarde, W. A., Basrur, V., Potapova, O., Appella, E. and Fornace, A. J. (2001). "Initiation of a G2/M checkpoint after ultraviolet radiation requires p38 kinase." *Nature* 411(6833): 102-107.

Cai, L., Morrow, E. M. and Cepko, C. L. (2000). "Misexpression of basic helix-loop-helix genes in the murine cerebral cortex affects cell fate choices and neuronal survival." *Development* 127(14): 3021-3030.

Cao, Y., Wei, W., Zhang, N., Yu, Q., Xu, W. B., Yu, W. J., Chen, G. Q., Wu, Y. L. and Yan, H. (2015). "Oridonin stabilizes retinoic acid receptor alpha through ROS-activated NF-kappaB signaling." *BMC Cancer* 15: 248.

Carreira, B. P., Morte, M. I., Inácio, Â., Costa, G., Rosmaninho-Salgado, J., Agasse, F., Carmo, A., Couceiro, P., Brundin, P., Ambrósio, A. F., Carvalho, C. M. and Araújo, I. M. (2010). "Nitric Oxide Stimulates the Proliferation of Neural Stem Cells Bypassing the Epidermal Growth Factor Receptor." *Stem Cells* 28(7): 1219-1230.

Chambers, R. A., Potenza, M. N., Hoffman, R. E. and Miranker, W. (2004). "Simulated apoptosis/neurogenesis regulates learning and memory capabilities of adaptive neural networks." *Neuropsychopharmacology* 29(4): 747-758.

Chatagnon, A., Veber, P., Morin, V., Bedo, J., Triqueneaux, G., Semon, M., Laudet, V., d'Alche-Buc, F. and Benoit, G. (2015). "RAR/RXR binding dynamics distinguish pluripotency from differentiation associated cis-regulatory elements." *Nucleic Acids Research* 43(10): 4833-4854.

Chiang, M.-Y., Misner, D., Kempermann, G., Schikorski, T., Giguère, V., Sucov, H. M., Gage, F. H., Stevens, C. F. and Evans, R. M. (1998). "An Essential Role for Retinoid Receptors RAR[beta] and RXR[gamma] In Long-Term Potentiation and Depression." *Neuron* 21(6): 1353-1361.

Chu, T., Zhou, H., Wang, T., Lu, L., Li, F., Liu, B., Kong, X. and Feng, S. (2015). "In vitro characteristics of valproic acid and all-trans-retinoic acid and their combined use in promoting neuronal differentiation while suppressing astrocytic differentiation in neural stem cells." *Brain Research* 1596: 31-47.

Conway, A. and Schaffer, D. V. (2014). "Biomaterial microenvironments to support the generation of new neurons in the adult brain." *Stem Cells* 32(5): 1220-1229.

Conway, A., Vazin, T., Spelke, D. P., Rode, N. A., Healy, K. E., Kane, R. S. and Schaffer, D. V. (2013). "Multivalent ligands control stem cell behaviour in vitro and in vivo." *Nat Nanotechnol* 8(11): 831-838.

Coolen, M., Katz, S. and Bally-Cuif, L. (2013). "miR-9: a versatile regulator of neurogenesis." *Front Cell Neurosci* 7: 220.

Corcoran, J. and Maden, M. (1999). "Nerve Growth Factor Acts *via* Retinoic Acid Synthesis to Stimulate Neurite Outgrowth." *Nat Neurosci* 2(4): 307-308.

Crandall, J., Sakai, Y., Zhang, J., Koul, O., Mineur, Y., Crusio, W. E. and McCaffery, P. (2004). "13-cis-retinoic acid suppresses hippocampal cell division and hippocampal-dependent learning in mice." *PNAS* 101(14): 5111-5116.

Curtis, M. A., Kam, M., Nannmark, U., Anderson, M. F., Axell, M. Z., Wikkelso, C., Holtas, S., van Roon-Mom, W. M., Bjork-Eriksson, T., Nordborg, C., Frisen, J., Dragunow, M., Faull, R. L. and Eriksson, P. S. (2007). "Human neuroblasts migrate to the olfactory bulb via a lateral ventricular extension." *Science* 315(5816): 1243-1249.

Curtis, M. A., Low, V. F. and Faull, R. L. (2012). "Neurogenesis and progenitor cells in the adult human brain: a comparison between hippocampal and subventricular progenitor proliferation." *Dev Neurobiol* 72(7): 990-1005.

Curtis, M. A., Penney, E. B., Pearson, J., Dragunow, M., Connor, B. and Faull, R. L. M. (2005). "The distribution of progenitor cells in the subependymal layer of the lateral ventricle in the normal and Huntington's disease human brain." *Neuroscience* 132(3): 777-788.

Delcea, M., Mohwald, H. and Skirtach, A. G. (2011). "Stimuli-responsive LbL capsules and nanoshells for drug delivery." *Adv Drug Deliv Rev* 63(9): 730-747.

Dilworth, F. J. and Chambon, P. (2001). "Nuclear Receptors Coordinate the Activities of Chromatin Remodeling Complexes and Coactivators to Facilitate Initiation of Transcription." *Oncogene* 20(24): 3047-3054.

Doetsch, F., Caille, I., Lim, D. A., García-Verdugo, J. M. and Alvarez-Buylla, A. (1999a). "Subventricular Zone Astrocytes Are Neural Stem Cells in the Adult Mammalian Brain." *Cell* 97: 703-716.

Doetsch, F., Garcia-Verdugo, J. M. and Alvarez-Buylla, A. (1999b). "Regeneration of a Germinal Layer in the Adult Mammalian Brain." *Proc Natl Acad Sci USA* 96(20): 11619-11624.

Doetsch, F., García-Verdugo, J. M. and Alvarez-Buylla, A. (1997). "Cellular Composition and Three-Dimensional Organization of the Subventricular Germinal Zone in the Adult Mammalian Brain." *The Journal of Neuroscience* 17(13): 5046-5061.

Doetsch, F., Petreanu, L., Caille, I., García-Verdugo, J.-M. and Alvarez-Buylla, A. (2002). "EGF Converts Transit-Amplifying Neurogenic Precursors in the Adult Brain into Multipotent Stem Cells." *Neuron* 36: 1021-1034.

Dvir, T., Banghart, M. R., Timko, B. P., Langer, R. and Kohane, D. S. (2010). "Photo-targeted nanoparticles." *Nano Letters* 10(1): 250-254.

Ekdahl, C. T., Kokaia, Z. and Lindvall, O. (2009). "Brain inflammation and adult neurogenesis: the dual role of microglia." *Neuroscience* 158(3): 1021-1029.

Episkopou, V. (2005). "SOX2 Functions in Adult Neural Stem Cells." *Trends Neurosci* 28(5): 219-221.

Eriksson, P. S., Perfilieva, E., Bjork-Eriksson, T., Alborn, A.-M., Nordborg, C., Peterson, D. A. and Gage, F. H. (1998). "Neurogenesis in the adult human hippocampus." *Nature Medicine* 4(11): 1313-1317.

Ernst, A., Alkass, K., Bernard, S., Salehpour, M., Perl, S., Tisdale, J., Possnert, G., Druid, H. and Frisén, J. (2014). "Neurogenesis in the Striatum of the Adult Human Brain." *Cell* 156(5): 1072-1083.

Esteves, M., Cristovao, A. C., Saraiva, T., Rocha, S. M., Baltazar, G., Ferreira, L. and Bernardino, L. (2015). "Retinoic acid-loaded polymeric nanoparticles induce neuroprotection in a mouse model for Parkinson's disease." *Front Aging Neurosci* 7: 20.

Estrada, C. and Murillo-Carretero, M. (2005). "Nitric oxide and adult neurogenesis in health and disease." *Neuroscientist* 11(4): 294-307.

Ferguson, B., Kunisada, T., Aoki, H., Handoko, H. Y. and Walker, G. J. (2015). "Hair follicle melanocyte precursors are awoken by ultraviolet radiation via a cell extrinsic mechanism." *Photochemical & Photobiological Sciences* 14(6): 1179-1189.

Ferreira, L., Karp, J. M., Nobre, L. and Langer, R. (2008a). "New opportunities: the use of nanotechnologies to manipulate and track stem cells." *Cell Stem Cell* 3(2): 136-146.

Ferreira, L., Karp, J. M., Nobre, L. and Langer, R. (2008b). "New Opportunities: The Use of Nanotechnologies to Manipulate and Track Stem Cells." *Cell Stem Cell* 3(2): 136-146.

Ferreira, L. S. (2009). "Nanoparticles as tools to study and control stem cells." *Journal of Cellular Biochemistry* 108(4): 746-752.

Finkel, T. (2011). "Signal transduction by reactive oxygen species." *Journal of Cell Biology* 194(1): 7-15.

Fomina, N., McFearin, C., Sermsakdi, M., Edigin, O. and Almutairi, A. (2010). "UV and near-IR triggered release from polymeric nanoparticles." *J Am Chem Soc* 132(28): 9540-9542.

Fujibayashi, T., Kurauchi, Y., Hisatsune, A., Seki, T., Shudo, K. and Katsuki, H. (2015). "Mitogen-activated protein kinases regulate expression of neuronal nitric oxide synthase and neurite outgrowth via non-classical retinoic acid receptor signaling in human neuroblastoma SH-SY5Y cells." *Journal of Pharmacological Sciences* In press.

Funato, Y., Michiue, T., Asashima, M. and Miki, H. (2006). "The thioredoxin-related redox-regulating protein nucleoredoxin inhibits Wnt-beta-catenin signalling through dishevelled." *Nature Cell Biology* 8(5): 501-508.

Germain, P., Gaudon, C., Pogenberg, V., Sanglier, S., Van Dorsselaer, A., Royer, C. A., Lazar, M. A., Bourguet, W. and Gronemeyer, H. (2009). "Differential Action on Coregulator Interaction Defines Inverse Retinoid Agonists and Neutral Antagonists." *Chem Biol* 16(5): 479-489.

Gil-Perotín, S., Duran-Moreno, M., Cebrián-Silla, A., Ramírez, M., García-Belda, P. and García-Verdugo, J. M. (2013). "Adult Neural Stem Cells From the Subventricular Zone: A Review of the Neurosphere Assay." *The Anatomical Record* 296(9): 1435-1452.

Gilardi, F. and Desvergne, B. (2014). "RXRs: collegial partners." *Subcell Biochem* 70: 75-102.

Gudas, L. J. (2013). "Retinoids induce stem cell differentiation via epigenetic changes." *Seminars in Cell & Developmental Biology* 24(10–12): 701-705.

Guerrero-Cazares, H., Gonzalez-Perez, O., Soriano-Navarro, M., Zamora-Berridi, G., Garcia-Verdugo, J. M. and Quinones-Hinojosa, A. (2011). "Cytoarchitecture of the lateral ganglionic eminence and rostral extension of the lateral ventricle in the human fetal brain." *Journal of Comparative Neurology* 519(6): 1165-1180.

Guerrero, S., Araya, E., Fiedler, J. L., Arias, J. I., Adura, C., Albericio, F., Giralt, E., Arias, J. L., Fernández, M. S. and Kogan, M. J. (2010). "Improving the brain delivery of gold nanoparticles by conjugation with an amphipathic peptide." *Nanomedicine* 5(6): 897-913.

Gutierrez-Mazariegos, J., Schubert, M. and Laudet, V. (2014). "Evolution of retinoic acid receptors and retinoic acid signaling." *Subcell Biochem* 70: 55-73.

Haditsch, U., Anderson, M. P., Freewoman, J., Cord, B., Babu, H., Brakebusch, C. and Palmer, T. D. (2013). "Neuronal Rac1 is required for learning-evoked neurogenesis." *Journal of Neuroscience* 33(30): 12229-12241.

Haditsch, U., Leone, D. P., Farinelli, M., Chrostek-Grashoff, A., Brakebusch, C., Mansuy, I. M., McConnell, S. K. and Palmer, T. D. (2009). "A central role for the small GTPase Rac1

in hippocampal plasticity and spatial learning and memory." *Molecular and Cellular Neuroscience* 41(4): 409-419.

Hajas, G., Bacsi, A., Aguilera-Aguirre, L., Hegde, M. L., Tapas, K. H., Sur, S., Radak, Z., Ba, X. and Boldogh, I. (2013). "8-Oxoguanine DNA glycosylase-1 links DNA repair to cellular signaling via the activation of the small GTPase Rac1." *Free Radic Biol Med* 61: 384-394.

Hanada, S., Fujioka, K., Inoue, Y., Kanaya, F., Manome, Y. and Yamamoto, K. (2014). "Cell-Based in Vitro Blood–Brain Barrier Model Can Rapidly Evaluate Nanoparticles' Brain Permeability in Association with Particle Size and Surface Modification." *Int J Mol Sci* 15(2): 1812.

He, L. and Hannon, G. J. (2004). "MicroRNAs: small RNAs with a big role in gene regulation." *Nat Rev Genet* 5(7): 522-531.

Hoglinger, G. U., Rizk, P., Muriel, M. P., Duyckaerts, C., Oertel, W. H., Caille, I. and Hirsch, E. C. (2004). "Dopamine depletion impairs precursor cell proliferation in Parkinson disease." *Nature Neuroscience* 7(7): 726-735.

Hsieh, J. and Gage, F. H. (2005). "Chromatin remodeling in neural development and plasticity." *Curr Opin Cell Biol* 17(6): 664-671.

Hsieh, J., Nakashima, K., Kuwabara, T., Mejia, E. and Gage, F. H. (2004). "Histone deacetylase inhibition-mediated neuronal differentiation of multipotent adult neural progenitor cells." *Proc Natl Acad Sci U S A* 101(47): 16659-16664.

Hua, S., Kittler, R. and White, K. P. (2009). "Genomic antagonism between retinoic acid and estrogen signaling in breast cancer." *Cell* 137(7): 1259-1271.

Huang, C., Chan, J. A. and Schuurmans, C. (2014). "Proneural bHLH genes in development and disease." *Curr Top Dev Biol* 110: 75-127.

Huang, T. T., Zou, Y. and Corniola, R. (2012a). "Oxidative stress and adult neurogenesis--effects of radiation and superoxide dismutase deficiency." *Seminars in Cell & Developmental Biology* 23(7): 738-744.

Huang, X., Hu, Q., Braun, G. B., Pallaoro, A., Morales, D. P., Zasadzinski, J., Clegg, D. O. and Reich, N. O. (2015). "Light-activated RNA interference in human embryonic stem cells." *Biomaterials* 63: 70-79.

Huang, Y. Y., Gupta, A., Vecchio, D., de Arce, V. J., Huang, S. F., Xuan, W. and Hamblin, M. R. (2012b). "Transcranial low level laser (light) therapy for traumatic brain injury." *J Biophotonics* 5(11-12): 827-837.

Hwang, N. S., Varghese, S. and Elisseeff, J. (2008). "Controlled differentiation of stem cells." *Adv. Drug Deliv. Rev.* 60(2): 199-214.

Imayoshi, I., Ishidate, F. and Kageyama, R. (2015). "Real-time imaging of bHLH transcription factors reveals their dynamic control in the multipotency and fate choice of neural stem cells." *Front Cell Neurosci* 9: 288.

Ito, H., Nakajima, A., Nomoto, H. and Furukawa, S. (2003). "Neurotrophins facilitate neuronal differentiation of cultured neural stem cells via induction of mRNA expression of basic helix-loop-helix transcription factors Mash1 and Math1." *J Neurosci Res* 71(5): 648-658.

Jacobs, S., Lie, D. C., DeCicco, K. L., Shi, Y., DeLuca, L. M., Gage, F. H. and Evans, R. M. (2006). "Retinoic acid is required early during adult neurogenesis in the dentate gyrus." *Proc Natl Acad Sci U S A* 103(10): 3902-3907.

Janesick, A., Wu, S. C. and Blumberg, B. (2015). "Retinoic acid signaling and neuronal differentiation." *Cellular and Molecular Life Sciences* 72(8): 1559-1576.

Jawerka, M., Colak, D., Dimou, L., Spiller, C., Lagger, S., Montgomery, R. L., Olson, E. N., Wurst, W., Gottlicher, M. and Gotz, M. (2010). "The specific role of histone deacetylase 2 in adult neurogenesis." *Neuron Glia Biol* 6(2): 93-107.

Jenuwein, T. and Allis, C. D. (2001). "Translating the histone code." *Science* 293(5532): 1074-1080.

Jessberger, S., Clark, R. E., Broadbent, N. J., Clemenson, G. D., Jr., Consiglio, A., Lie, D. C., Squire, L. R. and Gage, F. H. (2009). "Dentate gyrus-specific knockdown of adult neurogenesis impairs spatial and object recognition memory in adult rats." *Learn Mem* 16(2): 147-154.

Jessberger, S., Toni, N., Clemenson, G. D., Jr., Ray, J. and Gage, F. H. (2008). "Directed differentiation of hippocampal stem/progenitor cells in the adult brain." *Nat Neurosci* 11(8): 888-893.

Jiao, J. and Chen, D. F. (2008a). "Induction of neurogenesis in nonconventional neurogenic regions of the adult central nervous system by niche astrocyte-produced signals." *Stem Cells* 26(5): 1221-1230.

Jiao, J. W., Feldheim, D. A. and Chen, D. F. (2008b). "Ephrins as negative regulators of adult neurogenesis in diverse regions of the central nervous system." *Proc Natl Acad Sci U S A* 105(25): 8778-8783.

Jin, K., Peel, A. L., Mao, X. O., Xie, L., Cottrell, B. A., Henshall, D. C. and Greenberg, D. A. (2004). "Increased hippocampal neurogenesis in Alzheimer's disease." *Proc Natl Acad Sci U S A* 101(1): 343-347.

Jin, K., Wang, X., Xie, L., Mao, X. O., Zhu, W., Wang, Y., Shen, J., Mao, Y., Banwait, S. and Greenberg, D. A. (2006). "Evidence for stroke-induced neurogenesis in the human brain." *Proc Natl Acad Sci U S A* 103(35): 13198-13202.

Jin, K., Zhu, Y., Sun, Y., Mao, X. O., Xie, L. and Greenberg, D. A. (2002). "Vascular endothelial growth factor (VEGF) stimulates neurogenesis in vitro and in vivo." *Proc Natl Acad Sci U S A* 99(18): 11946-11950.

Johanson, C. E., Stopa, E. G. and McMillan, P. N. (2011). "The Blood-Cerebrospinal Fluid Barrier: Structure and Functional Significance." *Methods Mol Biol* 686: 101-131.

Kageyama, R., Ohtsuka, T., Hatakeyama, J. and Ohsawa, R. (2005). "Roles of bHLH genes in neural stem cell differentiation." *Exp Cell Res* 306(2): 343-348.

Kageyama, R., Ohtsuka, T. and Kobayashi, T. (2008). "Roles of Hes genes in neural development." *Dev Growth Differ* 50 Suppl 1: S97-103.

Kageyama, R., Shimojo, H. and Imayoshi, I. (2015). "Dynamic expression and roles of Hes factors in neural development." *Cell and Tissue Research* 359(1): 125-133.

Kam, M., Curtis, M. A., McGlashan, S. R., Connor, B., Nannmark, U. and Faull, R. L. (2009). "The cellular composition and morphological organization of the rostral migratory stream in the adult human brain." *Journal of Chemical Neuroanatomy* 37(3): 196-205.

Kang, M. A., So, E. Y., Simons, A. L., Spitz, D. R. and Ouchi, T. (2012). "DNA damage induces reactive oxygen species generation through the H2AX-Nox1/Rac1 pathway." *Cell Death Dis* 3: e249.

Kashyap, V., Gudas, L. J., Brenet, F., Funk, P., Viale, A. and Scandura, J. M. (2011). "Epigenomic reorganization of the clustered Hox genes in embryonic stem cells induced by retinoic acid." *Journal of Biological Chemistry* 286(5): 3250-3260.

Kastner, P., Mark, M., Ghyselinck, N., Krezel, W., Dupe, V., Grondona, J. M. and Chambon, P. (1997). "Genetic Evidence that the Retinoid Signal is Transduced by Heterodimeric RXR/RAR Functional Units During Mouse Development." *Development* 124(2): 313-326.

Kawahara, K., Suenobu, M., Ohtsuka, H., Kuniyasu, A., Sugimoto, Y., Nakagomi, M., Fukasawa, H., Shudo, K. and Nakayama, H. (2014). "Cooperative therapeutic action of retinoic acid receptor and retinoid x receptor agonists in a mouse model of Alzheimer's disease." *J Alzheimers Dis* 42(2): 587-605.

Kerever, A., Schnack, J., Vellinga, D., Ichikawa, N., Moon, C., Arikawa-Hirasawa, E., Efird, J. T. and Mercier, F. (2007). "Novel extracellular matrix structures in the neural stem cell niche capture the neurogenic factor fibroblast growth factor 2 from the extracellular milieu." *Stem Cells* 25(9): 2146-2157.

Kernie, S. G. and Parent, J. M. (2010). "Forebrain neurogenesis after focal Ischemic and traumatic brain injury." *Neurobiology of Disease* 37(2): 267-274.

Kim, D. H., Seo, Y. K., Thambi, T., Moon, G. J., Son, J. P., Li, G., Park, J. H., Lee, J. H., Kim, H. H., Lee, D. S. and Bang, O. Y. (2015). "Enhancing neurogenesis and angiogenesis with target delivery of stromal cell derived factor-1alpha using a dual ionic pH-sensitive copolymer." *Biomaterials* 61: 115-125.

Kim, E. J., Ables, J. L., Dickel, L. K., Eisch, A. J. and Johnson, J. E. (2011). "Ascl1 (Mash1) Defines Cells With Long-Term Neurogenic Potential in Subgranular and Subventricular Zones in Adult Mouse Brain." *PLoS ONE* 6(3): e18472.

Kim, E. J., Leung, C. T., Reed, R. R. and Johnson, J. E. (2007). "*In Vivo* Analysis of Ascl1 Defined Progenitors Reveals Distinct Developmental Dynamics During Adult Neurogenesis and Gliogenesis." *J Neurosci* 27(47): 12764-12774.

Kim, H. J., Leeds, P. and Chuang, D. M. (2009a). "The HDAC inhibitor, sodium butyrate, stimulates neurogenesis in the ischemic brain." *J Neurochem* 110(4): 1226-1240.

Kim, J. B., Greber, B., Arauzo-Bravo, M. J., Meyer, J., Park, K. I., Zaehres, H. and Scholer, H. R. (2009b). "Direct reprogramming of human neural stem cells by OCT4." *Nature* 461(7264): 649-643.

Kim, J. B., Sebastiano, V., Wu, G., Arauzo-Bravo, M. J., Sasse, P., Gentile, L., Ko, K., Ruau, D., Ehrich, M., van den Boom, D., Meyer, J., Hubner, K., Bernemann, C., Ortmeier, C., Zenke, M., Fleischmann, B. K., Zaehres, H. and Scholer, H. R. (2009c). "Oct4-induced pluripotency in adult neural stem cells." *Cell* 136(3): 411-419.

Kim, S., Yoon, Y. S., Kim, J. W., Jung, M., Kim, S. U., Lee, Y. D. and Suh-Kim, H. (2004). "Neurogenin1 is sufficient to induce neuronal differentiation of embryonal carcinoma P19 cells in the absence of retinoic acid." *Cell Mol Neurobiol* 24(3): 343-356.

Kong, L., Wang, Y., Wang, X. J., Wang, X. T., Zhao, Y., Wang, L. M. and Chen, Z. Y. (2015). "Retinoic acid ameliorates blood-brain barrier disruption following ischemic stroke in rats." *Pharmacological Research* 99: 125-136.

Konig, K. (2000). "Multiphoton microscopy in life sciences." *Journal of Microscopy (Oxford)* 200(Pt 2): 83-104.

Kouzarides, T. (2007). "Chromatin modifications and their function." *Cell* 128(4): 693-705.

Krezel, W., Kastner, P. and Chambon, P. (1999). "Differential Expression of Retinoid Receptors in the Adult Mouse Central Nervous System." *Neuroscience* 89(4): 1291-1300.

Lane, M. A. and Bailey, S. J. (2005). "Role of retinoid signalling in the adult brain." *Prog Neurobiol* 75(4): 275-293.

le Maire, A. and Bourguet, W. (2014). "Retinoic acid receptors: structural basis for coregulator interaction and exchange." *Subcell Biochem* 70: 37-54.

Lee, E. and Son, H. (2009). "Adult hippocampal neurogenesis and related neurotrophic factors." *BMB Rep* 42(5): 239-244.

Lee, J., Kotliarova, S., Kotliarov, Y., Li, A., Su, Q., Donin, N. M., Pastorino, S., Purow, B. W., Christopher, N., Zhang, W., Park, J. K. and Fine, H. A. (2006). "Tumor stem cells derived from glioblastomas cultured in bFGF and EGF more closely mirror the phenotype and genotype of primary tumors than do serum-cultured cell lines." *Cancer Cell* 9: 391-403.

Lee, J. E., Cho, K. E., Lee, K. E., Kim, J. and Bae, Y. S. (2014). "Nox4-mediated cell signaling regulates differentiation and survival of neural crest stem cells." *Mol Cells* 37(12): 907-911.

Lee, S. K., Lee, B., Ruiz, E. C. and Pfaff, S. L. (2005). "Olig2 and Ngn2 function in opposition to modulate gene expression in motor neuron progenitor cells." *Genes Dev* 19(2): 282-294.

Leone, D. P., Srinivasan, K., Brakebusch, C. and McConnell, S. K. (2010). "The rho GTPase Rac1 is required for proliferation and survival of progenitors in the developing forebrain." *Dev Neurobiol* 70(9): 659-678.

Li, J., Stouffs, M., Serrander, L., Banfi, B., Bettiol, E., Charnay, Y., Steger, K., Krause, K. H. and Jaconi, M. E. (2006). "The NADPH oxidase NOX4 drives cardiac differentiation: Role in regulating cardiac transcription factors and MAP kinase activation." *Mol Biol Cell* 17(9): 3978-3988.

Li, L., Li, Y., Ji, X., Zhang, B., Wei, H. and Luo, Y. (2008). "The effects of retinoic acid on the expression of neurogranin after experimental cerebral ischemia." *Brain Res* 1226: 234-240.

Li, X., Liu, X., Zhao, W., Wen, X. and Zhang, N. (2012). "Manipulating neural-stem-cell mobilization and migration in vitro." *Acta Biomater* 8(6): 2087-2095.

Lim, D. A. and Alvarez-Buylla, A. (2014). "Adult neural stem cells stake their ground." *Trends in Neurosciences* 37(10): 563-571.

Lim, D. A., Huang, Y. C., Swigut, T., Mirick, A. L., Garcia-Verdugo, J. M., Wysocka, J., Ernst, P. and Alvarez-Buylla, A. (2009). "Chromatin Remodelling Factor Mll1 Is Essential For Neurogenesis From Postnatal Neural Stem Cells." *Nature* 458(7237): 529-533.

Lim, D. A., Tramontin, A. D., Trevejo, J. M., Herrera, D. G., Garcia-Verdugo, J. M. and Alvarez-Buylla, A. (2000). "Noggin antagonizes BMP signaling to create a niche for adult neurogenesis." *Neuron* 28(3): 713-726.

Lim, T. C., Rokkappanavar, S., Toh, W. S., Wang, L. S., Kurisawa, M. and Spector, M. (2013). "Chemotactic recruitment of adult neural progenitor cells into multifunctional hydrogels

providing sustained SDF-1alpha release and compatible structural support." *FASEB J* 27(3): 1023-1033.

Lin, R., Cai, J., Nathan, C., Wei, X., Schleidt, S., Rosenwasser, R. and Iacovitti, L. (2015). "Neurogenesis is enhanced by stroke in multiple new stem cell niches along the ventricular system at sites of high BBB permeability." *Neurobiol Dis* 74: 229-239.

Liu, C., Teng, Z. Q., Santistevan, N. J., Szulwach, K. E., Guo, W., Jin, P. and Zhao, X. (2010). "Epigenetic regulation of miR-184 by MBD1 governs neural stem cell proliferation and differentiation." *Cell Stem Cell* 6(5): 433-444.

Liu, X. S., Chopp, M., Zhang, R. L., Hozeska-Solgot, A., Gregg, S. C., Buller, B., Lu, M. and Zhang, Z. G. (2009). "Angiopoietin 2 mediates the differentiation and migration of neural progenitor cells in the subventricular zone after stroke." *J Biol Chem* 284(34): 22680-22689.

Liu, X. S., Zhang, Z. G., Zhang, R. L., Gregg, S. R., Meng, H. and Chopp, M. (2007). "Comparison of *In Vivo* and *In Vitro* gene Expression Profiles in Subventricular Zone Neural Progenitor Cells From the Adult Mouse After Middle Cerebral Artery Occlusion." *Neuroscience* 146(3): 1053-1061.

Lledo, P.-M., Alonso, M. and Grubb, M. S. (2006). "Adult neurogenesis and functional plasticity in neuronal circuits." *Nat. Rev. Neurosci.* 7(3): 179-193.

Lois, C., García-Verdugo, J. M. and Alvarez-Buylla, A. (1996). "Chain migration of neuronal precursors." *Science* 271(5251): 978-981.

Lundell, T. G., Zhou, Q. and Doughty, M. L. (2009). "Neurogenin1 Expression in Cell Lineages of the Cerebellar Cortex in Embryonic and Postnatal Mice." *Dev Dyn* 238(12): 3310-3325.

Luskin, M. B. (1993). "Restricted proliferation and migration of postnatally generated neurons derived from the forebrain subventricular zone." *Neuron* 11(1): 173-189.

Lytle, J. R., Yario, T. A. and Steitz, J. A. (2007). "Target mRNAs are repressed as efficiently by microRNA-binding sites in the 5' UTR as in the 3' UTR." *Proc Natl Acad Sci U S A* 104(23): 9667-9672.

Ma, D. K., Marchetto, M. C., Guo, J. U., Guo-li, M., Gage, F. H. and Hongjun, S. (2010). "Epigenetic choreographers of neurogenesis in the adult mammalian brain." *Nature Neuroscience* 13(11): 1338-1344.

Maden, M. (2002). "Retinoid signalling in the development of the central nervous system." *Nature Reviews Neuroscience* 3(11): 843-853.

Maden, M. (2007). "Retinoic Acid in the Development, Regeneration and Maintenance of the Nervous System." *Nat Rev Neurosci* 8(10): 755-765.

Maia, J., Santos, T., Aday, S., Agasse, F., Cortes, L., Malva, J. O., Bernardino, L. and Ferreira, L. (2011). "Controlling the Neuronal Differentiation of Stem Cells by the Intracellular Delivery of Retinoic Acid-Loaded Nanoparticles." *ACS Nano* 5(1): 97-106.

Maire, C. L., Buchet, D., Kerninon, C., Deboux, C., Baron-Van Evercooren, A. and Nait-Oumesmar, B. (2009). "Directing human neural stem/precursor cells into oligodendrocytes by overexpression of Olig2 transcription factor." *J Neurosci Res* 87(15): 3438-3446.

Marin-Husstege, M., Muggironi, M., Liu, A. and Casaccia-Bonnefil, P. (2002). "Histone deacetylase activity is necessary for oligodendrocyte lineage progression." *J Neurosci* 22(23): 10333-10345.

Marti-Fabregas, J., Romaguera-Ros, M., Gomez-Pinedo, U., Martinez-Ramirez, S., Jimenez-Xarrie, E., Marin, R., Marti-Vilalta, J. L. and Garcia-Verdugo, J. M. (2010). "Proliferation in the human ipsilateral subventricular zone after ischemic stroke." *Neurology* 74(5): 357-365.

Martino, G., Pluchino, S., Bonfanti, L. and Schwartz, M. (2011). "Brain Regeneration in Physiology and Pathology: The Immune Signature Driving Therapeutic Plasticity of Neural Stem Cells." *Physiological Reviews* 91(4): 1281-1304.

Masiá, S., Alvarez, S., Lera, A. R. d. and Barettino, D. (2007). "Rapid, Nongenomic Actions of Retinoic Acid on Phosphatidylinositol-3-Kinase Signaling Pathway Mediated by the Retinoic Acid Receptor." *Molecular Endocrinology* 21(10): 2391-2402.

Mattson, M. P. (2008). "Glutamate and Neurotrophic Factors in Neuronal Plasticity and Disease." *Annals of the New York Academy of Sciences* 1144(1): 97-112.

McCaffery, P., Zhang, J. and Crandall, J. E. (2006). "Retinoic acid signaling and function in the adult hippocampus." *Journal of Neurobiology* 66(7): 780-791.

Mercier, F. and Arikawa-Hirasawa, E. (2012). "Heparan sulfate niche for cell proliferation in the adult brain." *Neurosci Lett* 510(2): 67-72.

Mercier, F., Kitasako, J. T. and Hatton, G. I. (2002). "Anatomy of the brain neurogenic zones revisited: fractones and the fibroblast/macrophage network." *J Comp Neurol* 451(2): 170-188.

Michaelis, K., Hoffmann, M. M., Dreis, S., Herbert, E., Alyautdin, R. N., Michaelis, M., Kreuter, J. and Langer, K. (2006). "Covalent linkage of apolipoprotein e to albumin nanoparticles strongly enhances drug transport into the brain." *J Pharmacol Exp Ther* 317(3): 1246-1253.

Ming, G.-l. and Song, H. (2011a). "Adult Neurogenesis in the Mammalian Brain: Significant Answers and Significant Questions." *Neuron* 70(4): 687-702.

Ming, G. L. and Song, H. (2011b). "Adult neurogenesis in the mammalian brain: significant answers and significant questions." *Neuron* 70(4): 687-702.

Mitsui, K., Tokuzawa, Y., Itoh, H., Segawa, K., Murakami, M., Takahashi, K., Maruyama, M., Maeda, M. and Yamanaka, S. (2003). "The homeoprotein Nanog is required for maintenance of pluripotency in mouse epiblast and ES cells." *Cell* 113(5): 631-642.

Mohamed Ariff, I., Mitra, A. and Basu, A. (2012). "Epigenetic regulation of self-renewal and fate determination in neural stem cells." *Journal of Neuroscience Research* 90(3): 529-539.

Mohyeldin, A., Garzon-Muvdi, T. and Quinones-Hinojosa, A. (2010). "Oxygen in stem cell biology: a critical component of the stem cell niche." *Cell Stem Cell* 7(2): 150-161.

Moreno-Estelles, M., Gonzalez-Gomez, P., Hortiguela, R., Diaz-Moreno, M., San Emeterio, J., Carvalho, A. L., Farinas, I. and Mira, H. (2012). "Symmetric expansion of neural stem cells from the adult olfactory bulb is driven by astrocytes via WNT7A." *Stem Cells* 30(12): 2796-2809.

Morshead, C. M., Reynolds, B. A., Craig, C. G., McBurney, M. W., Staines, W. A., Morassutti, D., Weiss, S. and Kooy, D. (1994). "Neural stem cells in the adult mammalian forebrain: A relatively quiescent subpopulation of subependymal cells " *Neuron* 13(5): 1071-1082.

Mura, S., Nicolas, J. and Couvreur, P. (2013). "Stimuli-responsive nanocarriers for drug delivery." *Nat Mater* 12(11): 991-1003.

Neo, W. H., Yap, K., Lee, S. H., Looi, L. S., Khandelia, P., Neo, S. X., Makeyev, E. V. and Su, I. H. (2014). "MicroRNA miR-124 controls the choice between neuronal and astrocyte differentiation by fine-tuning Ezh2 expression." *Journal of Biological Chemistry* 289(30): 20788-20801.

Niehrs, C. (2012). "The complex world of WNT receptor signalling." *Nature Reviews: Molecular Cell Biology* 13(12): 767-779.

Niwa, H., Miyazaki, J. and Smith, A. G. (2000). "Quantitative expression of Oct-3/4 defines differentiation, dedifferentiation or self-renewal of ES cells." *Nat Genet* 24(4): 372-376.

Nomura, T., Goritz, C., Catchpole, T., Henkemeyer, M. and Frisen, J. (2010). "EphB signaling controls lineage plasticity of adult neural stem cell niche cells." *Cell Stem Cell* 7(6): 730-743.

Núñez, V., Alameda, D., Rico, D., Mota, R., Gonzalo, P., Cedenilla, M., Fischer, T., Boscá, L., Glass, C. K., Arroyo, A. G. and Ricote, M. (2010). "Retinoid X receptor α controls innate inflammatory responses through the up-regulation of chemokine expression." *Proceedings of the National Academy of Sciences* 107(23): 10626-10631.

O'Sullivan, S. S., Johnson, M., Williams, D. R., Revesz, T., Holton, J. L., Lees, A. J. and Perry, E. K. (2011). "The effect of drug treatment on neurogenesis in Parkinson's disease." *Mov Disord* 26(1): 45-50.

Oh, H. J., Hwang do, W., Youn, H. and Lee, D. S. (2013). "In vivo bioluminescence reporter gene imaging for the activation of neuronal differentiation induced by the neuronal activator neurogenin 1 (Ngn1) in neuronal precursor cells." *Eur J Nucl Med Mol Imaging* 40(10): 1607-1617.

Oliva, A. A., Jr, Atkins, C. M., Copenagle, L. and Banker, G. A. (2006). "Activated c-Jun N-Terminal Kinase Is Required for Axon Formation." *J Neurosci* 26(37): 9462-9470.

Orive, G., Anitua, E., Pedraz, J. L. and Emerich, D. F. (2009). "Biomaterials for Promoting Brain Protection, Repair and Regeneration." *Nat Rev Neurosci* 10(9): 682-692.

Palmer, T. D., Willhoite, A. R. and Gage, F. H. (2000). "Vascular niche for adult hippocampal neurogenesis." *J Comp Neurol* 425(4): 479-494.

Parent, J. M., Vexler, Z. S., Gong, C., Derugin, N. and Ferriero, D. M. (2002). "Rat forebrain neurogenesis and striatal neuron replacement after focal stroke." *Ann Neurol* 52(6): 802-813.

Park, D., Lee, H. J., Joo, S. S., Bae, D. K., Yang, G., Yang, Y. H., Lim, I., Matsuo, A., Tooyama, I., Kim, Y. B. and Kim, S. U. (2012). "Human neural stem cells over-expressing choline acetyltransferase restore cognition in rat model of cognitive dysfunction." *Exp Neurol* 234(2): 521-526.

Park, D., Yang, Y. H., Bae, D. K., Lee, S. H., Yang, G., Kyung, J., Kim, D., Choi, E. K., Lee, S. W., Kim, G. H., Hong, J. T., Choi, K. C., Lee, H. J., Kim, S. U. and Kim, Y. B. (2013). "Improvement of cognitive function and physical activity of aging mice by human neural stem cells over-expressing choline acetyltransferase." *Neurobiol Aging* 34(11): 2639-2646.

Parker, M. A., Anderson, J. K., Corliss, D. A., Abraria, V. E., Sidman, R. L., Park, K. I., Teng, Y. D., Cotanche, D. A. and Snyder, E. Y. (2005). "Expression profile of an operationally-defined neural stem cell clone." *Experimental Neurology* 194(2): 320-332.

Paschaki, M., Lin, S. C., Wong, R. L., Finnell, R. H., Dolle, P. and Niederreither, K. (2012). "Retinoic acid-dependent signaling pathways and lineage events in the developing mouse spinal cord." *PLoS One* 7(3): e32447.

Pfaffl, M. W. (2001). "A New Mathematical Model for Relative Quantification in Real-Time RT-PCR." *Nucleic Acids Res* 29(9): e45.

Piskunov, A., Al Tanoury, Z. and Rochette-Egly, C. (2014). "Nuclear and extra-nuclear effects of retinoid acid receptors: how they are interconnected." *Subcell Biochem* 70: 103-127.

Piskunov, A. and Rochette-Egly, C. (2012). "A retinoic acid receptor RAR[alpha] pool present in membrane lipid rafts forms complexes with G protein [alpha]Q to activate p38MAPK." *Oncogene* 31(28): 3333-3345.

Plane, J. M., Whitney, J. T., Schallert, T. and Parent, J. M. (2008). "Retinoic Acid and Environmental Enrichment Alter Subventricular Zone and Striatal Neurogenesis After Stroke." *Exp Neurol*: 125-134.

Prozorovski, T., Schneider, R., Berndt, C., Hartung, H. P. and Aktas, O. (2015). "Redox-regulated fate of neural stem progenitor cells." *Biochimica et Biophysica Acta: Protein Structure and Molecular Enzymology* 1850(8): 1543-1554.

Qian, X., Shen, Q., Goderie, S. K., He, W., Capela, A., Davis, A. A. and Temple, S. (2000). "Timing of CNS cell generation: a programmed sequence of neuron and glial cell production from isolated murine cortical stem cells." *Neuron* 28(1): 69-80.

Qu, Q., Sun, G., Murai, K., Ye, P., Li, W., Asuelime, G., Cheung, Y. T. and Shi, Y. (2013). "Wnt7a regulates multiple steps of neurogenesis." *Molecular and Cellular Biology* 33(13): 2551-2559.

Quiñones-Hinojosa, A., Sanai, N., Soriano-Navarro, M., Gonzalez-Perez, O., Mirzadeh, Z., Gil-Perotin, S., Romero-Rodriguez, R., Berger, M. S., García-Verdugo, J. M. and Alvarez-Buylla, A. (2006). "Cellular Composition and Cytoarchitecture of the Adult Human Subventricular Zone: A Niche of Neural Stem Cells." *The Journal of Comparative Neurology* 494: 415-434.

Raha, S. and Robinson, B. H. (2000). "Mitochondria, oxygen free radicals, disease and ageing." *Trends in Biochemical Sciences* 25(10): 502-508.

Rana, T. M. (2007). "Illuminating the silence: understanding the structure and function of small RNAs." *Nat Rev Mol Cell Biol* 8(1): 23-36.

Reya, T. and Clevers, H. (2005). "Wnt signalling in stem cells and cancer." *Nature* 434(7035): 843-850.

Reznikov, K. Y. (1991). "Cell proliferation and cytogenesis in the mouse hippocampus." *Advances in anatomy, embriology and cell biology* 122: 1-74.

Rharass, T., Lemcke, H., Lantow, M., Kuznetsov, S. A., Weiss, D. G. and Panakova, D. (2014). "Ca2+-mediated mitochondrial reactive oxygen species metabolism augments Wnt/beta-catenin pathway activation to facilitate cell differentiation." *Journal of Biological Chemistry* 289(40): 27937-27951.

Rochette-Egly, C. (2015). "Retinoic acid signaling and mouse embryonic stem cell differentiation: Cross talk between genomic and non-genomic effects of RA." *Biochimica et Biophysica Acta: Protein Structure and Molecular Enzymology* 1851(1): 66-75.

Rochette-Egly, C., Plassat, J. L., Taneja, R. and Chambon, P. (2000). "The AF-1 and AF-2 activating domains of retinoic acid receptor-alpha (RARalpha) and their phosphorylation are differentially involved in parietal endodermal differentiation of F9 cells and retinoid-induced expression of target genes." *Molecular Endocrinology* 14(9): 1398-1410.

Rosa, A. I., Goncalves, J., Cortes, L., Bernardino, L., Malva, J. O. and Agasse, F. (2010). "The angiogenic factor angiopoietin-1 is a proneurogenic peptide on subventricular zone stem/progenitor cells." *J Neurosci* 30(13): 4573-4584.

Sakai, Y., Crandall, J. E., Brodsky, J. and McCaferry, P. (2004). "13-cis Retinoic Acid (Accutane) Suppresses Hippocampal Cell Survival in Mice." *Annals of the New York Academy of Sciences* 1021: 436-440.

Sanai, N., Nguyen, T., Ihrie, R. A., Mirzadeh, Z., Tsai, H.-H., Wong, M., Gupta, N., Berger, M. S., Huang, E., Garcia-Verdugo, J.-M., Rowitch, D. H. and Alvarez-Buylla, A. (2011). "Corridors of Migrating Neurons in the Human Brain and Their Decline During Infancy." *Nature* 478(7369): 382-386.

Sanai, N., Tramontin, A. D., Quiñones-Hinojosa, A., Barbaro, N. M., Gupta, N., Kunwa, S., Lawton, M. T., McDermott, M. W., Parsa, A. T., Verdugo, J. M.-G., Berger, M. S. and Alvarez-Buylla, A. (2004). "Unique astrocyte ribbon in adult human brain contains neural stem cells but lacks chain migration." *Nature* 427: 740-744.

Sandieson, L., Hwang, J. T. and Kelly, G. M. (2014). "Redox regulation of canonical Wnt signaling affects extraembryonic endoderm formation." *Stem Cells Dev* 23(10): 1037-1049.

Santos-Rosa, H., Schneider, R., Bannister, A. J., Sherriff, J., Bernstein, B. E., Emre, N. C. T., Schreiber, S. L., Mellor, J. and Kouzarides, T. (2002). "Active Genes Are Tri-Methylated at K4 of Histone H3." *Nature* 419(6905): 407-411.

Santos, T., Ferreira, R., Maia, J., Agasse, F., Xapelli, S., Cortes, L., Bragança, J., Malva, J. O., Ferreira, L. and Bernardino, L. (2012a). "Polymeric Nanoparticles to Control the Differentiation of Neural Stem Cells in the Subventricular Zone of the Brain." *ACS Nano* 6(12): 10463-10474.

Santos, T., Maia, J., Agasse, F., Xapelli, S., Ferreira, L. and Bernardino, L. (2012b). "Nanomedicine Boosts Neurogenesis: New Strategies for Brain Repair." *Integr Biol* 4(9): 973-981.

Sauer, H., Ruhe, C., Muller, J. P., Schmelter, M., D'Souza, R. and Wartenberg, M. (2008). "Reactive oxygen species and upregulation of NADPH oxidases in mechanotransduction of embryonic stem cells." *Methods Mol Biol* 477: 397-418.

Schieber, M. and Chandel, N. S. (2014). "ROS function in redox signaling and oxidative stress." *Current Biology* 24(10): R453-462.

Schmidt-Hieber, C., Jonas, P. and Bischofberger, J. (2004). "Enhanced synaptic plasticity in newly generated granule cells of the adult hippocampus." *Nature* 429(6988): 184-187.

Schmidt, A., Haas, S. J., Hildebrandt, S., Scheibe, J., Eckhoff, B., Racek, T., Kempermann, G., Wree, A. and Putzer, B. M. (2007). "Selective targeting of adenoviral vectors to neural precursor cells in the hippocampus of adult mice: new prospects for in situ gene therapy." *Stem Cells* 25(11): 2910-2918.

Sena, L. A. and Chandel, N. S. (2012). "Physiological roles of mitochondrial reactive oxygen species." *Molecular Cell* 48(2): 158-167.

Seri, B., García-Verdugo, J. M., Collado-Morente, L., McEwen, B. S. and Alvarez-Buylla, A. (2004). "Cell Types, Lineage, and Architecture of the Germinal Zone in the Adult Dentate Gyrus." *The Journal of Comparative Neurology* 478: 359-378.

Seri, B., García-Verdugo, J. M., McEwen, B. S. and Alvarez-Buylla, A. (2001). "Astrocytes Give Rise to New Neurons in the Adult Mammalian Hippocampus." *The Journal of Neuroscience* 21(18): 7158-7160.

Shen, Q., Goderie, S. K., Jin, L., Karanth, N., Sun, Y., Abramova, N., Vincent, P., Pumiglia, K. and Temple, S. (2004). "Endothelial cells stimulate self-renewal and expand neurogenesis of neural stem cells." *Science* 304(5675): 1338-1340.

Shen, Q., Wang, Y., Kokovay, E., Lin, G., Chuang, S.-M., Goderie, S. K., Roysam, B. and Temple, S. (2008). "Adult SVZ Stem Cells Lie in a Vascular Niche: A Quantitative Analysis of Niche Cell-Cell Interactions." *Cell Stem Cell* 3(3): 289-300.

Shen, S., Li, J. and Casaccia-Bonnefil, P. (2005). "Histone modifications affect timing of oligodendrocyte progenitor differentiation in the developing rat brain." *J Cell Biol* 169(4): 577-589.

Shimada, J.-I., Taniguchi, J., Mori, M., Sato, Y., Takuwa, H., Ito, H. and Kuwabara, S. (2013). "Retinol palmitate prevents ischemia-induced cell changes in hippocampal neurons through the Notch1 signaling pathway in mice." *Experimental Neurology* 247(0): 182-187.

Shitamukai, A. and Matsuzaki, F. (2012). "Control of asymmetric cell division of mammalian neural progenitors." *Development Growth & Differentiation* 54(3): 277-286.

Shors, T. J., Miesegaes, G., Beylin, A., Zhao, M., Rydel, T. and Gould, E. (2001). "Neurogenesis in the adult is involved in the formation of trace memories." *Nature* 410: 372-376.

Shyam, R., Ren, Y., Lee, J., Braunstein, K. E., Mao, H. Q. and Wong, P. C. (2015). "Intraventricular Delivery of siRNA Nanoparticles to the Central Nervous System." *Mol Ther Nucleic Acids* 4: e242.

Siegenthaler, J. A., Ashique, A. M., Zarbalis, K., Patterson, K. P., Hecht, J. H., Kane, M. A., Folias, A. E., Choe, Y., May, S. R., Kume, T., Napoli, J. L., Peterson, A. S. and Pleasure, S. J. (2009). "Retinoic Acid from the Meninges Regulates Cortical Neuron Generation." *Cell* 139(3): 597-609.

Sonavane, G., Tomoda, K. and Makino, K. (2008). "Biodistribution of colloidal gold nanoparticles after intravenous administration: Effect of particle size." *Colloids and Surfaces B: Biointerfaces* 66(2): 274-280.

Sousa, F., Mandal, S., Garrovo, C., Astolfo, A., Bonifacio, A., Latawiec, D., Menk, R. H., Arfelli, F., Huewel, S., Legname, G., Galla, H. J. and Krol, S. (2010). "Functionalized gold nanoparticles: a detailed in vivo multimodal microscopic brain distribution study." *Nanoscale* 2(12): 2826-2834.

Srikanth, M. and Kessler, J. A. (2012). "Nanotechnology-novel therapeutics for CNS disorders." *Nat Rev Neurol* 8(6): 307-318.

Suh, H., Consiglio, A., Ray, J., Sawai, T., D'Amour, K. A. and Gage, F. H. (2007). "In vivo fate analysis reveals the multipotent and self-renewal capacities of Sox2+ neural stem cells in the adult hippocampus." *Cell Stem Cell* 1(5): 515-528.

Suh, H., Deng, W. and Gage, F. H. (2009a). "Signaling in adult neurogenesis." *Annu Rev Cell Dev Biol* 25: 253-275.

Suh, Y., Obernier, K., Holzl-Wenig, G., Mandl, C., Herrmann, A., Worner, K., Eckstein, V. and Ciccolini, F. (2009b). "Interaction between DLX2 and EGFR regulates proliferation and neurogenesis of SVZ precursors." *Mol Cell Neurosci* 42(4): 308-314.

Sun, Y., Jin, K., Xie, L., Childs, J., Mao, X. O., Logvinova, A. and Greenberg, D. A. (2003). "VEGF-induced neuroprotection, neurogenesis, and angiogenesis after focal cerebral ischemia." *Journal Of Clinical Investigation* 111(12): 1843-1851.

Sun, Y., Nadal-Vicens, M., Misono, S., Lin, M. Z., Zubiaga, A., Hua, X., Fan, G. and Greenberg, M. E. (2001). "Neurogenin Promotes Neurogenesis and Inhibits Glial Differentiation by Independent Mechanisms." *Cell* 104(3): 365-376.

Szulwach, K. E., Li, X., Smrt, R. D., Li, Y., Luo, Y., Lin, L., Santistevan, N. J., Li, W., Zhao, X. and Jin, P. (2010). "Cross talk between microRNA and epigenetic regulation in adult neurogenesis." *J Cell Biol* 189(1): 127-141.

Szutowicz, A., Bielarczyk, H., Jankowska-Kulawy, A., Ronowska, A. and Pawelczyk, T. (2015). "Retinoic acid as a therapeutic option in Alzheimer's disease: a focus on cholinergic restoration." *Expert Rev Neurother* 15(3): 239-249.

Szuts, E. Z. and Harosi, F. I. (1991). "Solubility of Retinoids in Water." *Arch Biochem Biophys* 287(2): 297-304.

Takahashi, K., Okita, K., Nakagawa, M. and Yamanaka, S. (2007). "Induction of pluripotent stem cells from fibroblast cultures." *Nat Protoc* 2(12): 3081-3089.

Takebayashi, H., Nabeshima, Y., Yoshida, S., Chisaka, O. and Ikenaka, K. (2002). "The basic helix-loop-helix factor olig2 is essential for the development of motoneuron and oligodendrocyte lineages." *Curr Biol* 12(13): 1157-1163.

Takizawa, T., Nakashima, K., Namihira, M., Ochiai, W., Uemura, A., Yanagisawa, M., Fujita, N., Nakao, M. and Taga, T. (2001). "DNA methylation is a critical cell-intrinsic determinant of astrocyte differentiation in the fetal brain." *Dev Cell* 1(6): 749-758.

Tang, X., Luo, Y. X., Chen, H. Z. and Liu, D. P. (2014). "Mitochondria, endothelial cell function, and vascular diseases." *Front Physiol* 5: 175.

Tashiro, A., Sandler, V. M., Toni, N., Zhao, C. and Gage, F. H. (2006). "NMDA-receptor-mediated, cell-specific integration of new neurons in adult dentate gyrus." *Nature* 442(7105): 929-933.

Tavazoie, M., Van der Veken, L., Silva-Vargas, V., Louissaint, M., Colonna, L., Zaidi, B., Garcia-Verdugo, J. M. and Doetsch, F. (2008). "A Specialized Vascular Niche for Adult Neural Stem Cells." *Cell Stem Cell* 3(3): 279-288.

Thored, P. r., Wood, J., Arvidsson, A., Cammenga, J. r., Kokaia, Z. and Lindvall, O. (2007). "Long-Term Neuroblast Migration Along Blood Vessels in an Area With Transient Angiogenesis and Increased Vascularization After Stroke." *Stroke* 38(11): 3032-3039.

Tiwari, S. K., Agarwal, S., Seth, B., Yadav, A., Nair, S., Bhatnagar, P., Karmakar, M., Kumari, M., Chauhan, L. K., Patel, D. K., Srivastava, V., Singh, D., Gupta, S. K., Tripathi, A., Chaturvedi, R. K. and Gupta, K. C. (2014). "Curcumin-loaded nanoparticles potently induce adult neurogenesis and reverse cognitive deficits in Alzheimer's disease model via canonical Wnt/beta-catenin pathway." *ACS Nano* 8(1): 76-103.

Tiyaboonchai, W., Woiszwillo, J. and Middaugh, C. R. (2001). "Formulation and characterization of amphotericin B-polyethylenimine-dextran sulfate nanoparticles." *Journal of Pharmaceutical Sciences* 90(7): 902-914.

Tyssowski, K., Kishi, Y. and Gotoh, Y. (2014). "Chromatin regulators of neural development." *Neuroscience* 264: 4-16.

Ueki, T., Tanaka, M., Yamashita, K., Mikawa, S., Qiu, Z., Maragakis, N. J., Hevner, R. F., Miura, N., Sugimura, H. and Sato, K. (2003). "A novel secretory factor, Neurogenesin-1, provides neurogenic environmental cues for neural stem cells in the adult hippocampus." *J Neurosci* 23(37): 11732-11740.

Varkouhi, A. K., Scholte, M., Storm, G. and Haisma, H. J. (2011). "Endosomal escape pathways for delivery of biologicals." *J Control Release* 151(3): 220-228.

Vierbuchen, T., Ostermeier, A., Pang, Z. P., Kokubu, Y., Sudhof, T. C. and Wernig, M. (2010). "Direct Conversion of Fibroblasts to Functional Neurons by Defined Factors." *Nature* 463(7284): 1035-1041.

Voronova, A., Fischer, A., Ryan, T., Al Madhoun, A. and Skerjanc, I. S. (2011). "Ascl1/Mash1 Is a Novel Target of Gli2 during Gli2-Induced Neurogenesis in P19 EC Cells." *PLoS ONE* 6(4): e19174.

Wald, G. (1968). "The molecular basis of visual excitation." *Nature* 219(5156): 800-807.

Wang, T. W., Zhang, H. and Parent, J. M. (2005). "Retinoic Acid Regulates Postnatal Neurogenesis in the Murine Subventricular Zone-Olfactory Bulb Pathway." *Development* 132(12): 2721-2732.

Wang, Y., Cooke, M. J., Sachewsky, N., Morshead, C. M. and Shoichet, M. S. (2013). "Bioengineered sequential growth factor delivery stimulates brain tissue regeneration after stroke." *J Control Release* 172(1): 1-11.

Watt, F. M. and Huck, W. T. (2013). "Role of the extracellular matrix in regulating stem cell fate." *Nature Reviews: Molecular Cell Biology* 14(8): 467-473.

Wen, S., Li, H. and Liu, J. (2009). "Epigenetic background of neuronal fate determination." *Prog Neurobiol* 87(2): 98-117.

Wiley, D. T., Webster, P., Gale, A. and Davis, M. E. (2013). "Transcytosis and brain uptake of transferrin-containing nanoparticles by tuning avidity to transferrin receptor." *Proc Natl Acad Sci U S A* 110(21): 8662-8667.

Wilhelmsson, U., Faiz, M., de Pablo, Y., Sjoqvist, M., Andersson, D., Widestrand, A., Potokar, M., Stenovec, M., Smith, P. L., Shinjyo, N., Pekny, T., Zorec, R., Stahlberg, A., Pekna, M., Sahlgren, C. and Pekny, M. (2012). "Astrocytes negatively regulate neurogenesis through the Jagged1-mediated Notch pathway." *Stem Cells* 30(10): 2320-2329.

Wohlfart, S., Gelperina, S. and Kreuter, J. (2012). "Transport of drugs across the blood-brain barrier by nanoparticles." *J Control Release* 161(2): 264-273.

Wu, M., Zhang, Y., Wu, N. H. and Shen, Y. F. (2009). "Histone Marks and Chromatin Remodelers on the Regulation of Neurogenin1 Gene in RA Induced Neuronal Differentiation of P19 Cells." *J Cell Biochem* 107(2): 264-271.

Xavier, J. M., Morgado, A. L., Sola, S. and Rodrigues, C. M. (2014). "Mitochondrial translocation of p53 modulates neuronal fate by preventing differentiation-induced mitochondrial stress." *Antioxidants and Redox Signaling* 21(7): 1009-1024.

Xiao, Q., Luo, Z., Pepe, A. E., Margariti, A., Zeng, L. and Xu, Q. (2009). "Embryonic stem cell differentiation into smooth muscle cells is mediated by Nox4-produced H2O2." *American Journal of Physiology: Cell Physiology* 296(4): C711-723.

Xuan, W., Vatansever, F., Huang, L. and Hamblin, M. R. (2014). "Transcranial low-level laser therapy enhances learning, memory, and neuroprogenitor cells after traumatic brain injury in mice." *J Biomed Opt* 19(10): 108003.

Xuan, W., Vatansever, F., Huang, L., Wu, Q., Xuan, Y., Dai, T., Ando, T., Xu, T., Huang, Y. Y. and Hamblin, M. R. (2013). "Transcranial low-level laser therapy improves neurological performance in traumatic brain injury in mice: effect of treatment repetition regimen." *PLoS One* 8(1): e53454.

Yamada, T., Hasegawa, S., Inoue, Y., Date, Y., Yamamoto, N., Mizutani, H., Nakata, S., Matsunaga, K. and Akamatsu, H. (2013). "Wnt/beta-catenin and kit signaling sequentially regulate melanocyte stem cell differentiation in UVB-induced epidermal pigmentation." *J Invest Dermatol* 133(12): 2753-2762.

Yavlovich, A., Smith, B., Gupta, K., Blumenthal, R. and Puri, A. (2010). "Light-sensitive lipid-based nanoparticles for drug delivery: design principles and future considerations for biological applications." *Mol Membr Biol* 27(7): 364-381.

Yoo, C. B. and Jones, P. A. (2006). "Epigenetic therapy of cancer: past, present and future." *Nat Rev Drug Discov* 5(1): 37-50.

Young, S. Z., Taylor, M. M. and Bordey, A. (2011). "Neurotransmitters couple brain activity to subventricular zone neurogenesis." *Eur J Neurosci* 33(6): 1123-1132.

Yu, S., Levi, L., Siegel, R. and Noy, N. (2012). "Retinoic acid induces neurogenesis by activating both retinoic acid receptors (RARs) and peroxisome proliferator-activated receptor beta/delta (PPARbeta/delta)." *Journal of Biological Chemistry* 287(50): 42195-42205.

Zaehres, H., Lensch, M. W., Daheron, L., Stewart, S. A., Itskovitz-Eldor, J. and Daley, G. Q. (2005). "High-efficiency RNA interference in human embryonic stem cells." *Stem Cells* 23(3): 299-305.

Zhang, R. L., Chopp, M., Roberts, C., Liu, X., Wei, M., Nejad-Davarani, S. P., Wang, X. and Zhang, Z. G. (2014a). "Stroke increases neural stem cells and angiogenesis in the neurogenic niche of the adult mouse." *PLoS One* 9(12): e113972.

Zhang, W., Wang, P. J., Sha, H. Y., Ni, J., Li, M. H. and Gu, G. J. (2014b). "Neural Stem Cell Transplants Improve Cognitive Function Without Altering Amyloid Pathology in an APP/PS1 Double Transgenic Model of Alzheimer's Disease." *Mol Neurobiol*.

Zhao, Y. Z., Li, X., Lu, C. T., Lin, M., Chen, L. J., Xiang, Q., Zhang, M., Jin, R. R., Jiang, X., Shen, X. T., Li, X. K. and Cai, J. (2014). "Gelatin nanostructured lipid carriers-mediated intranasal delivery of basic fibroblast growth factor enhances functional recovery in hemiparkinsonian rats." *Nanomedicine* 10(4): 755-764.